이학박사 학위논문

A study on the regulatory mechanisms of *VERNALIZATION INSENSITIVE3* during vernalization in *Arabidopsis*

애기장대 춘화처리를 매개하는 ***VERNALIZATION INSENSITIVE3***의 조절 기작에 대한 연구

2022 년 8 월

서울대학교 대학원

생명과학부

정 구 원

A study on the regulatory mechanisms of *VERNALIZATION INSENSITIVE3* during vernalization in Arabidopsis

A dissertation submitted in partial fulfillment of the requirement for the degree of

DOCTOR OF PHILOSOPHY

to the Faculty of

School of Biological Sciences

at

Seoul National University

by

Goowon Jeong

June, 2022

Chair	Yoo-sun Noh	(Seal)
Vice Chair	Ilha Lee	(Seal)
Examiner	Youbong Hyun	(Seal)
Examiner	Yeonhee Choi	(Seal)
Examiner	Jaehoon Jung	(Seal)

Abstract

A study on the regulatory mechanisms of *VERNALIZATION INSENSITIVE3* during vernalization in *Arabidopsis*

Goowon Jeong

School of Biological Sciences

The Graduate School

Seoul National University

Vernalization, an acceleration of flowering after long-term winter cold, is an intensively studied flowering mechanism in winter annual plants. In the model plant *Arabidopsis*, Polycomb Repressive Complex 2 (PRC2)-mediated suppression of the strong floral

repressor, *FLOWERING LOCUS C* (*FLC*), is critical for vernalization and a PHD finger domain protein, VERNALIZATION INSENSITIVE 3 (VIN3), recruits PRC2 to *FLC* chromatin. The level of *VIN3* was found to gradually increase in proportion with the length of the cold period during vernalization. However, how plants finely regulate *VIN3* expression according to the cold environment has not been completely elucidated. As a result, I performed EMS mutagenesis using a transgenic line with a minimal promoter of *VIN3* fused to the GUS reporter gene and isolated two mutants, *hov1* and *P161*.

In chapter 1, I discuss the fine-tuning mechanism underlying *VIN3* regulation by a heat-shock transcription factor. I performed EMS mutagenesis using a transgenic line with a *VIN3* promoter fused to the GUS reporter gene and isolated a mutant with hyperactive *VIN3* with increased GUS signals and endogenous *VIN3* transcript levels. Using positional cloning combined with whole-genome resequencing, I found that *hov1* carries a nonsense mutation, leading to a premature stop codon in the *HsfB2b*, which encodes a repressive heat shock transcription factor. HsfB2b directly binds to the *VIN3* promoter, and *HsfB2b* overexpression leads to reduced acceleration of flowering after vernalization. These findings reveal a novel fine-tuning mechanism that regulates *VIN3* for proper vernalization responses.

In chapter 2, I discuss a eukaryotic chaperonin-mediated molecular mechanism of *VIN3* regulation. During a previous mutant screening procedure, I isolated the *P161* mutant that demonstrates reduced GUS signals and endogenous *VIN3* expression levels during vernalization treatment. Using positional cloning combined with whole-genome

resequencing, I found that *P161* carries a missense mutation, leading to an amino acid residue substitution in the CCT8, one of eight subunits of the cytosolic chaperonin complex. The mutation was found to be disrupt a rhythmic expression of a circadian clock gene, *RVE8*, specifically during vernalization treatment. RVE8 directly binds to the *VIN3* promoter, inducing circadian rhythm-controlled *VIN3* expression levels. Collectively, these findings reveal a novel mechanism that regulates *VIN3*, promoting a proper vernalization response.

Keyword: Flowering, Vernalization, VIN3, CCT8, RVE8*, Arabidopsis thaliana*

Student Number: 2013-20317

Table of Contents

Chapter 2 : Chaperonin-mediated regulation of *VIN3* via circadian clock

List of Figures

List of Tables

Abbreviations

ABRC	Arabidopsis biological resource center
AHA motif	Motifs with aromatic, large hydrophobic, and acidic amino acid residues
BAC	Bacterial artificial chromosome
CCA1	CIRCADIAN CLOCK ASSOCIATED 1
CCT	Chaperonin containing TCP-1
CLF	CURLY LEAF
CLSM	Confocal laser-scanning microscope
CME	Cold memory element
COLDAIR	COLD ASSISTED INTRONIC NONCODING RNA
COLDWRAP	COLD OF WINTER-INDUCED NONCODING RNA FROM THE PROMOTER
COOLAIR	COLD INDUCED LONG ANTISENSE INTRAGENIC RNA
CRT	C-repeat element
DAP	DNA Affinity Purification
DRE	Dehydration-responsive element
E. coli	*Escherichia coli*
EE	Evening element
eGFP	Enhanced green fluorescent protein
EMS	Ethyl methanesulfonate
EMSA	Electrophoretic Mobility-Shift Assay

FIE	FERTILIZATION INDEPENDENT ENDOSPERM
FLC	FLOWERING LOCUS C
FPLC	Fast protein liquid chromatography
FRI	FRIGIDA
FT	FLOWERING LOCUS T
GUS	*β-glucuronidase*
H3K27me3	Histone H3 lysine 27 trimethylation
HOV1	HYPERACTIVATION OF VIN3 1
HSE	Heat shock element
HsfB2b	Heat shock transcription factor B2b
Hsfs	Heat Shock Factors
HSPs	Heat shock proteins
LFY	LEAFY
LHP1	LIKE HETEROCHROMATIN PROTEIN 1
LHY	LATE ELONGATED HYPOCOTYL
MSI1	MULTICOPY SUPRESSOR OF IRA1
NTL8	NAC WITH TRANSMEMBRANE MOTIF 1-LIKE 8
PHD	Plant Homeo Domain
PI	Propidium iodide
PRC2	Polycomb repressive complex 2
RVE	REVEILLE

RT-qPCR	Quantitative real-time polymerase chain reaction
SD	Standard deviation
SEM	Standard error of the mean
SOC1	SUPPRESSOR OF OVEREXPRESSION OF CO 1
SWN	SWINGER
TRiC	T-complex protein Ring Complex
TUB	Tubulin
UTR	Untranslated region
VAL1	VP1/ABI3-LIKE 1
VAL2	VP1/ABI3-LIKE 2
VIN3	VERNALIZATION INSENSITIVE3
VRN2	VERNALIZATION 2
WT	Wild-type
Y1H	Yeast one-hybrid
ZT	Zeitgeber time

Background

Floral transition

Plant development occurs in a series of developmental phases. There are three distinct phases during post-embryonic development: a juvenile vegetative phase, an adult vegetative phase, and a reproductive phase (Poethig, 1990). As the transition from the vegetative to reproductive phase is usually irreversible, correct timing of the transition to flowering is one of the most important developmental processes in plants (Chouard, 1960).

The timing of the transition to flowering is controlled by the integration of external environmental factors and internal factors (Kim, 2020). Signal transduction initiated by those factors is integrated by so-called floral integrator genes, such as *FT*, SOC1, and *LFY* (Simpson and Dean, 2002). As plants are sessile organisms, environmental signals are critical factors influencing the timing of the transition. Plants have established specific mechanisms to sense signals from environmental changes and optimize the onset of flowering to maximize fitness.

Vernalization

Vernalization, an acceleration of flowering after long-term winter cold, is one of the mechanisms that render plants to flower in a timely manner. *Arabidopsis* winter annuals exhibit a late-flowering phenotype but their flowering time is dramatically accelerated by vernalization. In contrast, summer annuals exhibit an early-flowering phenotype regardless

of cold treatment (Michaels and Amasino, 2000). Before winter, the winter annuals display strong expression of *FLOWERING LOCUS C* (*FLC*), a MADS-box transcription factor that represses precocious flowering, however, *FLC* is gradually suppressed according to the winter cold period, which allows plants to flower in the spring (Michaels and Amasino, 1999; Michaels and Amasino, 2000; Sheldon et al., 1999). Thus, the molecular mechanism of vernalization in *Arabidopsis* involves the suppression of *FLC* by winter cold. Suppression of *FLC* by long-term cold exposure involves epigenetic silencing which undergoes three critical stages; stages before, during, and after cold. During stage before cold, the proteins containing plant specific B3 DNA-binding domain, VP1/ABI3-LIKE 1 (VAL1) and VP1/ABI3-LIKE 2 (VAL2) directly bind to the, so called, RY elements, or Cold Memory Element (CME) in 1st intron of *FLC* (Qüesta Julia et al., 2016; Yuan et al., 2016). VAL1 and VAL2 are expressed constitutively, regardless of surrounding temperature, and establish the nucleation region for histone modification marks, which is a prerequisite for the next stage. In stage during cold, H3K27me3 mark, a repressive histone modification, is accumulated on the nucleation region of *FLC* chromatin by a protein complex called PHD-PRC2 complex. It includes the core components of PRC2, CURLY LEAF (CLF) and SWINGER (SWN), Arabidopsis homologues of H3K27 methyltransferase, VERNALIZATION 2 (VRN2), FERTILIZATION INDEPENDENT ENDOSPERM (FIE), the WD-40 domain protein MULTICOPY SUPRESSOR OF IRA1 (MSI1), and VERNALIZATION INSENSITIVE3 (VIN3), a protein bearing a Plant Homeo Domain (PHD) motif (De Lucia et al., 2008; Sung and Amasino, 2004; Wood et al., 2006; Yang et al., 2017). PHD-PRC2 complex recognizes previously depositioned

histone mark on CME and play a role in accumulation of H3K27me3 during vernalization period. Several non-coding RNAs such as *COOLAIR* (*COLD INDUCED LONG ANTISENSE INTRAGENIC RNA*), *COLDAIR* (*COLD ASSISTED INTRONIC NONCODING RNA*), and *COLDWRAP* (*COLD OF WINTER-INDUCED NONCODING RNA FROM THE PROMOTER*) were suggested to have role in *FLC* regulation during vernalization period through epigenetic regulation (Heo and Sung, 2011; Kim and Sung, 2017b; Kim et al., 2017; Marquardt et al., 2014). During stage after cold, accumulated H3K27me3 on the nucleation region spreads all over the gene body by LIKE HETEROCHROMATIN PROTEIN 1 (LHP1) and CLF, which causes the suppression stabilized (Sung et al., 2006; Yang et al., 2017).

Among the genes encoding the components of PHD-PRC2 complex, *VIN3* is the only gene induced by vernalization. Until exposed to cold temperature, *VIN3* is known to be expressed rarely and sparsely throughout the meristematic regions (Sung and Amasino, 2004). If plants are exposed to cold temperature, *VIN3* is induced within few hours, and its expression is gradually increased in proportion to the length of the cold period (Sung and Amasino, 2004). However, such induction is transient such that the *VIN3* level gets reverted to non-vernalized conditions if plants are returned to warm temperature (Sung and Amasino, 2004). The *vin3* mutant fails to respond to vernalization treatment, while constitutive expression of *VIN3* is not sufficient for vernalization response. Therefore, these results indicate that *VIN3* is a factor required, but not sufficient for vernalization (Sung and Amasino, 2004). In addition to the cold exposure, there are many additional

factors capable of inducing *VIN3*, such as hypoxic condition and nicotinamide treatment. But the molecular mechanism behind the *VIN3* induction is still not known yet (Bond et al., 2009a; Bond et al., 2009c).

Chapter 1

HEAT SHOCK TRANSCRIPTION FACTOR B2b Acts as a Transcriptional Repressor of *VIN3*, a Gene Induced by Long-Term Cold for Flowering

I. Introduction

There were many efforts to understand the molecular mechanism of the *VIN3* regulation over decades. For example, epigenetic regulation has been found to be a molecular basis for gradual *VIN3* expression over long-term cold exposure (Bond et al., 2009a; Bond et al., 2009c). In detail, bivalent modification of active (H3Ac, H3K36me3) and repressive (H3K27me3) histone marks on the *VIN3* chromatin is revealed as a molecular mechanism of *VIN3* induction (Bond et al., 2009a; Bond et al., 2009c). In addition, transcriptional regulators also have been reported recently. For example, NAC WITH TRANSMEMBRANE MOTIF 1-LIKE 8 (NTL8) has been identified as a direct regulator of *VIN3* expression through its accumulation during long-term cold exposure (Zhao et al., 2020). Moreover, two circadian clock regulators, CIRCADIAN CLOCK ASSOCIATED 1 (CCA1) and LATE ELONGATED HYPOCOTYL (LHY), were identified as direct regulators of *VIN3,* which presumably render diurnal rhythms of *VIN3* expression (Kyung et al., 2021). Such findings provide supportive explanations for *VIN3* regulation under multiple thermosensory pathways which was previously constructed by mathematical modeling of *VIN3* dynamics (Antoniou-Kourounioti et al., 2018; Hepworth et al., 2018). However, such findings are still insufficient to understand regulatory mechanism of *VIN3*.

Cellular proteins are easily damaged when exposed to various environmental stresses. To protect cellular proteins from such cellular stresses, most eukaryotic organisms, including plants, have evolved molecular chaperones (Richter et al., 2010). The most well-studied molecular chaperones are heat shock proteins (HSPs), which are induced by

myriads of cellular stresses as well as heat shock (Feder and Hofmann, 1999). The activation of HSPs, a general stress response in most eukaryotic organisms, is induced by a family of transcription factors known as Heat Shock Factors (Hsfs). Hsfs act as components of signal transduction that induce the expression of *HSPs* in response to a broad range of abiotic stresses (Wu, 1995). By binding to the cis-elements, called Heat Shock Elements (HSEs; inverted repeat of a basal element 5′-nGAAn-3′), which are conserved in the promoters of heat stress–inducible genes of all eukaryotes, Hsfs directly regulate the transcription of stress-responsive genes, including HSPs (Amin et al., 1988; Busch et al., 2005; Enoki and Sakurai, 2011). There are 21 *Hsf* genes in the *Arabidopsis* genome and are divided into three classes; A, B and C (Nover et al., 2001; Nover et al., 1996). Class A contains the motif (AHA motif) with activation activity, which is characterized by aromatic, large hydrophobic, and acidic amino acid residues (Nover et al., 2001). Class A proteins have been reported to act as positive regulators in response to a broad range of stress conditions in plants (Andrási et al., 2021; Busch et al., 2005; von Koskull-Döring et al., 2007). In contrast, class B and C proteins are considered transcriptional repressors, as they lack AHA motifs and contain the repressive R/KLFGV motif (Ikeda and Ohme-Takagi, 2009). Among the five class B proteins, HsfB1 and HsfB2b have been reported to act as transcriptional repressors, but positively regulate redundantly the acquired thermotolerance, an enhanced thermotolerance by prior heat treatment (Ikeda et al., 2011). Besides the acquired thermotolerance, HsfB1 and HsfB2b have been shown to negatively regulate pathogen resistance redundantly (Kumar et al., 2009), while HsfB2b alone has been shown to mediate abiotic stress responses of the

circadian clock (Kolmos et al., 2014).

In the present study, I identified *HsfB2b* as a novel repressor of *VIN3*. Further, I isolated one mutant, *hov1,* with hyperactive *VIN3* from a mutant pool that originated from the *pVIN3::GUS* reporter lines. The mutant was identified to carry a nonsense mutation in exon 1 of *HsfB2b*. Overexpression of *HsfB2b* rescued hyperactive *VIN3* in *hov1,* and HsfB2b was found to bind to the conserved HSEs located in the 5′-UTR of *VIN3*. Moreover, overexpression of *HsfB2b* in the late-flowering *FRI* Col background resulted in defects in the vernalization response, suggesting that *HsfB2b* negatively regulates the vernalization response.

II. Materials and Methods

1.2.1. Plant Materials and Growth Conditions

All *Arabidopsis thaliana* lines used were in the Columbia (Col-0) background except L*er* ecotype used to generate mapping population for map-based gene cloning. The wild-type, Col:*FRI*^{Sf2} (*FRI* Col) have been previously described (Lee et al., 1994). *hsfb1, hsfb2b*, and *hsfb1 hsfb2b* mutants have been previously described (Ikeda et al., 2011).

To produce *pHsfB2b::HsfB2b-eGFP* construct, the genomic sequences including 2,624bp upstream of the promoter and the whole coding sequence of *HsfB2b* were amplified by polymerase chain reaction. The fragment was cloned into *pCR2.1-TOPO* vector, then fused in-frame to *pCAMBIA1300* vector containing eGFP. The construct was transformed into the *hov1* mutant. To produce *pHsfB2b::Hsfb2b-myc*, the 3 kb *HsfB2b* promoter and the HsfB2b-coding sequence were amplified and fused in-frame to *pPZP221* vector containing 4xmyc (EQKLISEEDL). The construct was transformed into the indicated lines using Agrobacterium (*Agrobacterium tumefaciens*)-mediated *Arabidopsis* floral dip method (Clough and Bent, 1998).

The plants were grown under 16 h/8 h light/dark cycle (long day) or 8 h/16 h light/dark cycle (short day) (22 °C/20 °C) in a controlled growth room with cool white fluorescent lights (125 μmol m-2 sec-1). Vernalization treatments were done as previously described (Kim and Sung, 2013). Nonvernalized seedlings were grown for 11 d. For 10V, 20V, 40V treatments, seedlings were grown for 10, 9, 7 d under short days respectively after

germination, then transferred to vernalization chamber at 4 ℃. After vernalization treatment, seedlings were sampled or transplanted to the soil. Flowering time was measured by counting the number of rosette leaves when the first flower opened using at least 20 plants.

1.2.2. EMS mutagenesis and positional cloning

EMS mutagenesis was performed as previously described (Kim et al., 2006). For the positional cloning of the causative gene of *hov1*, F2 progenies were obtained by crossing *hov1* to L*er*. Mapping procedure was followed using 135 GUS-hypersensitive F2 plants and molecular makers described as previous reports (Hou et al., 2010; Lukowitz et al., 2000b). After rough mapping, the genomes of *hov1* and the parental *-0.2kb pVIN3_U_I::GUS* were sequenced and compared by illumina Hiseq2000 platform (illumina) sequencing to find mutant-specific SNPs in *hov1* using BGI services.

1.2.3. Histochemical GUS Staining

GUS staining was done following the standard methods that have been previously described (Shin et al., 2018). Photographs were taken with a USB digital-microscope Dimis-M (Siwon Optical Technology, South Korea).

1.2.4. Quantitative PCR

For real-time quantitative PCR, total RNA was isolated using TRIzol solution (Sigma). Four micrograms of total RNA were treated with recombinant DNase I (TaKaRa, 2270A)

to eliminate genomic DNA. cDNA was generated using the RNA with reverse transcriptase (Thermo scientific, EP0441) and oligo(dT). Quantitative PCR was performed using the 2x SYBR Green SuperMix (Bio-Rad 170-8882) and monitored by the CFX96 real-time PCR detection system. The relative transcript level of each gene was determined by normalization of the resulting expression levels compared to that of UBC. The primer sequences used in real-time RT-PCR analyses were shown in Supplementary Table S1.

1.2.5. Immunoblotting

For immunoblot assay, the seedlings of *pHsfB2b::HsfB2b-eGFP* were harvested at each time point. Total proteins were prepared from 100mg of harvested samples in protein extraction buffer (50mM Tris-Cl pH 7.5, 150 mM NaCl, 10 mM $MgCl_2$, 1 mM ethylenediaminetetraacetic acid (EDTA), 1% Triton X-100, 1 mM phenylmethylsulfonyl fluoride (PMSF), 1 mM 1,4-Dithiothreitol (DTT), 1X complete Mini, and EDTA-free protease inhibitor cocktail (Roche). Total proteins were separated by sodium-dodecyl sulfate (SDS)-PAGE. For phosphatase assay, total proteins were treated with or without alkaline phosphatase (Thermo scientific, EF0652) for 1 hr at 37°C, then separated by SDS-PAGE. The proteins were transferred to PVDF membranes (Amersham Biosciences) and probed with anti-GFP (Clontech, JL-8, 1:10,000 dilution) or anti-myc (Santa Cruz Biotechnology, sc-40, 1:10,000 dilution) antibodies overnight at 4 °C. The samples were then probed with horseradish peroxidase-conjugated anti-mouse IgG (Cell Signaling, #7076, 1:10,000 dilution) antibodies at room temperature. The signals were detected using ImageQuant LAS 4000 (GE Healthcare) with WesternBrightTM Sirius ECL solution

(Advansta).

1.2.6. Confocal laser-scanning microscopic (CLSM) analysis

For microscopic observations, 5-day-old *pHsfB2b::HsfB2b-eGFP* seedlings with or without 5 days of additional cold treatment were prepared. Seedlings were pre-stained with propidium iodide (PI), mounted on glass slides, and observed using confocal microscopy (LSM700, Zeiss) following the manufacturer's instructions.

1.2.7. Promoter Analysis

The promoter sequences from plant species were downloaded from GBrowse at Phytozome (www.phytozome.net). The following *VIN3* loci (At5g57380) were identified using BLAST Search: *Arabidopsis lyrata* (AL8G33360), *Boechera stricta* (Bostr.26833s0518) and *Capsella rubella* (Carub.0008s1790). The sequences were processed and aligned in T-coffee (tcoffee.crg.eu)

1.2.8. Yeast one-hybrid assay

Yeast one-hybrid assay was performed following the previously described method with some modifications (Kyung et al., 2021). For the reporter constructs used in the Y1H analysis, four tandem repeats containing HSE_{VIN3} (5′-TTAGAAACATCTAGAAAAAACAAA-3′) were cloned into the *pHisi* vector. For the effector, the coding sequences of *HsfA1a, HsfA2, HsfA4a, HsfA6a, HsfA8, HsfB1, HsfB2b* and *HsfC1* were cloned in-frame with the sequences of the GAL4 activation domain into

pGADT7. The Y1H assay was performed following the manufacturer's instructions. In brief, the reporter construct and effector construct were transformed into yeast strain YM4271. The yeast cells were spotted on synthetic define (SD) medium lacking Leu, Ura, and His, with or without 5-mM 3-amino-1,2,4-triazole (3-AT).

1.2.9. Preparation of fusion protein and EMSA

Coding sequence encoding DNA binding domain of *HsfB2b* was fused to *pMAL-c2* vector. The MBP and MBP-HsfB2b^{DBD} proteins were expressed in *Escherichia coli* BL21 strain according to the manufacturer's instructions using the pMAL Protein Fusion and Purification System (#E8200; New England BioLabs) and purified using MBPtrap HP column (Cytiva) attached to ÄKTA FPLC system (Cytiva). The Cy5-labeled probes (HSE, 5′-Cy5- TTTCCTCCTTA**G**A**A**AC**A**T**C**TA**G**A**A**AAAACAAAAGGAGAGA-3′; mHSE, 5′-Cy5- TTTCCTCCTTA**A**A**A**AC**A**T**T**TA**A**A**A**AAAACAAAAGGAGAGA -3′) and unlabeled competitors were generated by annealing 40 bp-length oligonucleotides. 5 μM of purified proteins and 100 nM of Cy5-labeled probe were incubated at room temperature in binding buffer (10 mM Tris-HCl (pH 7.5), 50 mM NaCl, 1 mM EDTA, 5% glycerol and 5 mM DTT). For competition assay, 100-fold molar excess of each competitor was added to the reaction mixture before incubation. The reaction mixtures were resolved by electrophoresis through 6% polyacrylamide gel in 0.5X Tris-borate EDTA buffer at 100 V. The Cy5 signals were detected using WSE-6200H LuminoGraph II (ATTO).

1.2.10. Chromatin Immunoprecipitation

Approximately 4 g of whole *Arabidopsis* seedlings were collected and cross-linked using 1% (v/v) formaldehyde for 10 min and quenched by 0.125 M glycine for 5 min under vacuum. Seedlings were rinsed with distilled water, frozen in liquid nitrogen, and grounded to fine powder. The powder was resuspended in Nuclei Isolation Buffer [1 M hexylene glycol, 20 mM PIPES-KOH (pH 7.6), 10 mM $MgCl_2$, 15 mM NaCl, 1 mm EGTA, 1 mM PMSF, complete protease inhibitor mixture tablets (Roche)], and *Arabidopsis* nuclei were isolated by centrifugation, lysed by Nuclei Lysis Buffer [50 mM TRIS-HCl (pH 7.4), 150 mM NaCl, 1% Triton X-100, 1% SDS], and sonicated using a Branson sonifier to shear the DNA. Sheared chromatin solution was diluted 10-fold with a ChIP Dilution Buffer [50 mM TRIS-HCl (pH 7.4), 150 mM NaCl, 1% Triton X-100, 1 mM EDTA]. The beads, chromatins and GFP-Trap A beads (gta-20, ChromoTek, Planegg, Germany) or Binding control agarose (bab-20) were mixed and incubated for overnight at 4 °C. Beads were washed with ChIP dilution buffer for 4 times and DNA extraction was performed using Chelex 100 resin following the manufacturer's instruction. qPCR analysis was performed using 1% input and immunoprecipitated DNA.

1.2.11. Accession Numbers

The Arabidopsis Genome Initiative locus identifiers for the genes discussed in this chapter are as follows: *VIN3* (At5g57380), *FLC* (At5g10140), *FRI* (At4g00650), *HsfA1a* (At4g17750), *HsfA2* (At2g26150), *HsfA3* (At5g03720), *HsfA4a* (At4g18880), *HsfA6a*

(At5g43840), *HsfA8* (At1g67970), *HsfB1* (At4g36990), *HsfB2a* (At5g62020), *HsfB2b* (At4g11660), *HsfC1* (At3g24520), *CCA1* (At2g46830), *LHY* (At1g01060), and *PP2A* (At1g13320).

1.2.12. List of primers used in this chapter

Oligo Name	Primer Sequence (5'-3')	Usage
PP2A-F	TATCGGATGACGATTCTTCGTGCAG	qRT-PCR
PP2A-R	GCTTGGTCGACTATCGGAATGAGAG	qRT-PCR
VIN3-F	GTTTCAGGACAAGGTGACAAG	qRT-PCR
VIN3-R	TTCCCCTGAGACGAGCATTC	qRT-PCR
HSFB2b-F	CAGCTCAATACTTACGGATTTCG	qRT-PCR
HSFB2b-R	CCGTTGAATATCCCGAAGCAG	qRT-PCR
FLC-F	AGCCAAGAAGACCGAACTCA	qRT-PCR
FLC-R	TTTGTCCAGCAGGTGACATC	qRT-PCR
HSFB2b-GFP-F	CCATGGACCAAACAAACTTAATCAAGTG	Construct
HSFB2b-GFP-R	CCATGGTTCCGAGTTCAAGCCACGA	Construct
HSFB2b-myc-F	GTCGACACCAAACAAACTTAATCAAGTG	Construct
HSFB2b-myc-R	GTCGACTTTTCCGAGTTCAAGCCAC	Construct
$4xHSE_{VIN3}$	GCGAATTCTTAGAAACATCTAGAAAAAACAAATTAGAAA CATCTAGAAAAAACAAATTAGAAACATCTAGAAAAAACA AATTAGAAACATCTAGAAAAAACAAAACTAGTCG	Y1H BD
HSFA1A-CDS-F	GCCCGGGAATGTTTGTAAATTTCAAATACTTC	Y1H AD
HSFA1A-CDS-R	CGCTCGAGCTAGTGTTCTGTTTCTGATG	Y1H AD
HSFA2-CDS-F	GCCCGGGAATGGAAGAACTGAAAGTGG	Y1H AD
HSFA2-CDS-R	CGCTCGAGTTAAGGTTCCGAACCAAGAAAAC	Y1H AD
HSFA3-CDS-F	CGCCATATGAGCCCAAAAAAAGATGCTG	Y1H AD
HSFA3-CDS-R	CGCTCGAGCTAAGGATCATTCATTGGC	Y1H AD
HSFA4A-CDS-F	GCCCGGGAATGGATGAGAATAATCATGGA	Y1H AD
HSFA4A-CDS-R	CGCTCGAGTCAACTTCTCTCTGAAGAAGTC	Y1H AD

HSFA6A-CDS-F	GCCCGGGAATGGATTATAACCTTCCAATTC	Y1H AD
HSFA6A-CDS-R	CGCTCGAGTTATATAAAATGTTCCACTAAATC	Y1H AD
HSFA8-CDS-F	GCCCGGGAATGGTGAAATCGACGGAC	Y1H AD
HSFA8-CDS-R	CGCTCGAGCTATTCATTTGAAGCCAGC	Y1H AD
HSFB1-CDS-F	GCCCGGGAATGACGGCTGTGACGGC	Y1H AD
HSFB1-CDS-R	CGCTCGAGTTAGTTGCAGACTTTGCTGC	Y1H AD
HSFC1-CDS-F	CGCCATATGGAGGACGACAATAGTAAC	Y1H AD
HSFC1-CDS-R	CGCGAGCTCCTAAAAGCCACCTCGAAACAG	Y1H AD
HSFB2B-CDS-F	GTCGACATGCCGGGGGAACAAAC	Y1H AD
HSFB2B-CDS-R	GTCGACTCATTTTCCGAGTTCAAGCC	Y1H AD
HSE_{VIN3}-F	GAGGGTTTCCTCCTTAGAAACATCTAGAAA	EMSA target (HSE_{VIN3})
HSE_{VIN3}-R	TTTCTAGATGTTTCTAAGGAGGAAACCCTC	EMSA target (HSE_{VIN3})
HSEcontrol-F	ATTTACTCTCTGAGTATTTGTTTATTTTAA	EMSA target (negative)
HSEcontrol-R	TTAAAATAAACAAATACTCAGAGAGTAAAT	EMSA target (negative)
VIN3_A-F	TAACGGAACTTCTCATTTTCATATG	ChIP-qPCR
VIN3_A-R	TTTGCATCATCTACGTTAATTTGTG	ChIP-qPCR
VIN3_B-F	TCGAACATATAGTAGTGAGTCATA	ChIP-qPCR
VIN3_B-R	CGTTGGAAATATCTTCACGTGC	ChIP-qPCR
VIN3_C-F	GTGTTCTTCATCATCGTAAGTG	ChIP-qPCR
VIN3_C-R	GCCGAGATCCGATTTCACAC	ChIP-qPCR
VIN3_D-F	AGTACACTGGTCTTAACAAACC	ChIP-qPCR
VIN3_D-R	CGTATCATCGCATCCAAGCG	ChIP-qPCR

Table 1. List of primers used in this chapter

III. Results

1.3.1. Isolation and characterization of the mutant showing hyperactivation of *VIN3*, *hov1*

To identify upstream regulators of *VIN3*, the GUS reporter line (-0.2kb *pVIN3_U_I::GUS*) (Kyung et al., 2021) was mutagenized with ethyl methanesulfonate (EMS). A total of 3,412 M1 lines were generated and their seeds were harvested as M2 seeds. Approximately 25 M2 seedlings from each line were grown at room temperature for 10 days, and transferred to the cold chamber for 3 days, then analyzed for GUS staining. Throughout the screening, the first and second true leaves of the M2 seedlings were used for GUS staining when seedlings produced more than 5 leaves. One mutant showing the hyperactivation of GUS was identified and initially named *hov1*. Compared to the parental line, which showed a very weak GUS signal after 3 days of cold exposure (3V), *hov1* showed an enhanced GUS signal with the same treatment (Fig. 1A). Consistent with the results of the GUS assay, endogenous *VIN3* transcript levels were enhanced in the mutant after 3V (Fig. 1B). The mutant phenotype was not found in the F1 plants when backcrossed to the parental line, and the phenotype was segregated by approximately 3:1 (81 wild-type vs 29 mutants) in F2 population. Such results indicate that the mutant phenotype is completely recessive and is caused by a mutation in a single locus. Thereafter, I performed a time course analysis of *VIN3* levels in *hov1* for vernalization treatment. As shown in Fig. 1C, *hov1* plants displayed higher levels of *VIN3* than the controls without vernalization treatment, indicating that

HOV1 is necessary to completely suppress *VIN3* at room temperature. The *hov1* plants also had higher levels of *VIN3* throughout the vernalization time course and the mutant had higher levels of *VIN3* than the control plants after returning to room temperature for 5 days (40VT5). These results indicate that *HOV1* is required for the suppression of *VIN3* under all conditions.

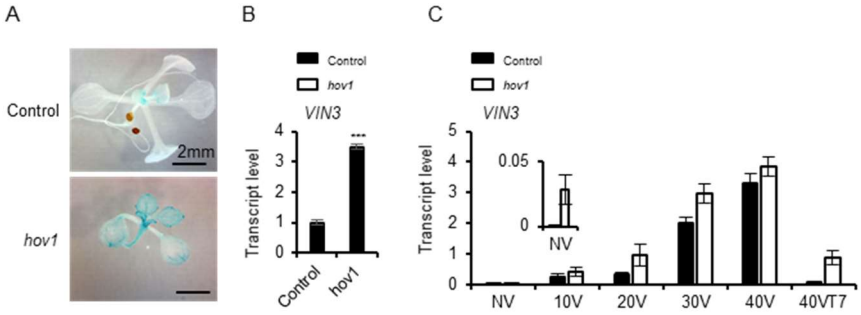

Figure 2. Isolation and characterization of the vernalization hypersensitive mutant, *hov1*.

(A-B) Characterization of the *hov1* mutant. Seedlings of control (*-0.2kb pVIN3_U_I::GUS*) and *hov1* were grown in room temperature for 10 days and analyzed after 3 days of cold treatment.

(A) Images of representative seedlings after GUS staining. (Scale bars, 2 mm)

(B) Endogenous *VIN3* transcript level in control and *hov1*. Transcript levels were normalized to *PP2A*. Data are shown as means ± SEM for three replicates. Asterisks indicate a significant difference compared to the control (Student's t test; ***P<0.001).

(C) Time course analysis of *VIN3* levels during vernalization. NV, Non-vernalized; 10V, 20V, 30V, and 40V, 10 d, 20 d, 30 d, and 40 d vernalized respectively; 40VT7, 7 d grown at room temperature after 40V. Transcript levels were normalized to *PP2A*. Data are shown as means ± SEM for three replicates. Inset in (C) is enlarged for NV.

1.3.2. Identification of causative mutation of increased *VIN3* expression in *hov1*

To identify the causative mutation, *hov1* was crossed with L*er* for positional cloning. A total of 156 F2 plants with enhanced GUS signals in the leaves were selected for mapping analysis. I mapped the mutation to the 590 kilobase pair interval on chromosome 4, which contained 142 genes (Fig. 2A and B). The genomes of *hov1* and parental *-0.2kb pVIN3_U_I::GUS* were sequenced using the Illumina sequencing method for comparison. Analysis of the sequence data revealed nine potentially disruptive point mutations, including one mutation within the At4g11660 gene (G to A, causing a nonsense mutation from Trp89 to the stop codon) (Fig. 2C). At4g11660 encodes the class B heat shock transcription factor, HEAT SHOCK TRANSCRIPTION FACTOR B2b (HsfB2b).

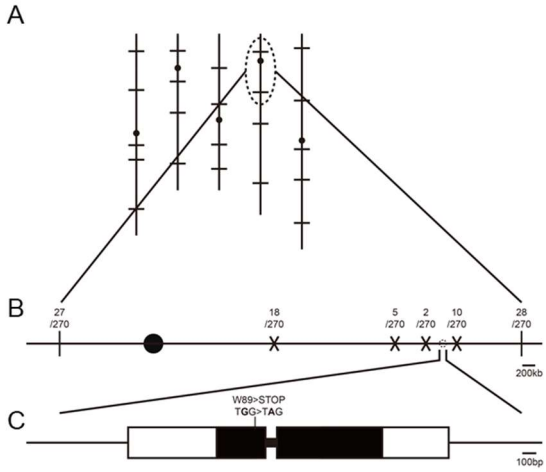

Figure 3. Simplified map-based cloning procedure for *hov1*.

(A) Schematic of the *Arabidopsis* chromosomes. Vertical lines represent five *Arabidopsis* chromosomes, horizontal lines represent molecular markers, and black circles indicate centromeres. (B) Genetic intervals and molecular markers. The uppermost numbers are the number of recombinants among the 270 chromatids analysed. Vertical lines and X-signs represent molecular markers. (C) Schematic of the *HsfB2b* structure. Black bars indicate exons and white boxes and lines represent untranslated regions and introns, respectively.

1.3.3. *HsfB2b* acts as a transcriptional repressor of *VIN3*

To verify that *HsfB2b* is the causative gene of the upregulation of *VIN3* level in *hov1*, the *VIN3* level in the T-DNA-inserted mutant, *hsfb2b-1* was examined. As expected, *hsfb2b-1* had higher levels of *VIN3* than wild-type Col-0 under non-vernalized conditions (Fig. 3A). Previously, *HsfB2b* was reported to display functional redundancy with *HsfB1* instead of *HsfB2a* for acquired thermotolerance, although the sequence of *HsfB2b* had higher homology with that of *HsfB2a* than *HsfB1* (Ikeda et al., 2011). To determine whether *HsfB2b* is functionally redundant with *HsfB1* for the vernalization response, *VIN3* levels among the *hsfb2b, hsfb1,* and *hsfb1 hsfb2b* mutants were compared. The *hsfb1* mutant displayed similar levels of *VIN3* to the wild-type under all conditions. However, the *hsfb1 hsfb2b* double mutant did not show any difference compared with *hsfb2b* in *VIN3* levels (Fig. 3A). Such finding suggests that *HsfB1* is not functionally redundant to *HsfB2b*, at least for *VIN3* regulation.

Finally, I introduced *HsfB2b::HsfB2b-myc* into the *hov1* mutant to determine whether *HsfB2b* can rescue the *hov1* mutation. The transcript levels of *HsfB2b* were found to be overexpressed in all obtained transgenic lines (Fig. 3C, Fig. 9A, and Fig. 10A). Here, I used two representative lines of *HsfB2b:HsfB2b-myc hov1,* #1, and #2. As expected, the phenotype of the GUS signal in *hov1* was complemented by *HSFB2b::HSFB2b-myc,* such that the GUS signal was barely detected after 3 d of cold exposure (Fig. 3B). Moreover, the endogenous *VIN3* transcript levels in both transgenic lines were lower than those in Col, as well as the *hov1* mutant, whereas *HsfB2b* transcript levels in the transgenic lines

were higher than those in Col (Fig. 3C and D). Taken together, my results indicate that *HsfB2b* is a causative gene that reduces *VIN3* level in *hov1* and acts as a transcriptional repressor of *VIN3*.

In a previous report, *VIN3* was found to gradually increase by long-term cold exposure from the first day of cold treatment (Bond et al., 2009c). Thus, whether HsfB2b affects *VIN3* expression during the initial stage of vernalization treatment was determined (Fig. 3E and F). As shown, *hsfb2b* caused strong derepression of *VIN3* from the initial phase, and the effect was strongest after 3 h of cold treatment. Of note, the derepression effect of *hsfb2b* is stronger at short-term cold and 40VT1 (1 d at room temperature after returning from 40 days of vernalization treatment) than during vernalization treatment (Fig. 3E and F).

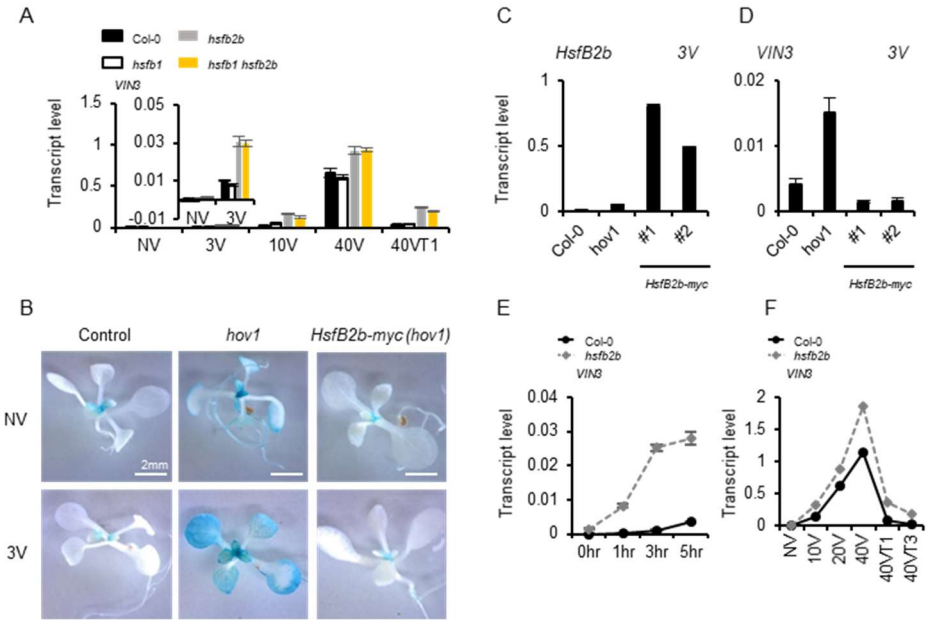

Figure 4. HsfB2b acts as a transcriptional repressor of *VIN3*.

(A) *HsfB1* is not functionally redundant to *HsfB2b* for the *VIN3* regulation. *VIN3* transcript levels in Col-0, *hsfb1, hsfb2b,*and *hsfb1 hsfb2b* during vernalization were determined by RT-qPCR. NV, Non-vernalized; 3V, 10V, 40V, 3, 10, and 40 d vernalized respectively; 40VT1, 1 d growth at RT after 40V. Transcript levels were normalized to *PP2A*. Data are shown as means ± SEM for three replicates. Inset in (A) is enlarged for NV and 3V.

(B-D) Complementation of *hov1* with *pHsfB2b::HsfB2b-myc*. (B) GUS staining for NV or 3V seedlings of parental line, *hov1*, and *pHsfB2b::HsfB2b-myc hov1* transgenic line. Images of representative seedlings after GUS staining are shown. (C) *HsfB2b* or (D) *VIN3* transcript levels in 3V Col-0, *hov1*, and two representative transgenic lines of *pHsfB2b::HsfB2b-myc hov1*. Transcript levels were normalized to *PP2A*. Data are shown

as means ± SD for three replicates.

(E-F) Effects of *hsfb2b* mutation on the *VIN3* levels. *VIN3* levels in Col-0 and *hsfb2b*, as determined by RT-qPCR after (E) short-term cold treatment (0 hr, 1 hr, 3 hr, 5 hr) or (F) long-term vernalization (NV, 10V, 20V, 40V, 40VT1, 40VT3). Transcript levels were normalized to *PP2A*. Data are shown as means ± SD for three replicates.

1.3.4. Effects of vernalization on HsfB2b

Hsfb2b expression is well-known to be induced by heat shock treatment to suppress hyperactivated heat shock-responsive genes (Ikeda et al., 2011). However, the effect of long-term cold treatment on *Hsfb2b* is unknown. Before vernalization treatment, the basal level of *Hsfb2b* was detected as previously reported (Fig. 4A). During the long-term cold treatment, such levels of *Hsfb2b* did not change significantly. In contrast, a slight increase of *Hsfb2b* was observed when returned to room temperature (Fig. 4A). HsfB2b protein levels using *pHsfB2b::HsfB2b-eGFP* transgenic lines during vernalization treatment was also checked (Fig. 4B). However, the protein levels were not found to be significantly affected by vernalization treatment. Nonetheless, vernalization treatment caused retarded migration of HsfB2b-eGFP proteins on polyacrylamide gel from the initial phase, suggesting that HsfB2b undergoes post-translational modifications, such as phosphorylation by cold (Fig. 4B). After returning to room temperature, such modifications may have been rapidly erased as 40VT1 displayed the same protein pattern as NV.

To confirm whether the retarded migration of HsfB2b protein is due to the phosphorylation, phosphatase assay was conducted using total protein extracted from vernalized or non-vernalized *pHsfB2b::HsfB2b-myc* seedlings. Subsequent immunoblot assay showed that the retarded migration of HsfB2b-myc from vernalized seedlings was abolished by phosphatase treatment, while migration of HsfB2b-myc from non-vernalized seedling was not changed by the treatment (Fig. 4C). These results indicate that retarded migration of

HsfB2b-myc from vernalized seedlings was due to the phosphorylation. Previously, HsfB2b has been reported as a protein that phosphorylated by SnRK2 kinases, which is activated by plant hormone abscisic acid (ABA) (Minkoff et al., 2015). Considering that ABA is known to play a role in broad range of stress response including cold response (Heino et al., 1990; Lång et al., 1989), the phosphorylation of HsfB2b is probably involved in stress responses triggered by ABA.

As the cellular localization of other Hsf is changed by post-translational modification (Evrard et al., 2013), whether cold treatment can change that of HsfB2b was checked (Fig. 4D and E). Using the *pHsfB2b::HsfB2b-eGFP* transgenic lines, the root tissue before and after 5 days of cold was observed. In both cases, GFP signals were observed in the nucleus, indicating that neither cold treatment nor phosphorylation altered the cellular localization of HsfB2b. This result is consistent with the fact that the protein sequence of HsfB2b has a nuclear localization signal (NLS), but lacks a nuclear export signal (NES) motif (Nover et al., 2001). Taken together, *HsfB2b* is neither transcriptionally induced nor is the subcellular localization of the proteins altered by vernalization treatment.

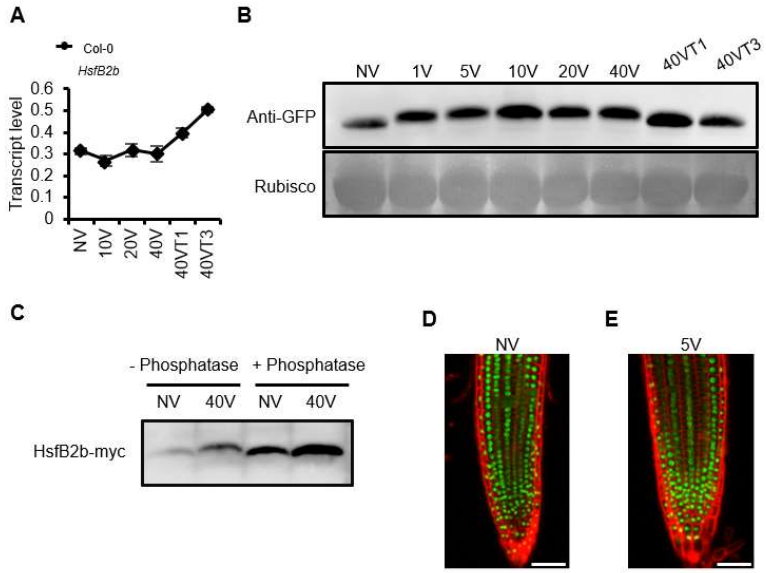

Figure 5. Characterization of *Hsfb2b* during cold and vernalization treatment.

(A) Effect of vernalization on the transcript levels of *HsfB2b*. Col-0 seedlings were vernalized before extracting total RNA for RT-PCR. Expression levels were normalized to *PP2A*. Data are shown as means ± SD for three technical replicates.

(B) Immunoblot analysis of HsfB2b-eGFP protein extracted from vernalized seedlings of *pHsfB2b::HsfB2b-eGFP*. Rubisco was used as a loading control. NV, Non-vernalized; 1V, 5V, 10V, 20V and 40V, 1 d, 5 d, 10 d, 20 d and 40 d vernalized, respectively; 40VT1, 40VT3, 1 d and 3 d grown at RT after 40V, respectively.

(C) Phosphorylation in HsfB2b under vernalization treatment. Total protein extracts were extracted from vernalized and non-vernalized seedlings of *pHsfB2b::HsfB2b-myc*. Extracts were treated with or without phosphatase for 1 hour at 37°C, and then separated

by SDS-PAGE and immunoblot was performed using anti-myc andibody. NV, Non-vernalized; 40V, 40 d vernalized.

(D-E) Confocal images of roots from NV or 5V plants expressing *pHsfB2b::HsfB2b-eGFP*. (Scale bars, 50 μm) Five days-old *Arabidopsis* seedlings without (NV) or with 5 d cold exposure (5V) were harvested and counterstained with propidium iodide.

1.3.5. *HsfB2b*-mediated *VIN3* repression is independent to *HsfB2b*-mediated circadian clock regulation

VIN3 expression is reported to show a circadian rhythm and *HsfB2b* acts as a negative regulator of the circadian clock regulator, *PSEUDO RESPONSE REGULATOR7* (*PRR7)* (Hepworth et al., 2018; Kolmos et al., 2014; Kyung et al., 2021). Thus, whether the *VIN3* rhythm was affected by *hsfb2b* during cold treatment was verified. Although the amplitude of the circadian rhythm was increased by *hsfb2b* mutation due to the increase in *VIN3* level, the rhythmic pattern was not significantly different (Fig. 5A and 5B). Therefore, *HsfB2b* seems to constitutively repress *VIN3,* and this repression is independent of the *HsfB2b*-regulated circadian clock.

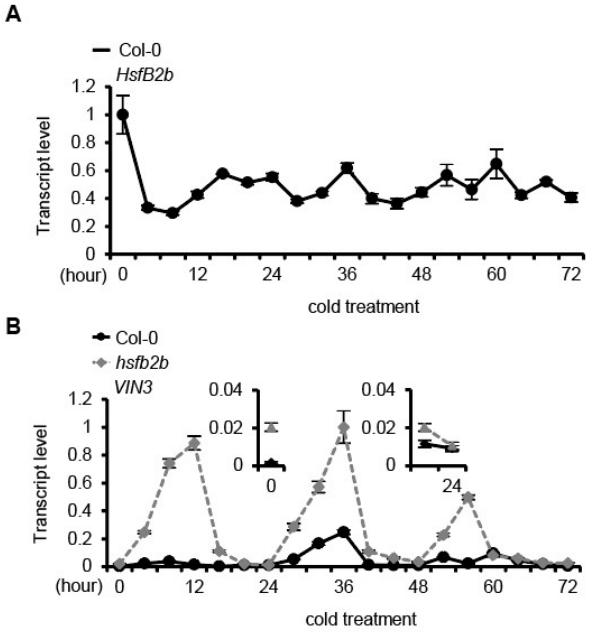

Figure 6. Effect of early phase of vernalization on the rhythmic expression.

(A) Effect of early phase of vernalization on the rhythmic expression of *HsfB2b* in Col-0. Expression levels were normalized to *PP2A*. Data are shown as means ± SD for three replicates.

(B) Effect of *hsfb2b* mutation on the rhythmic expression of *VIN3*. *VIN3* levels during early phase of vernalization were analyzed using seedlings of Col-0 and *hsfb2b* collected at 4-hour intervals over 72 hours in LD at 4°C. The x-axis indicates exposed time to cold. Data are shown as means ± SD for three replicates.

1.3.6. HSE exists in 5′-UTR of *VIN3*

Heat shock transcription factors regulate a variety of genes by directly binding to the HSE in the promoters (Amin et al., 1988; Busch et al., 2005). Consistently, HSE was detected near the *VIN3* promoter, approximately 40 bp downstream of the transcription start site (Fig. 7A). In addition, the HSE was highly conserved among the *VIN3* orthologs from Brassicaceae species (*Arabidopsis thaliana*, *Arabidopsis lyrata, Boechera stricta*, and *Capsella rubella*) (Fig. 6A). Therefore, whether HsfB2b directly binds to the 5′-UTR of *VIN3* was determined. In *silico* analyses using the DNA affinity purification (DAP)-seq database (O'Malley et al., 2016) showed that several heat shock transcription factors bind to the 5′-UTR of *VIN3*, where HSE is located (Fig. 6B).

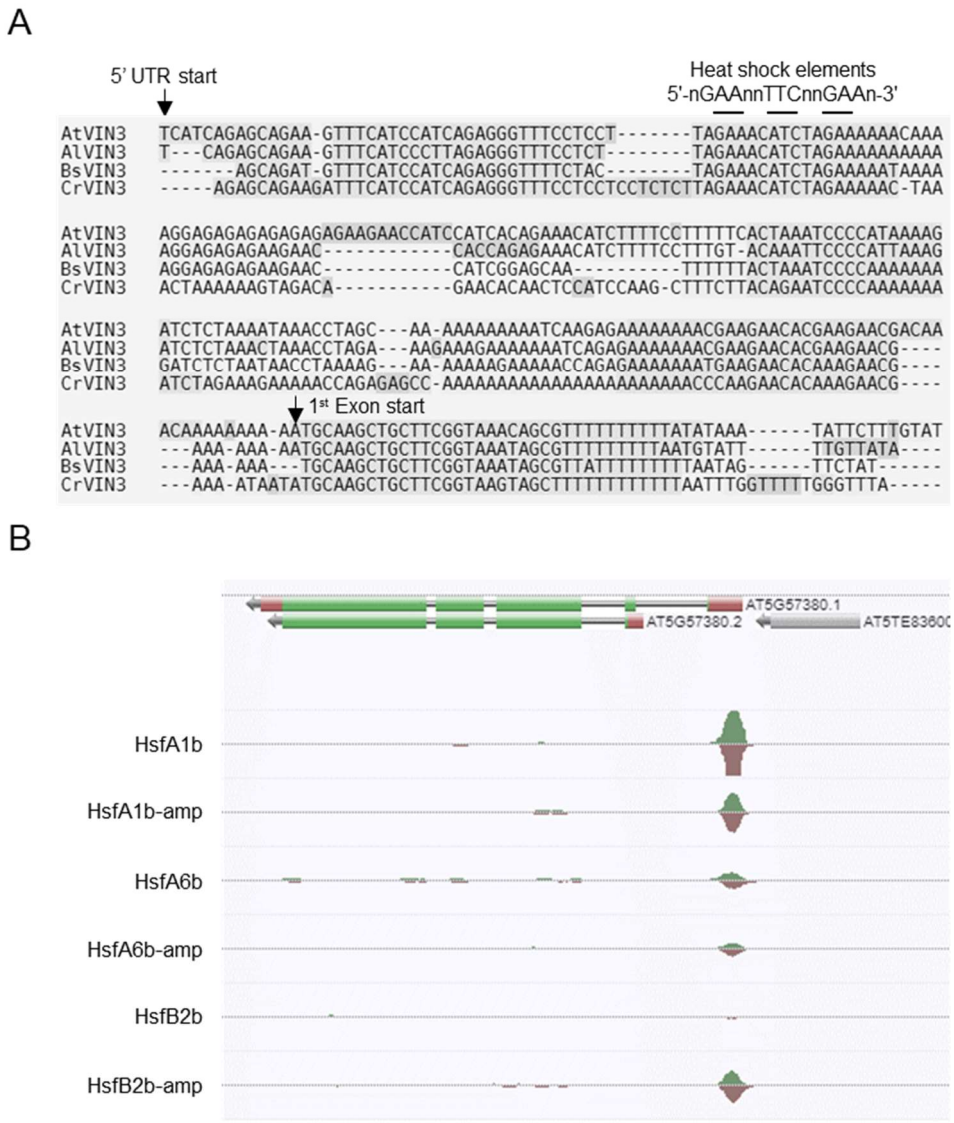

Figure 7. HSE exists in 5′-UTR of *VIN3*.

(A) HSE_{VIN3} is conserved among *Arabidopsis* relatives. Multiple sequence alignment of the *VIN3* orthologs from the *Brassica* family. The region shown is +1 to +269 bp (relative

to the transcription start site). At, *Arabidopsis thaliana*; Al, *Arabidopsis lyrata*; Bs, *Boechera stricta*; Cr, *Capsella rubella*. Shading represents the degree of similarity.

(B) DNA Affinity Purification (DAP)-seq reveals *in vitro* binding of HsfB2b to *VIN3.* DAP-seq results revealed enrichment of the Hsf proteins at the *VIN3* locus obtained from the Plant Cistrome Database (http://neomorph.salk.edu/dev/pages/shhuang/dap_web/pages/index.php (O'Malley et al., 2016). The top bars represent the structures of the alternatively spliced forms of the *VIN3* transcript. The green, grey, and red bars indicate exons, introns, and UTRs of *VIN3*, respectively. The peaks below represent the positions of Hsf enrichment. Hsf-amp: Amplification of DAP-seq results.

1.3.7. HsfB2b directly regulates *VIN3* repression

I proceeded to assess whether HsfB2b bound to HSE_{VIN3} using yeast one-hybrid assay (Fig. 7B). Among the nine Hsf proteins analyzed, HsfA1, HsfA6a, HsfB1, HsfB2b, and HsfC1 were found to interact with HSE_{VIN3}. To confirm *in planta* binding, I also performed ChIP-qPCR using transgenic *pHsfB2B::HsfB2b-eGFP,* grown under long days without cold treatment (Fig. 7C). HsfB2b-eGFP proteins were found to be enriched in the promoter region near the HSE location even without cold treatment, which is consistent with the elevated *VIN3* level in *hsfb2b*. EMSA was also conducted to assess whether HsfB2b specifically binds to HSE_{VIN3} DNA element *in vitro*. The purified recombinant protein, MBP-HsfB2b^{DBD}, DNA binding domain of HSFB2b fused with maltose binding protein (MBP), from *E. coli* indeed binds the HSE_{VIN3} probe but fails to bind the mutated version of HSE_{VIN3} probe (Fig. 7D). Taken together, these data strongly support the hypothesis that HsfB2b directly regulates *VIN3* repression.

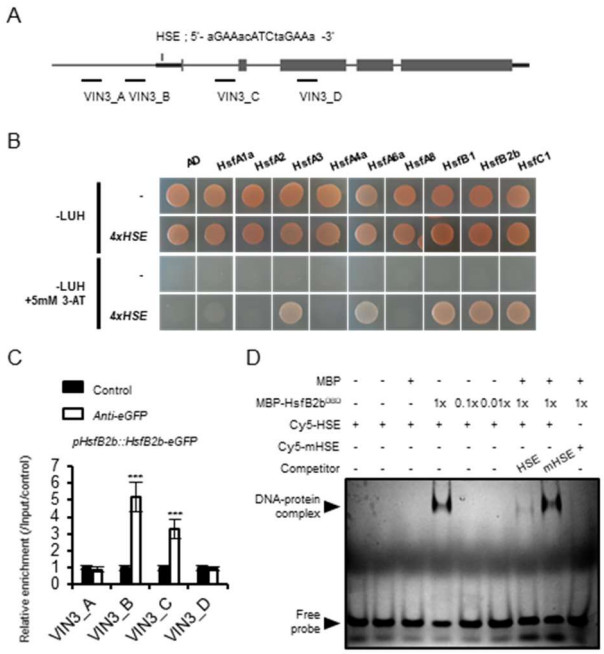

Figure 8. HsfB2b directly binds to the HSE on the *VIN3* locus.

(A) Schematic diagram of *VIN3* with description of HSE_{VIN3} sequence and PCR amplicons indicated as letters A-D used for ChIP-qPCR. Black bars indicate untranslated region, grey boxes and lines represent exons and introns, respectively.

(B) Yeast one-hybrid assay between heat shock factors and HSE_{VIN3} cis-element. As DNA baits, four tandem copies of the 24-bp sequences containing HSE_{VIN3} were inserted into the vector and used as the reporter construct. The CDS of HsfA1a, HsfA2, HsfA3, HsfA4a, HsfA6a, HsfA8, HsfB1, HsfB2b, HsfC1 was cloned into *pGADT7* and used as effector construct. GAL4 AD alone (AD) was used as control. The effecter and reporter constructs were co-transformed into the yeast strain AH109. Representative growth status

of yeast cells is shown on Synthetic Defined (SD)–LUH medium, with or without 5 mM 3-AT. –LUH, SD medium without Leu, Ura, His; -LUH +5 mM 3-AT, SD medium without Leu, Ura, His but containing 5 mM 3-Amino-1,2,4-triazole.

(C) ChIP-qPCR showing the enrichment of HsfB2b-eGFP. Chromatin of transgenic line expressing *pHsfB2b::HsfB2b-eGFP* was immunoprecipitated using control bead or GFP-trap beads. Histograms show mean values ± SEM (*n*=2 biological replicates, each each biological replicate is an average value of three replicates) for enrichment calculated by percent input normalized against control. Asterisks indicate significant difference compared to the control (Student's t test; ***P<0.001).

(D) EMSA of the binding of the. recombinant MBP-HsfB2b^{DBD} to HSE$_{VIN3}$ sequence. Recombinant purified MBP-HsfB2b^{DBD} or MBP was incubated with 40-bp of flanking sequences of HSE$_{VIN3}$ probes (HSE) labeled using Cy5. Same region with mutations in the HSE$_{VIN3}$ was used as another probe (mHSE). Unlabeled competitor DNA (100x molar excess) was added to each reaction, as indicated.

1.3.8. *hsfb2b* mutation does not change vernalization response under normal condition

To analyze the effect of *hsfb2b* on vernalization response, the *hsfb2b* mutation was introduced into *FRI* Col, a vernalization-sensitive line, by genetic cross (Lee et al., 1994). As shown in Fig. 8, the flowering time of *hsfb2b FRI* was similar to that *of FRI* Col, although *VIN3* levels were higher in *hsfb2b FRI* than in *FRI* Col throughout the time course of vernalization treatment (Fig. 8A-C). Consistently, the *FLC* levels were not significantly different between the two genotypes throughout vernalization treatment (Fig. 8D). Thus, the increased levels of *VIN3* in *hsfb2b* may not alter the vernalization response under normal growth conditions. Such findings suggest that *VIN3* levels in the *FRI* Col are sufficient for a proper vernalization response.

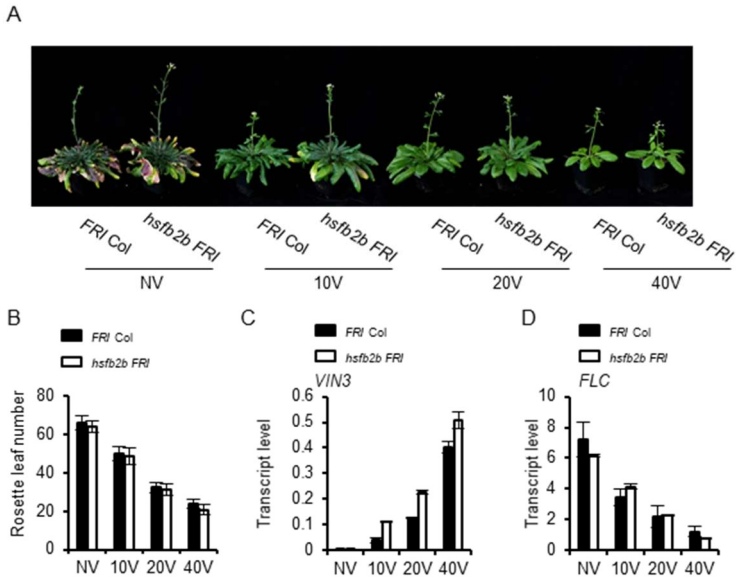

Figure 9. *hsfb2b* mutation does not change vernalization response under normal condition.

(A) Photographs of *FRI* Col and *hsfb2b FRI* without (NV) or with 10 d (10V), 20 d (20V), 40 d (40V) of vernalization. (B) Flowering time of *FRI* Col and *hsfb2b FRI* after vernalization. Flowering time was measured as the number of primary rosette leaves formed when bolting. Data are shown as means ± SD.

(C-D) *VIN3* or *FLC* transcript levels in *FRI* Col and *hsfb2b FRI* after vernalization treatment. The transcript levels were normalized to *UBC*. Data are shown as means ± SD for three replicates.

1.3.9. *VIN3* level is downregulated by overexpression of *HsfB2b* in vernalized plant

In my complementation analysis, all *HsfB2b* transgenic lines displayed overexpression of *HsfB2b*, although the transgenes were driven by the endogenous promoter. Thus, I analyzed the vernalization response in *HsfB2b* overexpressing lines. The *hov1* mutant, containing a nonsense mutation in the first exon of *HsfB2b*, showed approximately 3-fold higher *HsfB2b* levels than Col-0, which might be due to the negative feedback regulation (Fig. 9A). When the transgenes, *pHsfB2b::HsfB2b-myc* or *pHsfB2b::HsfB2b-eGFP*, were introduced into the *hov1* background, the *HsfB2b* levels were increased by 20–50-fold relative to that of Col-0, indicating that the transgenic lines were *HsfB2b* overexpressors (Fig. 9A). The GUS and endogenous *VIN3* levels among the parental lines (*-0.2kb pVIN3_U_I::GUS*), *hov1* (in *-0.2kb pVIN3_U_I::GUS* background), and *pHsfB2b::HsfB2b-myc hov1* (Fig. 9B and C) were subsequently compared after 40 days of vernalization treatment. The overexpression of *HsfB2b* was found to markedly reduce *VIN3* levels after 40 days of vernalization treatment. Such finding is consistent with the hypothesis that HsfB2b represses *VIN3* transcription.

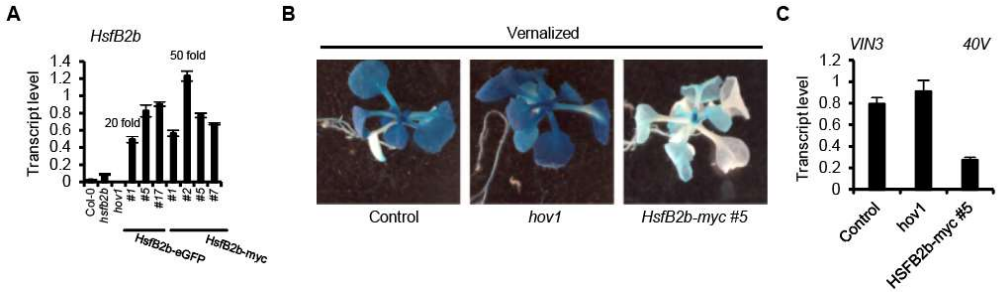

Figure 10. *VIN3* level is downregulated by overexpression of *HsfB2b* in vernalized plant.

(A) Comparison of *HsfB2b* transcript levels in Col-0, *hov1*, *hsfb2b,* and the transgenic lines expressing *pHsfB2b::HsfB2b-eGFP* or *pHsfB2b::HsfB2b-myc* in *hov1*. Transcript levels were normalized to *PP2A*. Fold changes compared to Col-0 were marked for comparison. Data are shown as means ± SD for three technical replicates.

(B) GUS staining for 40V seedlings of parental lines (*-0.2kb pVIN3_U_I::GUS*), *hov1*, and *pHsfB2b::HsfB2b-myc hov1*. Images of representative seedlings after GUS staining are shown.

(C) *VIN3* levels in 40V seedlings of parental line, *hov1* and *pHsfB2b::HsfB2b-myc hov1*. Transcript levels were normalized to *PP2A*. Data are shown as means ± SD for three technical replicates.

1.3.10. *HsfB2b* overexpression leads to hyposensitive response to vernalization

I proceeded to verify whether *HsfB2b* overexpression caused any changes in the vernalization response. Briefly, I introduced *pHsfB2b::HsfB2b-eGFP* into *FRI* Col by transformation. As expected, all 10 transgenic lines showed overexpression of *HsfB2b* (3~10 folds) based on the level after 20 days of vernalization (20V) (Fig. 10A). In these transgenic lines, *VIN3* levels were lower than those in both *FRI* Col and *hsfb2b FRI* after 20V, which supports the hypothesis that *HsfB2b* overexpression causes the repression of *VIN3* in *FRI* Col plants (Fig. 10A). Consistent with the fact that *VIN3* is required for the suppression of *FLC* (Sung and Amasino, 2004), the *FLC* levels in *pHsfB2b::HsfB2b-eGFP FRI* lines were slightly higher than those in *FRI* Col after 20V (Fig. 10A). Finally, the flowering time of the transgenic lines, *pHsfB2b::HsfB2b-eGFP FRI,* was less accelerated than that of both *FRI* Col and *hsfb2b FRI* by 20V (Fig. 10B and C). Therefore, in contrast to *hsfb2b* mutation, *HsfB2b* overexpression causes defects in the vernalization response under normal growth conditions.

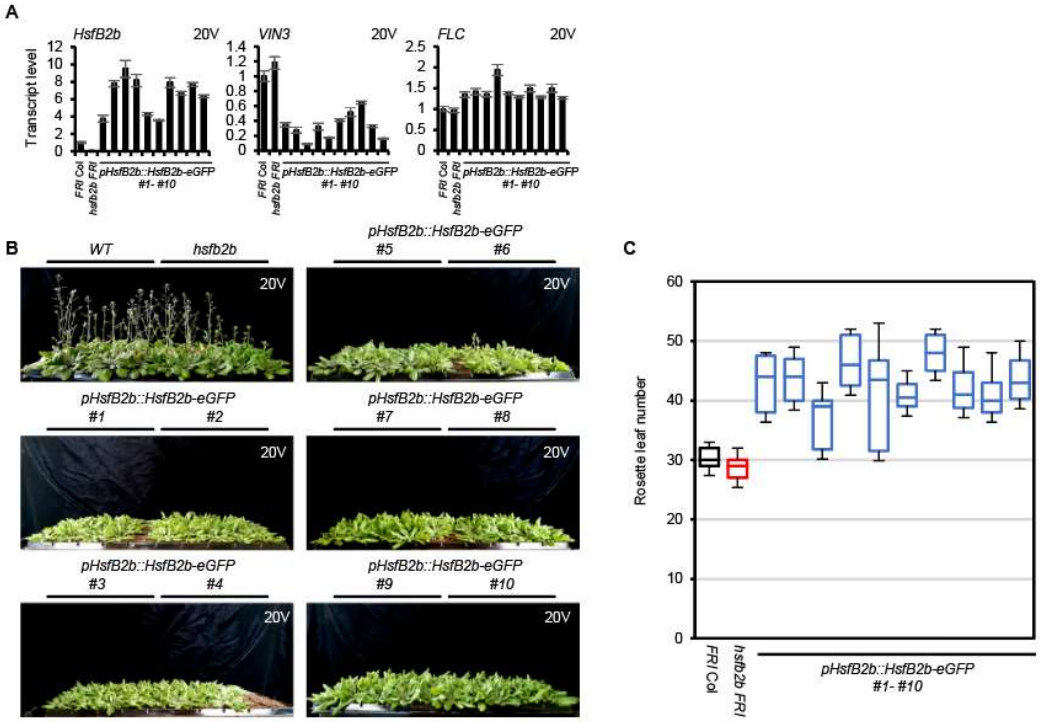

Figure 11. *HsfB2b* overexpression leads to hyposensitive response to vernalization.

(A) Transcript levels of *HsfB2b*, *VIN3*, and *FLC* in *FRI* Col, *hsfb2b FRI*, and transgenics expressing *pHsfB2b::HsfB2b-eGFP* in *FRI* Col after 20V. Transcript levels were normalized to *PP2A*. Data are shown as means ± SD for three replicates.

(B) Photographs of wild-type (*FRI* Col), *hsfb2b FRI*, and transgenics expressing *pHsfB2b::HsfB2b-eGFP* in *FRI* Col after 20V. Photos taken when 20V wild-type and *hsfb2b* plants were fully flowered.

(C) Flowering time is presented as a box plot. The number of primary leaves when bolting was counted for flowering time. The center lines show the medians. Box limits indicate the 25th and 75th percentiles.

IV. Discussion

VIN3 is required for proper vernalization in *Arabidopsis*, particularly winter annuals. However, the molecular mechanism by which *VIN3* is finely regulated has not been fully elucidated. In this study, I isolated a mutant, *hov1,* that showed hyperactivation of *VIN3*. By map-based cloning combined with whole-genome resequencing, *HsfB2b* was defined as the causative gene for *VIN3* derepression in *hov1*. Interestingly, *hsfb2b* exhibited higher *VIN3* levels under all conditions, including before and after vernalization. Therefore, *HsfB2b* might act as a general repressor of *VIN3*, regardless of cold treatment. Nonetheless, the intensity of the derepression in *hsfb2b* was strongest at the initial stages of cold treatment and stronger at the phase of return to room temperature after 40V than during vernalization treatment. Taken together, *HsfB2b* might act in a fine-tuning mechanism, suppressing precocious *VIN3* activation during the fall when temperature drops abruptly and suppressing *VIN3* levels rapidly after spring.

Higher *VIN3* levels in *hsfb2b* failed to show a stronger vernalization response in the late-flowering *FRI* Col background. This result is consistent with that of previous studies where ectopic expression of *VIN3* was not found to alter the vernalization response, despite complementing *vin3* mutation (Kim and Sung, 2017a; Lee et al., 2015). In contrast, the lower *VIN3* levels in the *HsfB2b* overexpression lines caused a weak vernalization response in both the acceleration of flowering time and *FLC* suppression by 20V. This result is also consistent with the fact that the *vin3* mutation causes failure of the vernalization response (Sung and Amasino, 2004; Yang et al., 2017). Finally, HsfB2b was

found to directly repress *VIN3,* a key factor in the vernalization process, by binding to the HSE on the 5′-UTR of *VIN3* (Fig. 7). Of note, the HSE_{VIN3} sequences on the 5′-UTR of the *VIN3* orthologues are highly conserved*,* whereas other regions of the 5′-UTR are relatively diversified among Brassicaceae species. As vernalization responses have been observed throughout Brassicaceae, conservation of such cis-elements suggests that *VIN3* regulation by Hsfs may also be conserved across the Brassicaceae family (Anderson et al., 2011; Guo et al., 2012; Kuittinen et al., 2008).

In *Arabidopsis,* Hsfs have been reported to regulate diverse stress responses, including responses to both biotic and abiotic stresses, such as bacterial infection, fungal infection, and heat and drought stresses (Bechtold et al., 2013; Nishizawa et al., 2006; Ogawa et al., 2007; Yoshida et al., 2011). During such responses, both class A and class B Hsfs are incorporated into complex and multi-layered regulatory systems, and different combinations of Hsfs seem to act on each stress response (Andrási et al., 2021). Although most of *Hsfs* are induced by heat stress, they usually show basal expression level without heat or cold stress similar to *Hsfb2b*. Such basal expression level may be required for the rapid response to diverse stresses. Here, *HsfB1* was not functionally redundant with *HsfB2b* for *VIN3* regulation (Fig. 3). However, several Hsfs, besides HsfB2b, including HsfB1, bound to the HSE_{VIN3} elements present in the 5′-UTR of *VIN3* in the yeast one-hybrid assay (Fig. 7). Therefore, other Hsfs, recognizing $HSE_{VIN3,}$ may regulate *VIN3* transcription in response to other stresses, such as low oxygen conditions at which *VIN3* is induced (Banti et al., 2010). This notion is consistent with the finding that Hsfs are required

for a broad range of stress responses (Andrási et al., 2021; Busch et al., 2005; von Koskull-Döring et al., 2007). It would be interesting to determine whether VIN3 acts as a hub for the stress responses mediated by Hsfs.

Plants perceive winter cold as a signal for vernalization, but simultaneously perceive it as long-term cold stress. In *Arabidopsis*, several HSPs and factors are strongly induced by cold stress, and the roles of both HSPs and Hsfs in the cellular response to cold stress have been reported previously (Busch et al., 2005; Sabehat et al., 1998; Swindell et al., 2007; Ul Haq et al., 2019). The HsfB2b protein displayed retarded migration on polyacrylamide gels during vernalization treatment. Such cold-induced phosphorylation indicate that *HsfB2b* is involved in a subset of cold signal transduction (Fig. 4B and C). Moreover, the transcript level of *HsfB2b* was slightly elevated after returning from cold temperatures to warm temperatures (Fig. 4A). Such observations may indicate that *HsfB2b* is required for sensing temperature changes, which are inevitable during vernalization treatment. Thus, *VIN3* regulation by *HsfB2b* may have evolved from a mechanism that senses cold stress.

The circadian clock was previously demonstrated to be involved in the regulation of *VIN3*, and components of the circadian clock, *CCA1* and *LHY*, directly regulate the diurnal rhythm of *VIN3* during vernalization treatment (Hepworth et al., 2018; Kyung et al., 2021). One of the circadian clock regulators, *PRR7*, has also been reported to be a transcription factor repressed by *HsfB2b* (Kolmos et al., 2014), which is required for proper abiotic stress responses. However, my data indicate that *HsfB2b* is not involved in regulating the diurnal rhythm of *VIN3* under cold treatment, despite affecting the amplitude (Fig. 5A and

B). As the circadian clock has rhythmic robustness due to multiple feedback loops consisting of diverse transcription factors, the defect in clock regulation by *hsfb2b* seems to be minor for the *VIN3* rhythm (Shalit-Kaneh et al., 2018a).

Under natural conditions, where environmental changes markedly occur, plants must avoid and distinguish between uncertain signals. For vernalization, plants must distinguish transient changes in temperature from winter cold. For example, plants often experience a sudden cold during late fall or a sudden warmth in early spring. Thus, plants must have an elaborate mechanism to regulate *VIN3* expression in response to ever-changing environmental conditions. Consistently, *VIN3* has been demonstrated to display dynamic expression patterns depending on fluctuating temperature (Hepworth et al., 2018). For such elaborate regulation of *VIN3*, *HsfB2b* may provide a fine-tuning mechanism to prevent unintentional flowering from sudden cold.

Chapter II

Chaperonin-mediated regulation of *VIN3* via circadian clock

I. Introduction

Chaperonins are a molecular chaperone, have a high-molecular mass double ring structure approximately 800~1000 kDa, composed of several protein subunits (Skjærven et al., 2015). Chaperonins are barrel-shaped and have a large internal cavity to hold a client substrate polypeptide and provide a microenvironment for the proper folding (Skjærven et al., 2015; Spiess et al., 2004). Chaperonin is evolutionary conserved in most life forms and mediates protein folding. Chaperonins were previously classified into two paralog groups, Group I and Group II (Spiess et al., 2004). Group I chaperonins are chaperonins that exist in bacteria, chloroplasts and mitochondria. Group II chaperonins are archaeal and cytosolic, exist in the eukaryotic cell cytosol and have been found to be essential for cell survival in yeast and mammals (Llorca et al., 2000; Muñoz et al., 2011). The eukaryotic chaperonin, Chaperonin containing TCP-1 (CCT), otherwise known as tailless-complex polypeptide 1 Ring Complex (TRiC), is predicted to be required for protein folding of many newly synthesized polypeptides, which is essential mechanism for cell viability (Horwich et al., 2007). In *Arabidopsis*, null mutation of CCT subunits are lethal (Xu et al., 2011). Despite the importance of plant cytosolic chaperonin, only a few studies have been conducted. Like in mammals and yeast, plant chaperonin plays a role in microtubule regulation through its folding activity (Ahn et al., 2019). However, plant chaperonin also seems to demonstrate specificity in substrate recognition and plays a role in regulating cellular or developmental processes. Previous report have shown that cytosolic chaperonin facilitates cell-to-cell trafficking of transcription factors, suggesting that role of cytosolic chaperonin is not

limited to general house-keeping functions (Xu et al., 2011).

Because a large part of environmental signaling is correlated with the presence of sunlight, plants develop an internal clock, the so-called circadian clock, to respond to diurnal changes. In *Arabidopsis*, the circadian clock is described as a multiple-feedback loop comprising many genes that regulate each other, resulting in sustained daily oscillation in the expression of their target genes (Fogelmark and Troein, 2014; Harmer et al., 2000). Among those clock genes, *CIRCADIAN CLOCK ASSOCIATED 1* (*CCA1*) and *LATE ELONGATED HYPOCOTYL* (*LHY*), two morning-phase clock transcription factors, bind to and repress their target genes, mostly evening-phase genes (Nagel Dawn et al., 2015). For example, TIMING OF CAB EXPRESSION 1 (TOC1) is an evening-phase clock transcription factor regulated by CCA1 and LHY binding to its promoter (Gendron et al., 2012). CCA1 and LHY have long been known to be core clock components (Alabadí et al., 2001). However, other morning-phase clock transcription factors homologous to CCA1 and LHY, REVEILLE (RVE) family transcription factors are included as morning-expressed clock regulators (Fogelmark and Troein, 2014; Gray et al., 2017; Hsu et al., 2013; Rawat et al., 2011). Like CCA1 and LHY, RVEs have myb-like DNA binding domains and directly bind to evening elements (EEs); however, RVEs activate target genes, including clock genes, instead of repressing them (Hsu et al., 2013; Rawat et al., 2011). Recently, *RVE* genes were determined to activate *CBF3*, which is essential for the cold acclimation process, by directly binding to the EE in *CBF3* promoter, while CCA1 and LHY act as repressors of *CBF3* (Kidokoro et al., 2021).

In this chapter, I report the novel upstream regulators of *VIN3* transcription during long-term cold exposure in *Arabidopsis*. Using a forward genetic approach, I isolated a mutant with reduced *VIN3* transcript levels in the fully vernalized plant, which normally demonstrates induced *VIN3* expression. The mutant carries a missense mutation in the gene that encodes one of eight cytosolic chaperonin subunits, CCT8. I performed RNA-seq analysis using non-vernalized and vernalized wild type or *cct8* mutant seedlings and identified cis-elements present in the promoter of genes with similar kinetics to those of *VIN3*. Among the identified cis-elements, an EE, which is frequently exists on promoters of genes that regulated by morning-phase circadian transcription factors, was present in the *VIN3* promoter. One of the circadian clock regulators, RVE8, was found to be a chaperonin-mediated *VIN3* transcription factor. I postulate that *RVE8* is involved in the rhythmic expression of *VIN3* during vernalization and that *RVE8*-mediated *VIN3* expression is crucial for vernalization responses.

II. Materials and methods

2.2.1. Plant Materials and Growth Conditions

All *Arabidopsis thaliana* lines used were in the Columbia (Col-0) background except L*er* ecotype used to generate mapping population for map-based gene cloning, Ws-2 ecotype used to examine *cct8-1* mutant. The wild type, Col:FRI^{Sf2} (*FRI* Col) have been previously described (Lee et al., 1994). *vin3-4*, *rve34568* and *lhy-7* mutant have been previously described (Bond et al., 2009b; Gray et al., 2017; Park et al., 2016). The *cca1-1* mutant in Col-0 background (CS67781) was obtained from Arabidopsis Biological Resource Center (https://abrc.osu.edu/). The seeds of *cca1-1 lhy-7* were generated by crossing.

To produce *35S::myc-RVE8* construct, RVE8-coding sequence were amplified and fused in-frame to *myc-pBA* vector. To produce *pFRI:gFRI* construct, genomic sequences including 1 kbp upstream of the promoter and the FRI-coding sequence from FRI^{Sf2} were amplified and fused into *pPZP211* vector. The construct was transformed into the indicated lines using Agrobacterium (*Agrobacterium tumefaciens*)-mediated *Arabidopsis* floral dip method (Clough and Bent, 1998).

The plants were grown under 16 h/8 h light/dark cycle (long day) or 8 h/16 h light/dark cycle (short day) (22 °C/20 °C) in a controlled growth room with cool white fluorescent lights (125 μmol m-2 sec-1). Vernalization treatments were done as previously described (Kim and Sung, 2013). Non-vernalized seedlings were grown for 11 d. For 10V, 20V, 40V treatments, seedlings were grown for 10, 9, 7 d under short days respectively after

germination, then transferred to vernalization chamber at 4 ℃. After vernalization treatment, seedlings were collected or transplanted to the soil. Flowering time was measured by counting the number of rosette leaves when the first flower opened using at least 20 plants.

2.2.2. EMS mutagenesis and positional cloning

EMS mutagenesis was performed as previously described (Kim et al., 2006). For the positional cloning of the causative gene of *P161*, F2 progenies were obtained by crossing *P161* to L*er*. Mapping procedure was followed using 94 GUS-inactive F2 plants and molecular makers described as previous reports (Hou et al., 2010; Lukowitz et al., 2000a). After rough mapping, the genomes of *P161* and the parental -*0.2kb pVIN3_U_I::GUS* were sequenced and compared by illumina Hiseq4000 platform (illumina) sequencing to find mutant-specific SNPs in *P161* using LabGenomics services.

2.2.3. Histochemical GUS Staining

GUS staining and were performed following standard methods that have been previously described (Shin et al., 2018). Photographs were taken with a USB digital-microscope Dimis-M (Siwon Optical Technology, South Korea).

2.2.4. Quantitative PCR

For real-time quantitative PCR, total RNA was isolated using TRIzol solutuion(Sigma). Four micrograms of total RNA was treated with recombinant DNaseI (TaKaRa, 2270A) to

eliminate genomic DNA. cDNA was generated using RNA with reverse transcriptase (Thermo scientific, EP0441) and oligo(dT). Quantitative PCR was performed using the 2x SYBR Green SuperMix (Bio-Rad 170-8882) and monitored by the CFX96 real-time PCR detection system. The relative transcript level of each gene was determined by normalization of the resulting expression levels compared to that of *UBC*.

2.2.5. Chromatin Immunoprecipitation

Approximately 4 g of whole *Arabidopsis* seedlings were collected and cross-linked using 1% (v/v) formaldehyde for 10 min and quenched by 0.125 M glycine for 5 min under vacuum. Seedlings were rinsed with distilled water, frozen in liquid nitrogen, and grounded to fine powder. The powder was resuspended in Nuclei Isolation Buffer [1 M hexylene glycol, 20 mM PIPES-KOH (pH 7.6), 10 mM $MgCl_2$, 15 mM NaCl, 1 mm EGTA, 1 mM PMSF, complete protease inhibitor mixture tablets (Roche)], and *Arabidopsis* nuclei were isolated by centrifugation, lysed by Nuclei Lysis Buffer [50 mM TRIS-HCl (pH 7.4), 150 mM NaCl, 1% Triton X-100, 1% SDS], and sonicated using a Branson sonifier to shear the DNA. Sheared chromatin solution was diluted 10-fold with a ChIP Dilution Buffer [50 mM TRIS-HCl (pH 7.4), 150 mM NaCl, 1% Triton X-100, 1 mM EDTA]. The beads (Santa Cruz Biotechnology, sc-2003), chromatins and anti-trimethyl-Histone H3 (Millipore,07-449) or anti-myc (Santa Cruz Biotechnology, sc-40) antibodies or mormal mouse IgG_1 (Santa Cruz Biotechnology, sc-3877) antibodies were mixed and incubated for overnight at 4 °C. Beads were washed with ChIP dilution buffer for 4 times and DNA extraction was performed using Chelex 100 resin following the manufacturer's instruction. qPCR analysis

was performed using 1% input and immunoprecipitated DNA.

2.2.6. Transcriptome analysis

Total RNA was isolated from *Arabidopsis* plants as described above. Bioanalyzer RNA Pico 6000 chip was applied to qualifying sample availability. An RNA-Seq library was constructed using TruSeq RNA Sample Preparation kit (Illumina, CA, USA), according to the manufacturer's guidelines. The RNA-Seq library was sequenced to generate paired-end (2 × 100 bp) reads using the Illumina Novaseq system (Illumina, CA, USA) using Macrogen services.

2.2.7. Immunoblotting

For immunoblot assay, the seedlings of *35S::RVE8-myc* were harvested at each time point. Total proteins were prepared from 100mg of harvested samples in protein extraction buffer (50mM Tris-Cl pH 7.5, 150 mM NaCl, 10 mM $MgCl_2$, 1 mM ethylenediaminetetraacetic acid (EDTA), 1% Triton X-100, 1 mM phenylmethylsulfonyl fluoride (PMSF), 1 mM 1,4-Dithiothreitol (DTT), 1X complete Mini, and EDTA-free protease inhibitor cocktail (Roche). Total proteins were separated by sodium-dodecyl sulfate (SDS)-PAGE. The proteins were transferred to PVDF membranes (Amersham Biosciences) and probed with anti-myc (Santa Cruz Biotechnology, sc-40, 1:10,000 dilution) antibodies or anti-α TUB (Santa Cruz Biotechnology, sc-23948, 1:10,000 dilution) overnight at 4 ℃. The samples were then probed with horseradish peroxidase-conjugated anti-mouse IgG (Cell Signaling, #7076, 1:10,000 dilution) antibodies at room temperature. The signals were detected using

ImageQuant LAS 4000 (GE Healthcare) with WesternBrightTM Sirius ECL solution (Advansta).

2.2.8. Preparation of fusion protein and EMSA

Coding sequence encoding RVE4 and RVE8 was fused to *pMAL-c2* vector. The MBP, MBP-RVE4 and MBP-RVE8 proteins were expressed in *Escherichia coli* BL21 strain according to the manufacturer's instructions using the pMAL Protein Fusion and Purification System (#E8200; New England BioLabs) and purified using MBPtrap HP column (Cytiva) attached to ÄKTA FPLC system (Cytiva). The Cy5-labeled probes (GEE, 5′-Cy5- CTTCCAAAGCACGTGAAGATATTTCCAACG-3′) and unlabeled competitors (GEE, 5′-CTTCCAAAGCACGTGAAGATATTTCCAACG-3′; mG, 5′-CTTCCAAAGGCCAGTAAGATATTTCCAACG-3′; mEE, 5′-CTTCCAAAGCACGTGAAATTGTATCCAACG-3′; mGEE, 5′-CTTCCAAAGGCCAGTAAATTGTATCCAACG-3′) were generated by annealing 40 bp-length oligonucleotides. 5 μM of purified proteins and 100 nM of Cy5-labeled probe were incubated at room temperature in binding buffer (10 mM Tris-HCl (pH 7.5), 50 mM NaCl, 1 mM EDTA, 5% glycerol and 5 mM DTT). For competition assay, 100-fold molar excess of each competitor was added to the reaction mixture before incubation. The reaction mixtures were resolved by electrophoresis through 6% polyacrylamide gel in 0.5X Tris-borate EDTA buffer at 100 V. The Cy5 signals were detected using WSE-6200H LuminoGraph II (ATTO).

2.2.9. Transient Expression Assays with Arabidopsis Mesophyll Protoplasts

Transient transformation of Arabidopsis mesophyll protoplasts was performed as described with minor modifications (Yoo et al., 2007). Protoplast was isolated from leaves of SD-grown wild type plant (Col-0) using a buffer containing 150 mg Cellulase Onozuka™ R-10 (Yakult), 50 mg Maceroenzyme™ R-10 (Yakult), 20 mM KCl, 20 mM MES-KOH (pH 5.6), 0.4 M D-mannitol, 10 mM CaCl2, 5 mM β-mercaptoethanol, 0.1 g bovine serum albumin. For protoplast transfection, 20 μg of plasmid DNA and isolated protoplast were incubated together in buffer containing 0.1 M D-mannitol, 50 mM CaCl2, and 20% (w/v) PEG. Luciferase activity in protoplast was measured using Luciferase Assay System (Promega) and MicroLumat Plus LB96V microplate luminometer (Berthold Technologies).

2.2.10. Accession Numbers

The Arabidopsis Genome Initiative locus identifiers for the genes discussed in this chapter are as follows: *VIN3* (At5g57380), *FLC* (At5g10140), *FRI* (At4g00650), *CCT8* (At3g03960), *CCA1* (At2g46830), *LHY* (At1g01060), *TOC1* (At5G61380), *GI* (At1g22770), *RVE3* (At1g01520), *RVE4* (At5g02840), *RVE5* (At4g01280), *RVE6* (At5g52660), *RVE8* (At3g09600), *UBC* (At5g25760), *Actin* (At5g09810), *FUS3* (At3g26790).

2.2.11. List of primers used in this chapter

Oligo Name	Primer Sequence (5'-3')	Usage
cct8-4 geno F	GTTCGTGTTTCCAAGCTCTAG	cct8-4 genotyping
cct8-4 geno R	CTTCGCTTTCTCCATTCGC	cct8-4 genotyping
cct8-1 geno F	TGCAGGTTATTTGCCCTTAAATAA	cct8-1 genotyping
cct8-1 geno R	GACTTAATCCTGGAAGATAATGC	cct8-1 genotyping
FRIgenomic-F	CGGGATCCCCCAATCACTCGTGGTAGG	Construct
FRIgenomic-R	CGCGTCGACGATGTATCTGAGGTTGACTAAAAC	Construct
RVE8CDS-F	GCGAGATCTATATGAGCTCGTCGCCGTC	Construct
RVE8CDS-R	CGCACTAGTTTATGCTGATTTGTCGCTTGTTG	Construct
myc-pBA-F	CGTCTAGACGGTATCGATTCAAAGCTATGG	Construct
RVE8CDS-R	CGTCTAGATTATGCTGATTTGTCGCTTGTTG	Construct
PP2A-F	TATCGGATGACGATTCTTCGTGCAG	RT-qPCR
PP2A-R	GCTTGGTCGACTATCGGAATGAGAG	RT-qPCR
UBC-F	TTGTGCCATTGAATTGAACCC	RT-qPCR
UBC-R	CATCCTAATGTTCATTTCAAGACAG	RT-qPCR
VIN3-F	GTTTCAGGACAAGGTGACAAG	RT-qPCR
VIN3-R	TTCCCCTGAGACGAGCATTC	RT-qPCR
FLC-F	AGCCAAGAAGACCGAACTCA	RT-qPCR
FLC-R	TTTGTCCAGCAGGTGACATC	RT-qPCR
LHY-F	CTTCTTCACAGTTGAATCAGGC	RT-qPCR
LHY-R	TTCAATGTCGCCACTTACCTG	RT-qPCR
CCA1-F	AGAGACATCAAACGCAAGCAC	RT-qPCR
CCA1-R	AGCACAGGGATATGCATCGG	RT-qPCR
PRR5-F	CAATAGGCAATCACATTGATCAG	RT-qPCR
PRR5-R	CGTAACGAACCTTTTTCTCATAAC	RT-qPCR
PRR7-F	TTGGAGAAGATGCCAAAGTTCT	RT-qPCR
PRR7-R	GTTCCGCTCTCACTTCCACTAC	RT-qPCR
PRR9-F	GCTGGACAAAGCAGTAGCAC	RT-qPCR
PRR9-R	CTGGTACCGAACCTTTTTGTC	RT-qPCR

TOC1-F	GGAAAATGAGTGGTCTGTTGC	RT-qPCR
TOC1-R	TGAAGAAAATTGCGCTGGATTACT	RT-qPCR
GI-F	CTGTTTAAACTGGGAAGCTCAC	RT-qPCR
GI-R	GGTGCTCGTTATTGGGACAAG	RT-qPCR
RVE3-F	GCCACATAGAGTGGCGCC	RT-qPCR
RVE3-R	GATATCAACTTCCGTTGTTCATC	RT-qPCR
RVE4-F	GTGGAGCAGAAGTTGATGTTG	RT-qPCR
RVE4-R	CAGGAAGACCATGCATTGAGG	RT-qPCR
RVE5-F	GCCACATAGAGTGATGCCG	RT-qPCR
RVE5-R	CAACCTCCTTTGCTCTGCAAAC	RT-qPCR
RVE6-F	CTCCTGCTCCTGCTTTTGGG	RT-qPCR
RVE6-R	CAAGAATGTGCAACTGCAAGTAC	RT-qPCR
RVE8-F	GGGAAGCTCAAGCCGAACAGTATC	RT-qPCR
RVE8-R	GGCCTCTCGTTTCAGGATCAAAGA	RT-qPCR
FUS3-F	GTGGCAAGTGTTGATCATGG	ChIP-qPCR
FUS3-R	AGTTGGCACGTGGGAAATAG	ChIP-qPCR
FLC_E-F	CGACAAGTCACCTTCTCCAAA	ChIP-qPCR
FLC_E-R	AGGGGGAACAAATGAAAACC	ChIP-qPCR
pTUB2-F	ACAAACACAGAGAGGAGTGAGCA	ChIP-qPCR
pTUB2-R	ACGCATCTTCGGTTGGATGAGTGA	ChIP-qPCR
pTOC1-F	GATTTTGATATGGAGATGCATCTTC	ChIP-qPCR
pTOC1-R	CCAAGGAGATGACGTGGACA	ChIP-qPCR
VIN3_A-F	CAAATTTGAATCCATTAAGCGTTATC	ChIP-qPCR
VIN3_A-R	CTGATTACTTTAGTTCATCTTTTTTTG	ChIP-qPCR
VIN3_B-F	TCGAACATATAGTAGTGAGTCATA	ChIP-qPCR
VIN3_B-R	CGTTGGAAATATCTTCACGTGC	ChIP-qPCR
VIN3_C-F	GTGTTCTTCATCATCGTAAGTG	ChIP-qPCR
VIN3_C-R	GCCGAGATCCGATTTCACAC	ChIP-qPCR
VIN3_D-F	AGTACACTGGTCTTAACAAACC	ChIP-qPCR
VIN3_D-R	CGTATCATCGCATCCAAGCG	ChIP-qPCR
VIN3_E-F	AATCGGTCTATTTATTAACTCGCT	ChIP-qPCR
VIN3_E-R	TTGAGTTTTTCACTAAGCATCAG	ChIP-qPCR

VIN3_WT_Cy5-F	Cy5-CTTCCAAAGCACGTGAAGATATTTCCAACG	Cy5-GEE
VIN3_WT_Cy5-R	Cy5-CGTTGGAAATATCTTCACGTGCTTTGGAAG	Cy5-GEE
VIN3_WT-F	CTTCCAAAGCACGTGAAGATATTTCCAACG	GEE
VIN3_WT-R	CGTTGGAAATATCTTCACGTGCTTTGGAAG	GEE
VIN3_mG-F	CTTCCAAAGGCCAGTAAGATATTTCCAACG	mG
VIN3_mG-R	CGTTGGAAATATCTTACTGGCCTTTGGAAG	mG
VIN3_mEE-F	CTTCCAAAGCACGTGAAATTGTATCCAACG	mEE
VIN3_mEE-R	CGTTGGATACAATTTCACGTGCTTTGGAAG	mEE
VIN3_mGEE-F	CTTCCAAAGGCCAGTAAATTGTATCCAACG	mGEE
VIN3_mGEE-R	CGTTGGATACAATTTACTGGCCTTTGGAAG	mGEE
pVIN3LUC-F	CGCCTGCAGGATTTTACATATCGTAATATTTCG	Reporter construct
pVIN3LUC-R	CTTCCATGGCAGCTTGCATTTTTTTTTTGTTTGTC	Reporter construct
NLSRVE8GFP-F	CGCAGATCTATGAGCTCGTCGCCGTCAA	Effector construct
NLSRVE8GFP-R	CGCAGGCCTTGCTGATTTGTCGCTTGTTGAG	Effector construct

Table 2. List of primers used in chapter 2

III. Results

2.3.1. Isolation and Characterization of *P161*, a mutant with reduced *VIN3* transcript levels

To identify upstream regulators of *VIN3*, the GUS reporter line (-0.2kb *pVIN3_U_I::GUS*) was mutagenized with ethyl methanesulfonate (EMS). A total of 3,412 M1 lines were generated, and their seeds were harvested as M2 seeds. Approximately 25 M2 seedlings from each line were grown at room temperature for 10 days, transferred to the cold chamber for 40 days, then analyzed by GUS staining. Throughout the screening, the whole seedlings derived from M2 seeds were used for GUS staining. One mutant with a reduced GUS signal was identified and initially referred to as *P161*. Compared to the parental line, which showed a strong GUS signal in whole tissues after 40 days of cold exposure (40V), *P161* showed a reduced GUS signal when exposed to the same treatment (Fig. 11). The mutant showed reduced GUS signals during the entire vernalization treatment process; however, no differences were observed in the non-vernalized condition (Fig. 11). Interestingly, the mutant displayed growth retardation and gradually increasing pigment accumulation during vernalization treatment (Fig. 12). The mutant phenotype was not found in the F1 plants when backcrossed to the parental line, and the phenotype was segregated approximately 3:1 (290 wild-type vs 94 mutants) in the F2 population. Such results indicate that the mutant phenotype is completely recessive and is caused by a mutation in a single locus. Thereafter, I performed a time course analysis of *VIN3* levels in

P161 during vernalization treatment. Consistent with the results of the GUS assay, endogenous *VIN3* transcript levels were reduced in the mutant during vernalization treatment (Fig. 13). *P161* and control plants displayed similar levels of *VIN3* in the absence of vernalization treatment, indicating that the mutation in *P161* specifically affects *VIN3* during vernalization treatment. The *P161* plants also expressed lower levels of *VIN3* throughout the vernalization time course and after returning to room temperature for 1 day (40VT1). These results indicate that *P161* carries a mutation in a gene required to activate *VIN3* under vernalization conditions.

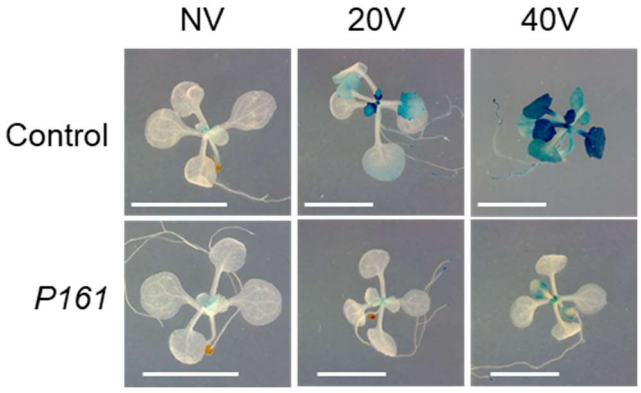

Figure 12. *P161* shows reduced GUS signal during vernalization treatment.

Images of representative Control (-*0.2kb pVIN3_U_I::GUS*) and *P161* seedlings after GUS-staining. NV, Non-vernalized; 20V and 40V, 20 d and 40 d vernalized. (Scale bars, 5 mm)

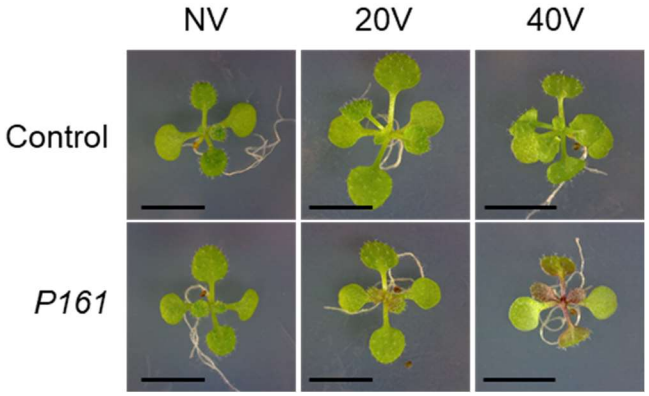

Figure 13. *P161* displays pigment accumulation during vernalization treatment.

Images of representative Control (-*0.2kb pVIN3_U_I::GUS*) and *P161* seedlings after vernalization treatment. NV, Non-vernalized; 20V and 40V, 20 d and 40 d vernalized. (Scale bars, 5 mm)

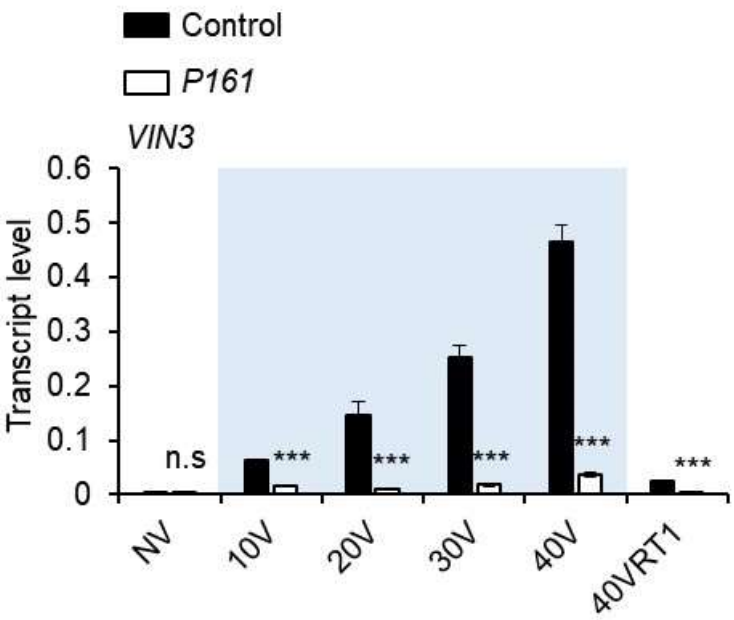

Figure 14. Endogenous *VIN3* transcript levels in control and *P161*

VIN3 transcript levels in control (-*0.2kb pVIN3_U_I::GUS*) and *P161* during vernalization treatment. NV, non-vernalized; 10V, 20V, 30V, and 40V, 10, 20, 30, and 40 d vernalized respectively. The transcript levels were normalized to UBC. Data are shown as means ± SD for three replicates. Asterisks indicate a significant difference compared to the control (Student's t test; ***P<0.001).

2.3.2. Map-based cloning reveals disruptive point mutations in *P161*

To identify the causative mutation, *P161* was crossed with L*er* for positional cloning. A total of 94 F2 plants with reduced GUS signals in the leaves were selected for mapping analysis. I mapped the mutation to the 744 kilobase pair interval on chromosome 3, which contained 234 genes (Fig. 14). The genomes of *P161* and parental *-0.2kb pVIN3_U_I::GUS* were sequenced using the Illumina sequencing method for comparison. Analysis of the sequence data revealed 5 potentially disruptive point mutations, including one mutation within the At3g03960 gene (G to A, causing an amino acid substitution from Gly^{212} to Arg^{212}) (Fig. 15). At3g03960 encodes one of the eight cytosolic chaperonin subunits, CCT8, and mutation was at a residue that is highly conserved in different organisms (Fig. 16). Thus, *P161* was renamed *cct8-4*.

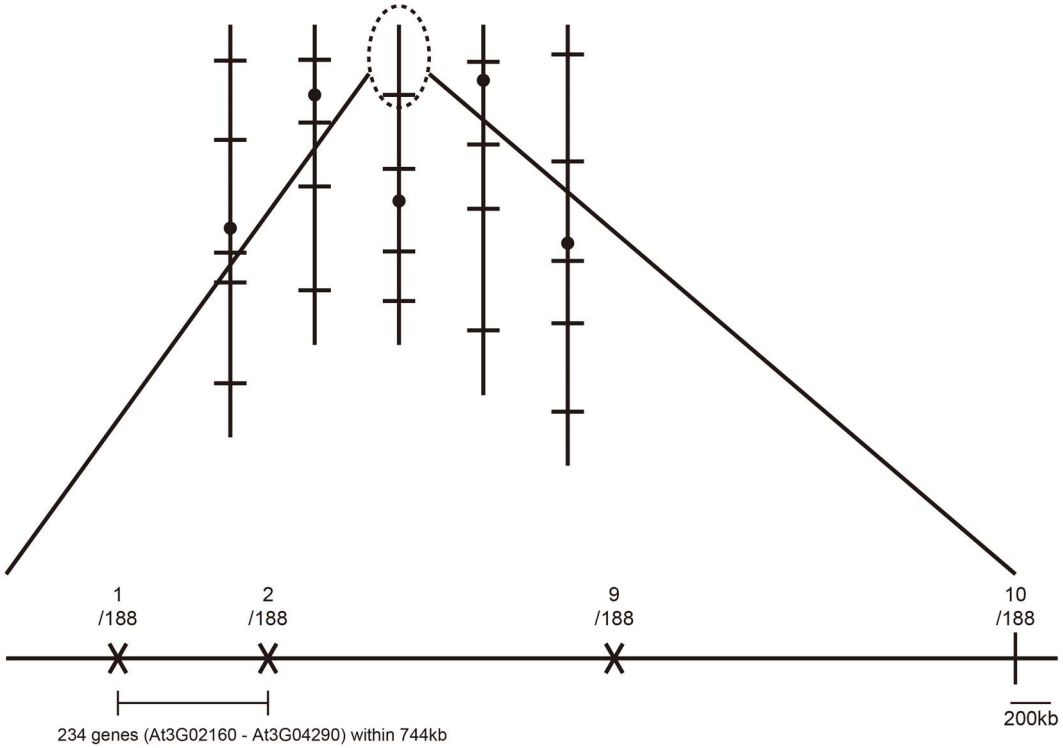

Figure 15. Genetic map of *P161* on chromosome 3.

Upper, simplified map-based cloning procedure for *P161*. Vertical lines represent five *Arabidopsis* chromosomes, horizontal lines represent molecular markers, and black circles indicate centromeres.

Lower, genetic intervals and molecular markers. The uppermost numbers are the number of recombinants among the 94 chromatids analysed. Vertical lines and X-signs represent molecular markers.

Figure 16. Schematic structure of genomic *CCT8.*

Different mutant alleles are shown. Black boxes indicate exon, grey boxes and black lines represent untranslated regions and introns, respectively. T-DNA insertions and point mutations are shown as triangles and asterisks, respectively.

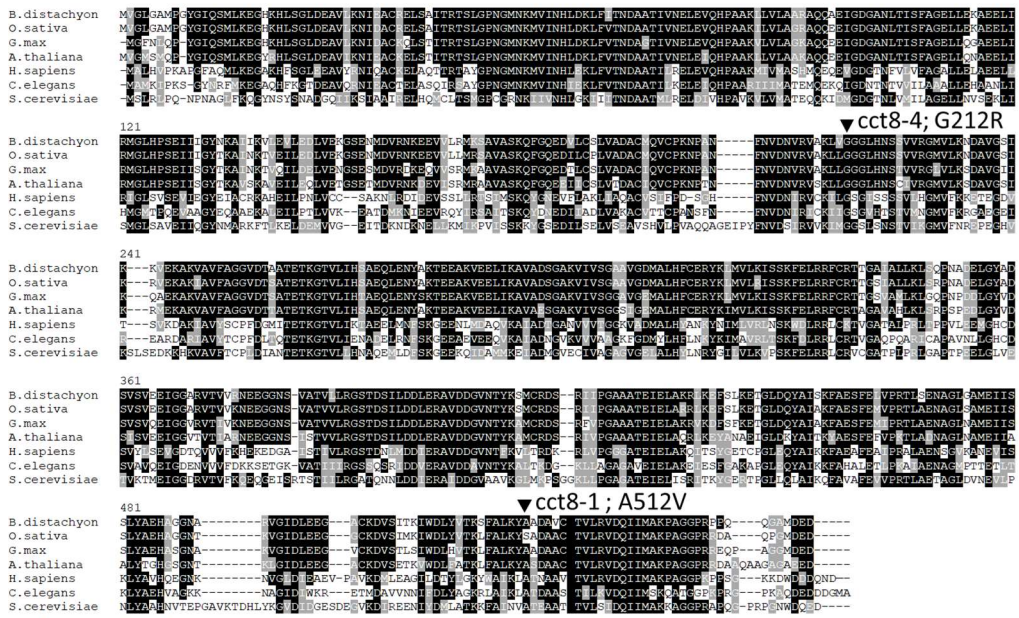

Figure 17. Multiple alignment of amino-acid sequences of the CCT8 orthologs from 7 species.

Mutated sites in *cct8-1* or *cct8-4* are indicated. B. distachyon, *Brachypodium distachyon;* O. sativa, *Oryza sativa*; G. max, *Glycine max*; A. thaliana, *Arabidopsis thaliana*; H. sapiens, *Homo sapiens*; C. elegans, *Caenorhabditis elegans*; S. cerevisiae, *Saccharomyces cerevisiae.* Shading represents the degree of similarity.

2.3.3. *CCT8* is causative gene of reduced *VIN3* expression in *P161*

Because there were multiple potentially disruptive point mutations, further analyses were conducted to clarify that *CCT8* is a causative gene of reduced *VIN3* expression in *P161*. Firstly, *VIN3* expression level in *cct8-1* was examined. *cct8-1*, an amino acid substitution mutant (Ala^{512} to Val^{512}), displayed upwardly curled leaves and dwarfism, whereas *cct8-4* did not showed any of those phenotypes in normal condition. *cct8-1* also showed reduced *VIN3* expression levels and pigment accumulation during 20 days of cold exposure (**Fig. 17B**). For complementation test, an F1 plant from a cross of *P161* with *cct8-1* was examined by GUS staining, and *VIN3* levels were measured. The GUS signal and *VIN3* level were reduced after 20 days of cold treatment (**Fig. 17A and B**). Next, CCT8-GFP was introduced into *P161* to examine whether CCT8 can recapitulate the reduced GUS signal in *P161*. After 20 days of cold treatment, GUS staining was performed on control, *P161* and *pCCT8::CCT8-GFP*-introduced *P161* plants. The GUS signal was successfully recovered in the *pCCT8::CCT8-GFP cct8* plant (**Fig. 18A**). Moreover, the introduction of *pCCT8::CCT8-GFP* recapitulates endogenous *VIN3* expression, which was reduced in *P161* (**Fig. 18B**). These assays revealed that *CCT8* is indeed the causative gene.

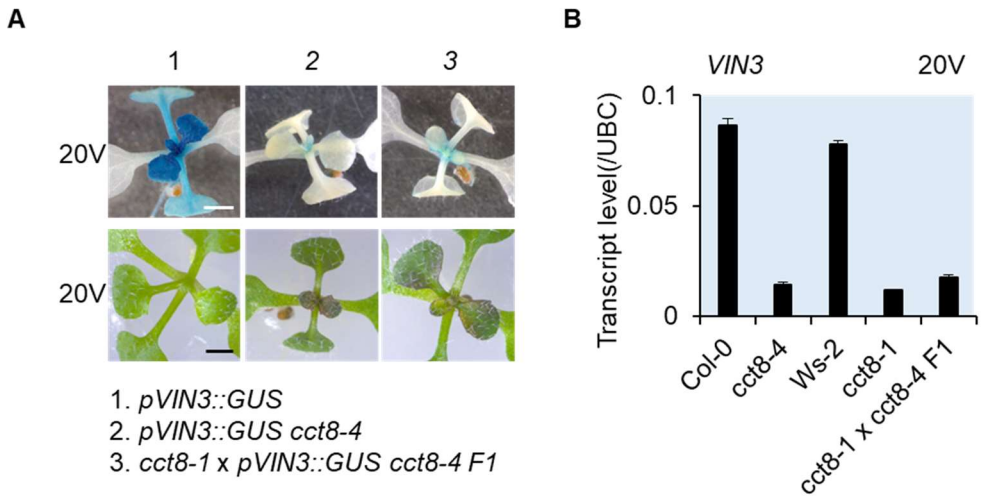

Figure 18. Complementation test using two allele of *CCT8.*

(A) 10-day old Control (*-0.2kb pVIN3_U_I::GUS*), *pVIN3::GUS cct8-4* and F1 hybrid (*cct8-1* x *pVIN3::GUS cct8-4*) seedlings were exposed to cold for 20 days, then GUS stained. Representative images of before (top) or after (bottom) GUS staining.

(B) Transcript level of *VIN3* in 20V Col-0, *cct8-4*, Ws-2, *cct8-1* and F1 hybrid after 20 days of cold treatment. The transcript levels were normalized to *UBC*. Data are shown as means ± SEM for three replicates.

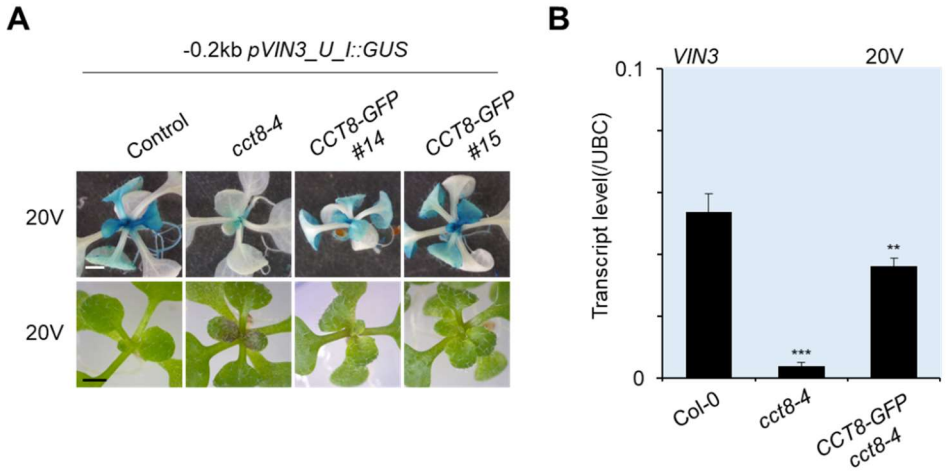

Figure 19. Introduction of CCT8-GFP recapitulates *P161* phenotype.

(A) 10-day old Control (-0.2kb *0.2kb pVIN3_U_I::GUS*), *P161* and CCT8-GFP in *P161* seedlings were exposed to cold for 20 days, then GUS stained. Representative images of before (bottom) or after (top) GUS staining.

(B) Transcript level of *VIN3* in 20V Col-0, *cct8-4*, CCT8-GFP *cct8-4*. The transcript levels were normalized to *UBC*. Data are shown as means ± SD for three replicates. Asterisks indicate a significant difference compared to the control (Student's t test; **P<0.01, ***P<0.001).

2.3.4. The chaperonin complex is attenuated in *cct8* during vernalization treatment

As CCT8 is one of 8 subunits of chaperonin complex, whether whole chaperonin complex is disrupted in *cct8-4* was examined. In chaperonin-deficient cells, cortical microtubules are depleted, and those depletion is accompanied by reduction of cellular α or β tubulin levels. Previous report have shown that depletion of CCT2, one of chaperonin subunits, causes reduced tubulin level in *Arabidopsis*, suggests that chaperonin is involved in the folding of tubulins (Ahn et al., 2019). To determine whether a mutation in one subunit of chaperonin also affects the function of chaperonin, Immunoblotting was performed with anti-α tubulin antibodies. The result showed that α tubulin levels in *cct8-4* were reduced according to duration of vernalization treatment, whereas those in wild-type is not affected by vernalization treatment (Fig. 19). These results suggest that the chaperonin complex is attenuated in cct8 during vernalization treatment.

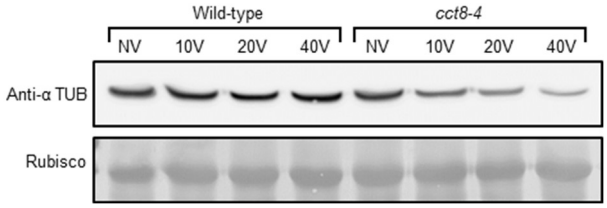

Figure 20. *cct8-4* lost its chaperonin function during vernalization.

Immunoblot analysis of the α-Tubulin protein extracted from vernalized seedlings of wild-type and *cct8-4*. Rubisco was used as loading control. NV, non-vernalized; 10V, 20V and 40V, 10 d, 20 d, 40 d vernalized, respectively.

2.3.5. The *cct8* mutant shows a defective vernalization response

The *cct8* mutation was introduced into *FRI* Col, a vernalization-sensitive line, by genetic crossing to analyze the effect of *cct8* on the vernalization response. As shown in Fig. 19, *cct8 FRI* showed a similar flowering time in the non-vernalized condition but delayed flowering compared to *FRI* Col at the early vernalization stage (Fig. 20). However, *cct8 FRI* showed a similar flowering time after 30 days of vernalization treatment, indicating that the delay in *cct8* is no longer present after a certain period of cold exposure (Fig. 20). Next, the effect of the duration of cold exposure on *VIN3* and *FLC* transcript levels was examined. *VIN3* expression levels were significantly decreased at every cold-exposed time point in *cct8*, but increased with cold treatment (Fig. 21A). *cct8 FRI* had a similar *FLC* level to that of *FRI* Col before cold exposure but showed a delayed decrease of *FLC* under continuing cold exposure, consistent with the delayed flowering of *cct8 FRI* (Fig. 21B). Next, I conducted a time-course analysis of H3K27me3 enrichments on *FLC* chromatin by ChIP-PCR. *cct8 FRI* showed decreased enrichment of H3K27me3, a repressive histone mark, which is accumulated by *VIN3*-mediated histone modification, but the enrichment is shown to increase with duration of cold treatment (Fig. 21C). These results indicate that decreased *VIN3* level in *cct8* is insufficient to the histone modification as wild-type, but sufficient for modification to occur. Taken together, chaperonin is supposed to be required for the control of *VIN3* and *FLC* expression to achieve a proper vernalization response during cold exposure.

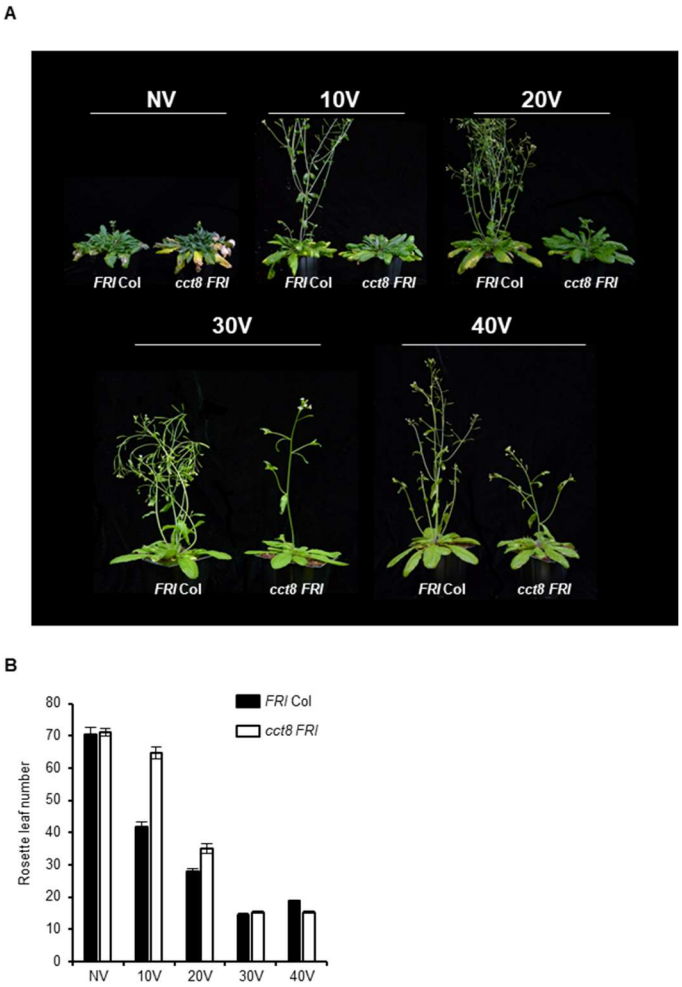

Figure 21. Effect of *cct8* on vernalization response.

(A) Photographs of *FRI* Col and *cct8 FRI* without (NV) or with 10 days (10V), 20 days (20V), 40 days (40V) of vernalization.

(B) Flowering time of *FRI* Col and *cct8 FRI* after vernalization. Flowering time was measured as the number of primary rosette leaves formed when bolting. Data are shown as means ± SD.

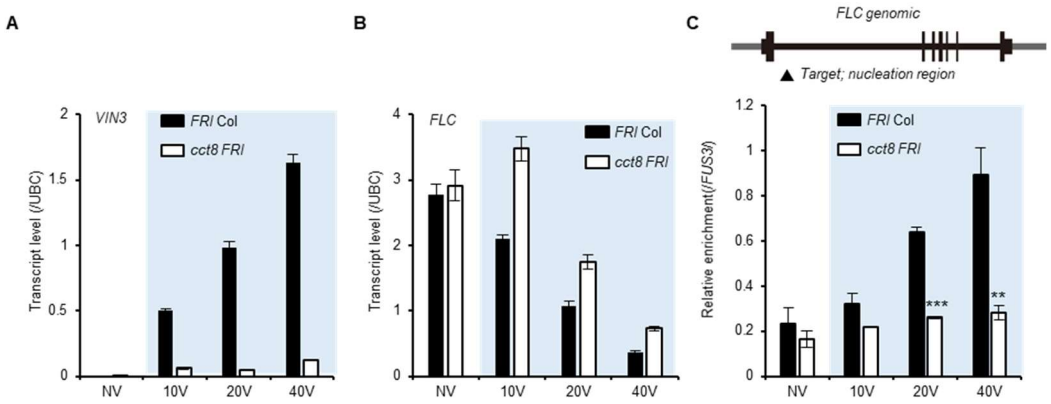

Figure 22. Effect of *cct8* on gene expression during vernalization treatment.

(A) *VIN3* or (B) *FLC* transcript levels in *FRI* Col and *cct8 FRI* during vernalization were determined by RT-qPCR. NV, non-vernalized; 10V, 20V, 40V, 10, 20, 40 d vernalized respectively. The transcript levels were normalized to UBC. Data are shown as means ± SEM for three replicates.

(C) ChIP-qPCR showing the enrichment of H3K27me3 in *FLC* locus. Upper: Schematic diagram of the *FLC* locus and enrichment of H3K27me3 DNA fragment. Thick black boxes indicate exon, thin black boxes and black lines represent untranslated regions and introns, respectively. Arrowhead indicates a region used for ChIP-qPCR analysis. Lower: Chromatin of *FRI* Col or *cct8 FRI* under indicated durations of cold treatment were harvested and analyzed. Histograms show mean values ± SEM (n=2 biological replicates, each biological replicate is an average value of three technical replicates). Each enrichment are calculated by percent input normalized against *FUS3*. Asterisks indicate significant difference compared to the *FRI* Col (Student's t test; **P<0.01, ***P<0.001).

2.3.6. Transcriptome analysis of differentially expressed genes in *cct8* mutant plants under long-term cold exposure

I assessed the gene expression profiles in *FRI* Col and *cct8 FRI* mutant plants exposed to 20 days of cold by RNA-seq analysis to identify the roles of the chaperonin complex in vernalization-responsive gene expression changes. DEG analysis was conducted, and a total of 3682 DEGs were obtained (fold change>1.8199, P<0.05) (**Fig**. 22). Next, GO analysis using the obtained DEGs was conducted. GO terms such as 'rhythmic process', 'circadian rhythm', 'cold acclimation', 'cellular transition metal ion homeostasis' and 'response to reactive oxygen species' were overrepresented in the genes upregulated in the wild-type upon cold treatment (WT NV vs 20V) and downregulated in mutant compared to wild-type (20V WT vs mt) (**Fig**. 23). Next, the enrichment of known motifs in the promoters of the genes showing similar kinetics to *VIN3* was analyzed. First, 98 genes showing similar kinetics to *VIN3* during vernalization treatment in wild-type and *cct8* plants were isolated. Those genes were upregulated in the wild-type upon cold treatment and downregulated in the mutant compared to in the wild-type. Then, the promoters of those genes were analyzed using Hypergeometric Optimization of Motif Enrichment (HOMER) software to identify overrepresented cis-elements. As a result, EE, G-Box, and C-repeat (CRT)/dehydration-responsive element (DRE) were found to be overrepresented in the genes showing *VIN3*-like kinetics (Table I). Among 3 of the representative overrepresented cis-elements among the DEGs, G-Box and EE were identified as cis-regulatory elements of *VIN3* regulation, while CRT/DRE was not detected in the vicinity

of the *VIN3* promoter (Kyung et al., 2022). Combined with the GO analysis results, these findings indicate that the EE is likely to be involved in CCT8-mediated *VIN3* regulation as EEs are known to be enriched in evening-phase clock genes.

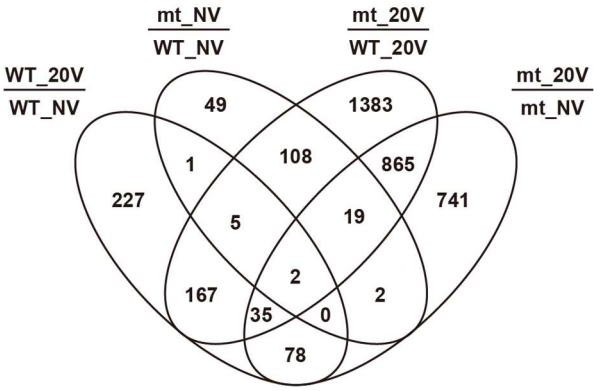

Figure 23. The expression profile of the DEGs across non-vernalized or 20 days of vernalized *FRI* Col and *cct8 FRI*.

The Venn diagram shows the overlapped DEGs among *FRI Col* and *cct8 FRI* without or with 20 d of vernalization. WT_NV, non-vernalized *FRI* Col; WT_20V, 20 d vernalized *FRI* Col; mt_NV, non-vernalized *cct8 FRI;* mt_20V, 20 d vernalized *cct8 FRI*

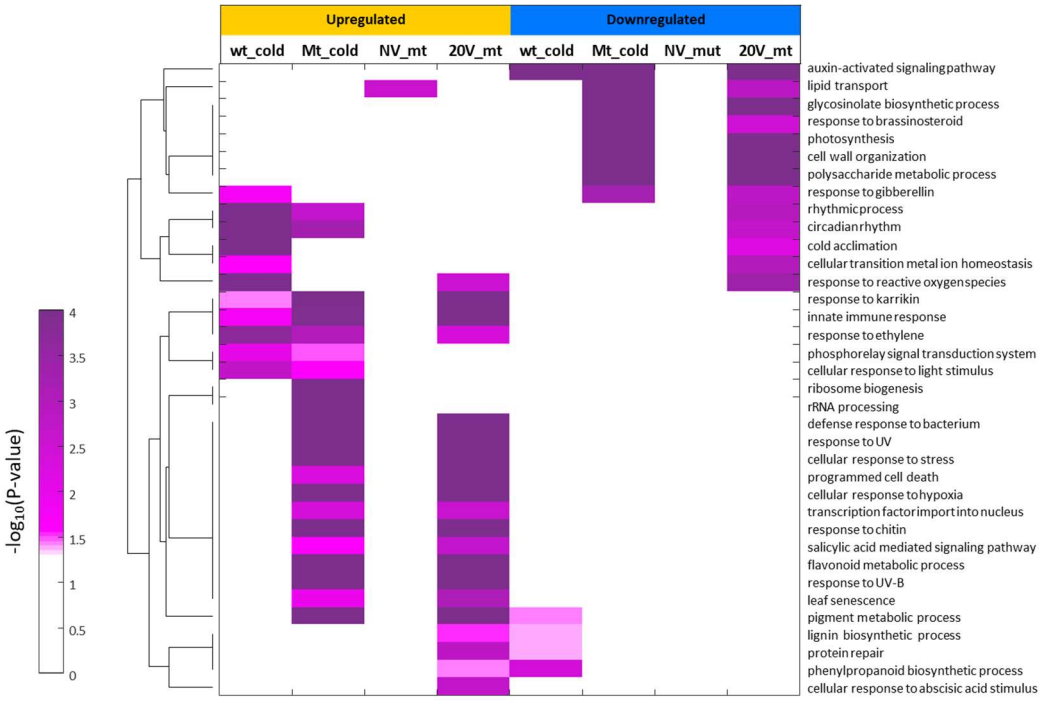

Figure 24. Gene ontology term enrichment analysis of differentially expressed genes.

The heatmap showing the enriched GO terms using DEG in response to vernalization treatment. The color scale represents enrichment folds after P-value of different GO terms. WT_cold, DEGs in wild-type by vernalization treatment; mt_cold, DEGs in *cct8* by vernalization treatment; NV_mt, DEGs between wild-type and *cct8* in non-vernalized condition; 20V_mt, DEGs between wild-type and *cct8* in vernalized condition.

Transcription factor name	DNA binding domain	Motif name	P-value	% of Target Sequences with Motif	% of Background Sequences with Motif
LCL1	Myb-related	EE	1.E-08	26.6%	6.8%
ERF36	AP2EREBP	CRT/DRE	1.E-07	23.4%	6.4%
DREB1A	AP2EREBP	CRT/DRE	1.E-06	23.4%	6.5%
IBL1	bHLH	G-Box	1.E-06	43.6%	20.2%
ERF38	AP2EREBP	CRT/DRE	1.E-06	21.3%	5.9%
ERF34	AP2EREBP	CRT/DRE	1.E-06	16.0%	3.4%
ERF37	AP2EREBP	CRT/DRE	1.E-05	29.8%	11.3%
CCA1	Myb-related	EE	1.E-05	50.0%	27.3%
SPCH	bHLH	G-Box	1.E-05	44.7%	22.9%
CBF2	AP2EREBP	CRT/DRE	1.E-05	22.3%	7.2%

Table 3. Result of motif analysis using genes having VIN3-like kinetics.

Result of HOMER DNA-motif enrichment analyses of 98 transcript, which shows similar kinetics in transcriptome analysis. Transcription factor name, DNA binding domain, Motif name, P-value, % of target sequences with motif, and % of target sequences with motif of top 10 identified DNA-motifs are shown.

2.3.7. Anthocyanin biosynthesis-associated genes are upregulated in *cct8* during vernalization treatment

GO analysis revealed that the GO terms associated with anthocyanin biosynthesis, such as 'flavonoid metabolic process' and 'pigment metabolic process', were overrepresented in the *cct8* mutant subjected to cold treatment for 20 days. As the *cct8* mutant exhibited pigment accumulation (Fig. 12), the expression levels of anthocyanin biosynthesis-associated genes were examined using the RNAseq data. Regulatory (*PAP2*, *MYB11*, *MYB12*, and *MYB111*) and structural (*CHS*, *F3H*, *PAL1*, *DFR*) genes were shown to be upregulated in the RNAseq data (Xu et al., 2017) (Fig. 24B and C). Moreover, *HY5* and *HYH*, which are bZIP transcription factors that positively regulate the expression of both regulatory and structural genes in anthocyanin biosynthesis pathways (Catalá et al., 2011; Zhang et al., 2011), were also found to be upregulated in *cct8* mutants subjected to cold treatment (Fig. 24A). These results suggest that pigment accumulation in cold-treated *cct8* mutants is due to the upregulation of anthocyanin biosynthesis-associated genes.

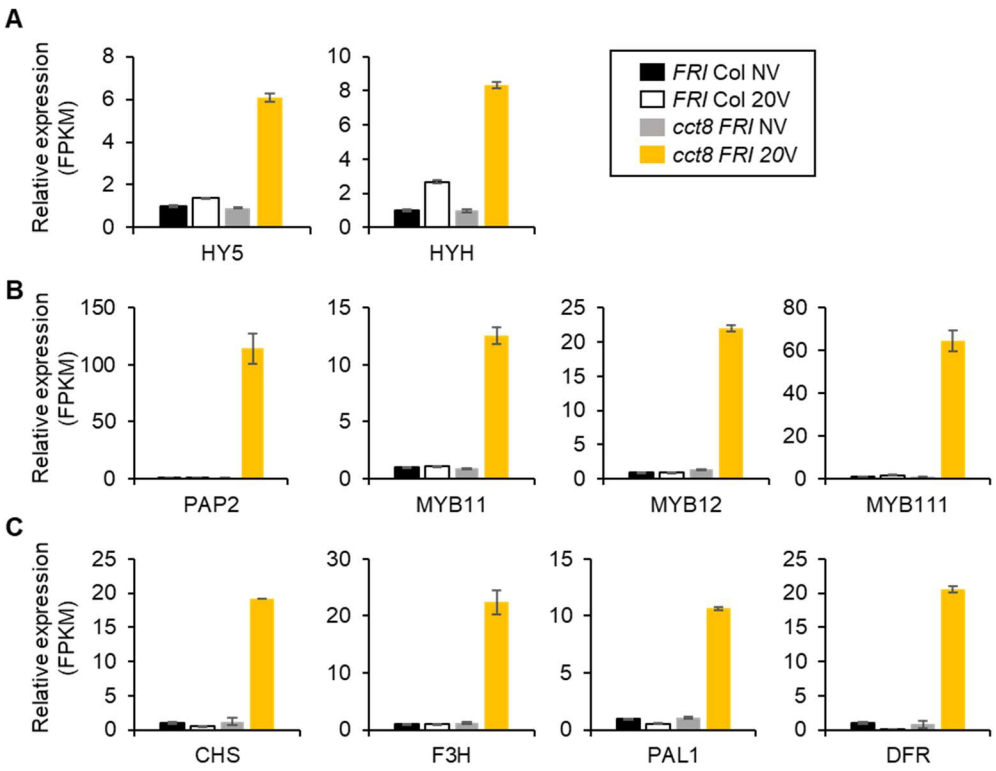

Figure 25. Anthocyanin biosynthesis-associated genes were upregulated in vernalized *cct8*.

Expression levels of (A) *HY5* and *HYH* or (B) Anthocyanin biosynthesis regulatory genes or (C) Anthocyanin biosynthesis structural genes in *FRI* Col and *cct8 FRI* during vernalization were determined by RNAseq. Expression by RNA-seq is expressed in normalized FPKM. NV, non-vernalized; 20V, 20 d vernalized. Data are shown as means ± SD for two replicates.

2.3.8. *VIN3* has a diurnal rhythm during vernalization treatment

Genes with EE in their promoter show diurnal oscillation of gene expression, regulated by MYB-like transcription factors, such as *CCA1*, *LHY* and *RVE*. Therefore, the effect of the circadian rhythm on *VIN3* expression was assessed. First, *VIN3* levels in *FRI* Col during vernalization treatment were examined at 4 hr intervals to verify that *VIN3* expression shows a circadian rhythm. *VIN3* levels showed a diurnal rhythm over 20 days of vernalization treatment, with peak of expression at ZT 4 (Fig. 25A). Next, I assessed to whether that diurnal rhythm was controlled by light or circadian clock. Twenty-day vernalized *FRI* Col was subjected to free-running with continuous light, and *VIN3* levels were analyzed at 4 hr intervals. I found that *VIN3* expression oscillation persists in 20V *FRI* Col, indicating that the circadian clock, instead of white light, is responsible for the diurnal regulation of *VIN3* (Fig. 25B). Such findings are consistent with previous reports that *VIN3* has diurnal rhythm and is regulated by circadian clock (Hepworth et al., 2018; Kyung et al., 2022).

Next, whether initial *VIN3* induction is gated by the circadian clock was verified. First, the induction efficiency of *VIN3* was assessed. A subset of seedlings was subjected or not subjected to cold treatment for 4 hrs at different ZT timepoints with 4 hr interval, and then collected for RT-qPCR. Compared to control seedlings that were not treated with cold, cold-treated seedlings showed enhanced induction when cold treatment was initiated at daytime (Fig. 26A). This result suggests that this time-dependent *VIN3* induction is regulated by the circadian clock. However, the result could be interpreted to indicate that

light is involved in *VIN3* regulation. To solve this problem, A gating experiment was performed to check whether *VIN3* induction is dependent on light or the circadian clock. Col-0 seedlings grown in an 8-h light/16-h dark cycle for 10 days were transferred to continuous light conditions for 3 days and subjected to cold exposure for 4 hrs at different zeitgeber times at 4 hr intervals. *VIN3* levels were strongly induced after cold treatment at ZT 76 and ZT 80, which is a subjective day, indicating that *VIN3* induction is gated by the circadian clock (Fig. 26B).

Then, the effect of the circadian rhythm on *VIN3* expression was assessed in the wild-type and *cct8 FRI* mutant plants. Both wild-type and *cct8 FRI* exhibited similar *VIN3* expression patterns, with a peak of expression at ZT 8 in the non-vernalized condition. However, in 20V and 40V plants, *cct8 FRI* exhibited impaired rhythmic expression, while wild-type *FRI* Col exhibited a rhythmic expression pattern (Fig. 27A). Interestingly, *VIN3* levels at night, such as at ZT 16 or ZT 20, were similar in *FRI* Col and *cct8 FRI*, indicating that *CCT8*-mediated *VIN3* regulation is not in effect at night. Experiments using *cct8-1 FRI* showed similar results, indicating that the absence of rhythmic expression of *VIN3* during vernalization is a result of the mutation in *CCT8* (Fig. 27B). Taken together, these findings indicate that the circadian clock regulator, which is inactive at night, strongly shapes *VIN3* rhythms during vernalization.

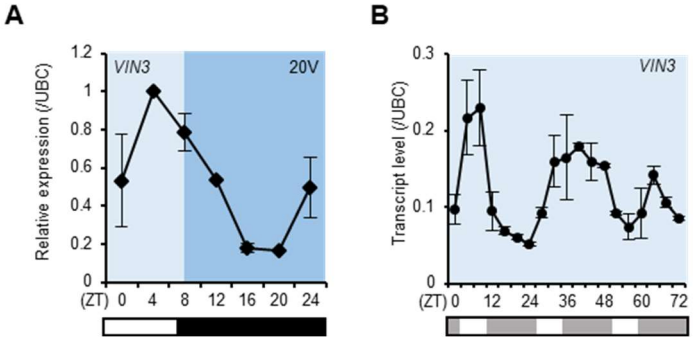

Figure 26. Rhythmic expression of *VIN3* is regulated by circadian clock.

(A) Rhythmic expression of *VIN3* during vernalization treatment. *FRI* Col seedlings were vernalized and harvested at indicated ZT timepoint. Transcript level of *VIN3* is determined by RT-qPCR. The transcript levels were normalized to UBC. Data are shown as means ± SEM for three replicates. The white and black boxes indicate the day and night, respectively.

(B) The free-running rhythms of *VIN3* level in continuous light. 20 d vernalized *FRI* Col was subjected to free-running with continuous light and analyzed at 4 hr intervals. The transcript levels were normalized to *UBC*. Data are shown as means ± SEM for two replicates. The x-axis indicates exposed time to continuous light. The white and pale grey boxes indicate the subjective day and night, respectively.

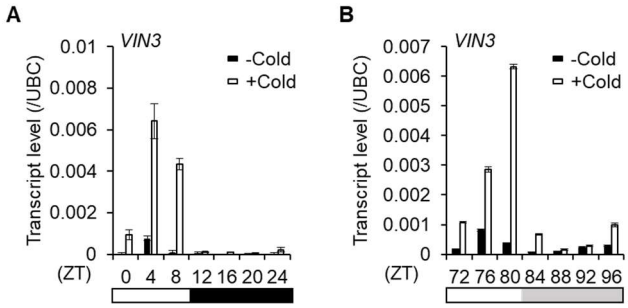

Figure 27. Initial *VIN3* induction is gated by circadian clock.

(A) Transcript level of *VIN3* in Col-0 with or without 4 hrs of cold treatment at indicated ZT timepoint. The transcript levels were normalized to *UBC*. Data are shown as means ± SEM for three replicates. The white and black boxes indicate the day and night, respectively. (B) A gating experiment. 10-day-old Col-0 seedlings grown in an 8-h light/16-h dark cycle were transferred to continuous light for 3 days and subjected to cold exposure for 4 hrs at indicated timepoint and harvested for RT-qPCR. The transcript levels were normalized to *UBC*. Data are shown as means ± SEM for three replicates. The x-axis indicates exposed time to continuous light. The white and pale grey boxes indicate the subjective day and night, respectively.

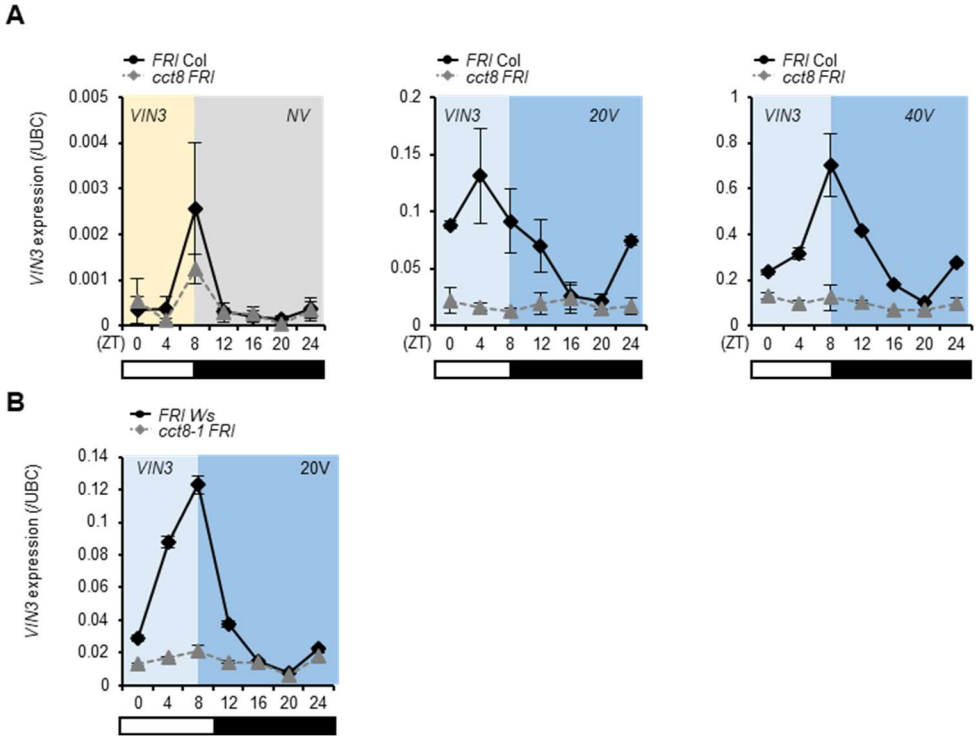

Figure 28. Effect of *cct8* on rhythmic expression of *VIN3*.

(A) Rhythmic expressions of *VIN3* in wild-type and *cct8 FRI*, according to various durations of vernalization treatment. The transcript levels were normalized to *UBC*. Data are shown as means ± SEM for three replicates. The white and black boxes indicate the day and night, respectively.

(B) Rhythmic expressions of *VIN3* in *FRI* Ws-2 and *cct8-1 FRI* after 20 days of vernalization treatment. The transcript levels were normalized to *UBC*. Data are shown as means ± SEM for three replicates. The white and black boxes indicate the day and night, respectively.

2.3.9. Circadian clock is disturbed by *cct8* mutation during vernalization

As the circadian clock regulates *VIN3* expression, the expression pattern of clock genes in the chaperonin mutant under vernalization treatment was examined. Initially, the expression patterns of clock genes including *CCA1*, *PRR9*, *PRR7*, *PRR5*, *GI*, and *TOC1,* were examined in wild-type and *cct8* after 20 days of cold treatment. *CCA1* expression exhibited decreased amplitude, and its peak of expression was shifted to ~4 hr later than that of the wild-type (Fig. 28). Similarly, *TOC1* exhibited a shifted expression peak, although no amplitude changes were present (Fig. 28). Expression patterns of other investigated clock genes, except *PRR7*, were also exhibited a delayed phase, although each of them showed a different amplitude (Fig. 28). These data suggest that the circadian clock in *cct8* has a robust diurnal rhythm with phase delaying, which is common aspect can be found in clock-gene mutants, especially in activator mutants (Shalit-Kaneh et al., 2018b).

As *VIN3* exhibits a midday peak and has an EE motif in its promoter region, I hypothesized that an EE-binding morning clock gene is responsible for impaired *VIN3* expression in *cct8.* However, CCA1 and LHY, the most known EE-binding transcription factors, are transcriptional repressors, in contrast with the apparent role of the EE in the *VIN3* promoter as an activator of *VIN3* expression. RVEs are homologs of CCA1 and LHY, and RVEs are known to be EE-binding transcriptional activators, which fits well with the *VIN3* regulator hypothesis. Therefore, the expression pattern of *RVE* family genes, including *RVE3, RVE4, RVE5, RVE6*, and *RVE8* in *cct8* was examined. *RVE* genes

exhibited impaired diurnal rhythm in *cct8* with reduced expression level (Fig. 29), which suggests that the chaperonin complex is responsible for the proper gene expression pattern of *RVEs* during vernalization. Experiments using *cct8-1* showed similar results, but more severe *RVE* downregulation, suggest that severity of *cct8-1* is reflected on rhythmic expression of *RVE* (Fig. 30).

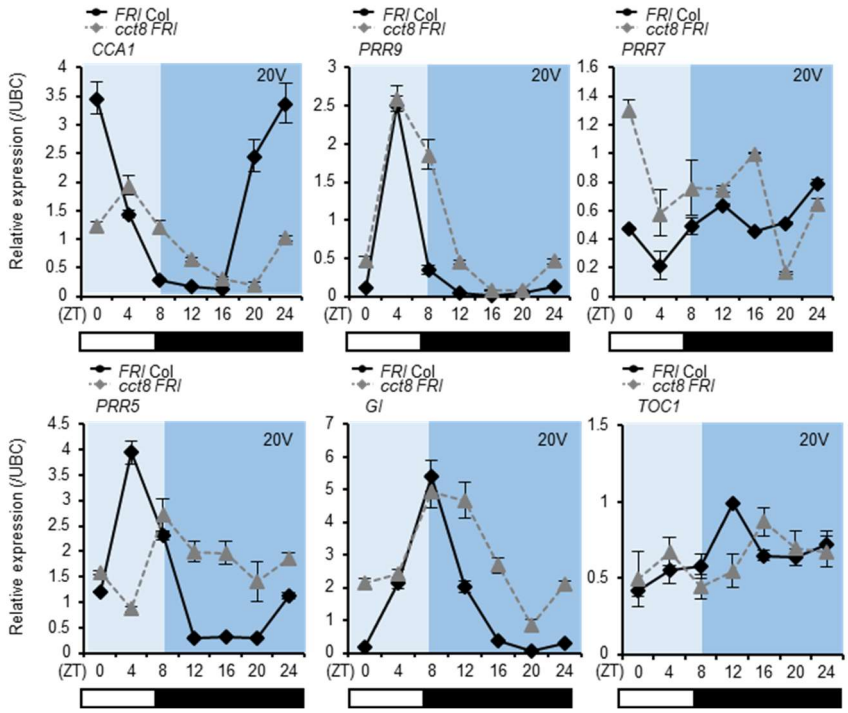

Figure 29. Rhythmic expression of clock genes is disturbed in *cct8*

Rhythmic expression of clock genes, *CCA1*, *PRR9*, *PRR7*, *PRR5*, *GI*, and *TOC1* in wild-type and *cct8 FRI*, during 20 days of vernalization treatment. The transcript levels were normalized to *UBC*. Data are shown as means ± SEM for three replicates. The white and black boxes indicate the day and night, respectively.

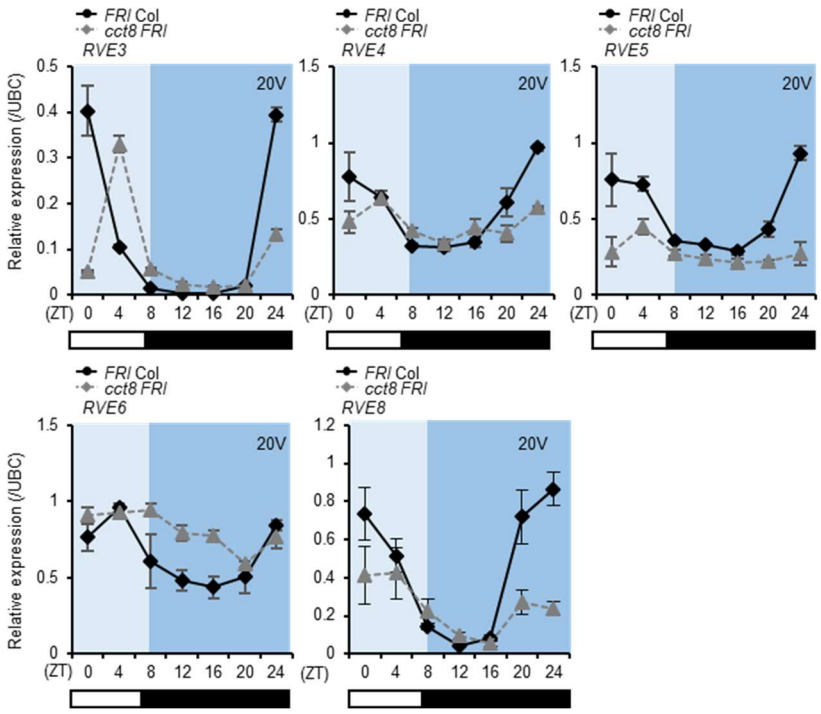

Figure 30. Rhythmic expression of *RVE* genes is disturbed in *cct8*.

Rhythmic expression of *RVE* genes, *RVE3*, *RVE4*, *RVE5*, *RVE6*, and *RVE8* in wild-type and *cct8 FRI*, during 20 days of vernalization treatment. The transcript levels were normalized to *UBC*. Data are shown as means ± SEM for three replicates. The white and black boxes indicate the day and night, respectively.

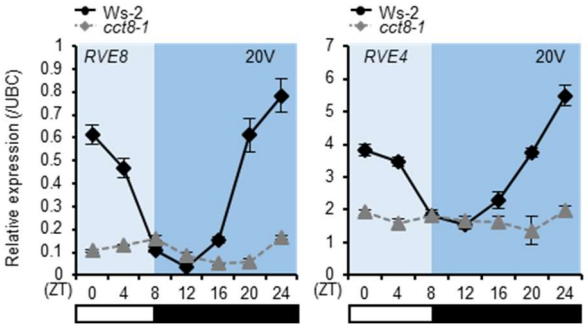

Figure 31. Rhythmic expression of *RVE4* and *RVE8* is disturbed in *cct8-1*.

Rhythmic expression of *RVE4* and *RVE8* in Ws-2 and *cct8-1*, during 20 days of vernalization treatment. The transcript levels were normalized to *UBC*. Data are shown as means ± SEM for three replicates. The white and black boxes indicate the day and night, respectively.

2.3.10. Circadian regulators, *RVEs,* are required for vernalization response

Because *RVE* gene expression in *cct8* was disrupted under vernalization treatment, I assessed the expression level of *VIN3* in several *rve* mutants to dissect the regulation process of *VIN3* by *RVEs*. Among 8 *RVE* family genes, *RVE3, RVE4, RVE5, RVE6* and *RVE8* have been reported to have clock regulation roles. Therefore, the expression pattern of *VIN3* at ZT 4 was examined in *rve3, rve4, rve5, rve6, rve8* (single), *rve468* (triple), *rve34568* (quintuple) under long-term cold treatment. Each single mutant showed a slightly reduced *VIN3* level, whereas the triple and quintuple mutants showed substantially reduced *VIN3* levels (Fig. 31A and B). Moreover, *rve34568* showed reduced *VIN3* levels at every assayed time point during and after long-term cold treatment (Fig. 31C).

Next, diurnal gene expression of *VIN3* was examined to determine whether circadian regulation of *VIN3* was regulated by *RVEs.* Therefore, diurnal rhythm of *VIN3* level in 20V Col-0, *cca1 lhy*, and *rve34568* were examined. Col-0 showed a rhythmic expression pattern with a peak of expression at ZT 8, while *cca1 lhy* showed reduced amplitude with a shifted peak of expression at ZT 4 (Fig. 32A). *rve34568* exhibited a disrupted diurnal rhythm of *VIN3* expression, similar to the expression pattern in *cct8* (Fig. 32A). I proceeded to verify that the clock gene expression pattern is affected by mutations in other clock genes. *RVE8* expression in *cca1 lhy* mutants and *CCA1* expression in *rve34568* mutants were assessed. Surprisingly, *RVE8* expression was not affected in the *cca1 lhy* mutant, whereas *CCA1* expression was reduced in the *rve34568* mutant (Fig. 32B). This

suggests that *RVE8* is regulated independently from *CCA1* or *LHY* under cold exposure, and in contrast, *CCA1* is affected by the absence of *RVEs.* Considering that the *RVE8* level in *cca1 lhy* is similar to that in Col-0 and its amplitude is not significantly changed, *VIN3* expression seems to be largely affected by *RVE* genes.

Next, I introduced *35S::myc-RVE8* into *rve34568*, to examine whether ectopic expression of *RVE8* can recapitulate reduced *VIN3* levels in *rve34568.* Then, *VIN3* levels in 20V treated Col-0, *rve34568,* and *35S::myc-RVE8 rve34568* plants were examined by RT-qPCR. Ectopic expression of *RVE8* was sufficient to recapitulate the reduced *VIN3* levels in *rve34568* (Fig. 33). However, introduction of *35S::myc-RVE8* into *cct8* failed to recover the reduced *VIN3* level in *cct8* during vernalization treatment, while RVE8 protein levels were not affected by the *cct8* mutation (Fig. 34). These data suggest that stability of RVE8 is not affected by attenuated chaperonin. Also, data suggests that ectopic expression of *RVE8* is not sufficient to recover the *VIN3* level in *cct8*.

Finally, to assess the effect of loss of *RVEs* on the vernalization response, the flowering time of the *rve34568* quintuple mutant was measured. For precise analysis, *pFRI::gFRI* was introduced into Col-0 and the *rve34568* mutant to enhance vernalization sensitivity. First-generation transgenic *pFRI::gFRI* and *pFRI::gFRI rve34568* showed similar flowering times under non-vernalized conditions (Fig. 35). However, *pFRI::gFRI rve34568* plants exhibited delayed flowering time compared to *pFRI::gFRI* plants (Fig. 35). These data indicate that *RVEs* are required for proper vernalization responses.

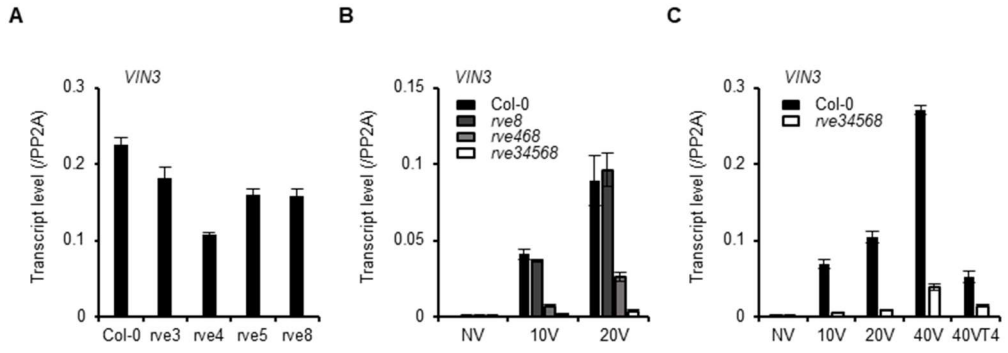

Figure 32. Effect of degree of *rve* mutation on *VIN3* level during vernalization treatment.

(A) *VIN3* transcript level in 20 days cold exposed Col-0, *rve3*, *rve4*, *rve5*, *rve8*.

(B) Effect of grade of mutation of *RVEs* on *VIN3* level. *VIN3* transcript level in NV, 10V and 20V Col-0, *rve8*, *rve468*, *rve34568* was examined by RT-qPCR.

(C) Time course analysis of *VIN3* level in wild-type and *rve34568* under all conditions, including before and after vernalization. The transcript levels were normalized to *PP2A*. Data are shown as means ± SEM for three replicates.

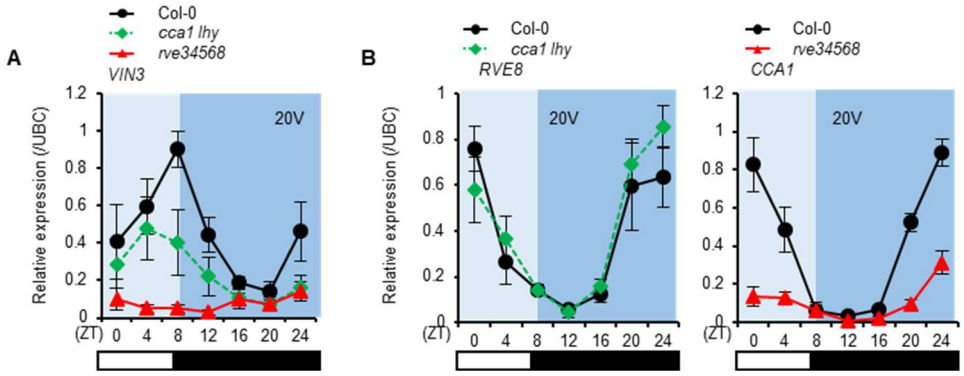

Figure 33. *VIN3* expression is largely affected by *RVE* genes.

(A) Diurnal *VIN3* expression in Col-0, *cca1 lhy*, and *rve34568* during vernalization treatment. 20V seedlings were harvested at indicated ZT timepoint and analyzed by RT-qPCR.

(B) Diurnal *RVE8* expression in Col-0 and *cca1 lhy*, and *CCA1* expression in Col-0 and *rve34568*. The transcript levels were normalized to *UBC*. Data are shown as means ± SEM for three replicates. The white and black boxes indicate the day and night, respectively.

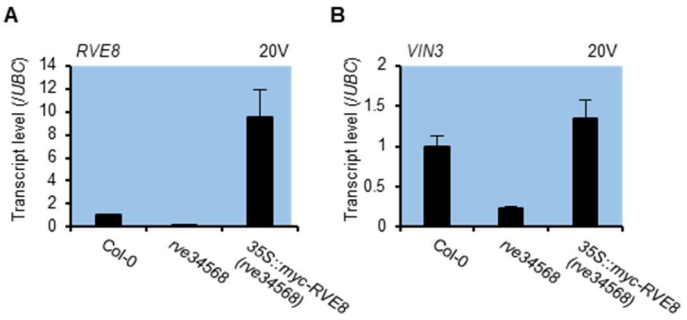

Figure 34. Ectopic expression of *RVE8* recapitulates the reduced *VIN3* levels in *rve34568*.

(A and B) *RVE8* and *VIN3* expression in Col-0, *rve34568*, and myc-RVE8 transgenic seedling after 20 days of vernalization treatment. Transcript levels were analyzed by RT-qPCR. The transcript levels were normalized to *UBC*. Data are shown as means ± SEM for three replicates.

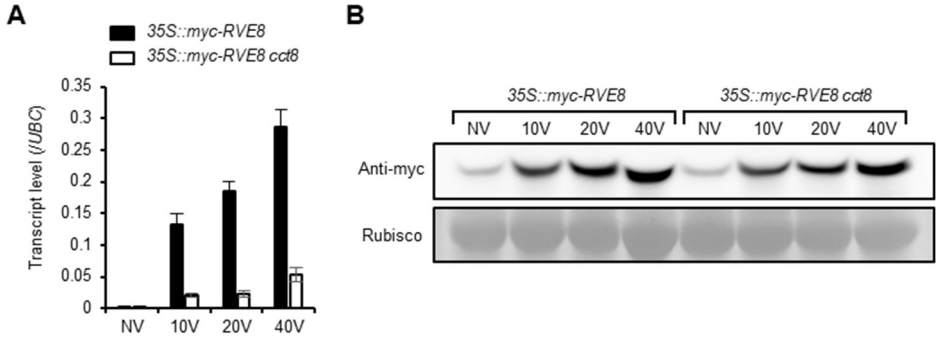

Figure 35. Ectopic expression of *RVE8* fails to recapitulate the reduced *VIN3* level in *cct8*.

(A) *VIN3* level in *35S::myc-RVE8* and *35S::myc-RVE8 cct8* during vernalization treatment. NV, non-vernalized; 10V, 20V, 40V, 10, 20, 40 d vernalized respectively. The transcript levels were normalized to *UBC*. Data are shown as means ± SEM for three replicates.

(B) Immunoblot analysis of the HsfB2b-eGFP protein extracted from vernalized seedlings of *35S::myc-RVE8* and *35S::myc-RVE8 cct8*. Rubisco was used as loading control. NV, non-vernalized; 10V, 20V and 40V, 10 d, 20 d, 40 d vernalized, respectively.

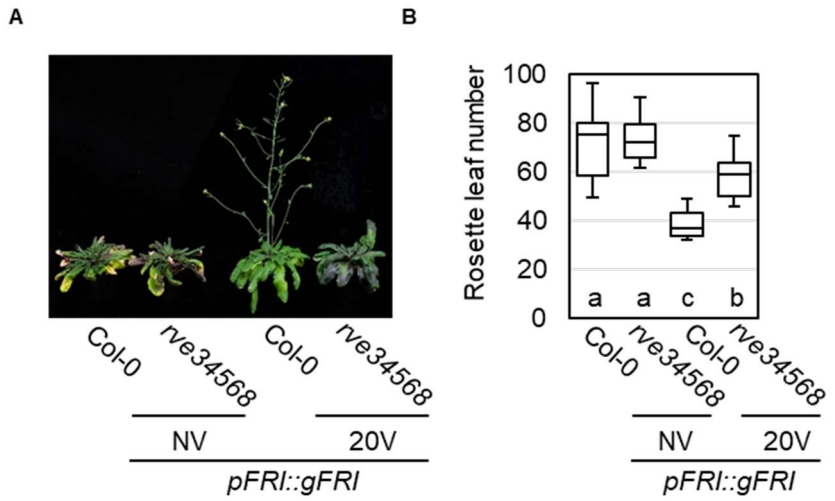

Figure 36. *RVEs* are required for proper vernalization responses.

(A) Images of *pFRI::gFRI* transgenic line and *pFRI::gFRI rve34568* transgenic line, without (NV) or with 20 d (20V) of vernalization. Images captured when *pFRI::gFRI rve34568* plants were bolted.

(B) Flowering time is presented as a box plot. The number of primary leaves when bolting was counted for flowering time. The center lines indicate the medians. Box limits indicate the 25th and 75th percentiles. Different letters represent a significant difference ($P < 0.05$) determined by one-way analysis of variance (ANOVA) with post hoc Tukey test.

2.3.11. *RVE8* activates *VIN3* by binding to the gene promoter

I hypothesized that RVEs directly activate *VIN3* using the EE motif located in the *VIN3* promoter. I performed electrophoresis mobility shift assays to determine whether RVE directly binds to the EE in the *VIN3* promoter. RVE4 and RVE8 were expressed as an MBP fusion protein (MBP-RVE4, MBP-RVE8) in *E. coli*, and purified by affinity chromatography. Following incubation with the EE and G-box containing promoter fragment of *VIN3*, shifted bands were detected, and the addition of a cold competitor led to the loss of the shifted bands (Fig. 36A and B). Next, the effect of mutations in the G-Box or EE motif in promoter fragment of *VIN3* was assessed. Mutations in the EE motif or both the G-Box or EE motif did not abolish the shifted band, while mutations in G-Box completely abolished the shifted band (Fig. 36A and B). These results indicate that RVE4 and RVE8 bind to the EE motif in the *VIN3* promoter and that this binding is independent of the G-Box, found to be overrepresented cis-element by motif analysis.

Subsequently, chromatin immunoprecipitation (ChIP) using *35S::myc-RVE8* transgenic plants was conducted to examine the *in vivo* binding of *RVE8* to the *VIN3* promoter. myc-RVE8 was enriched in the promoter region near the EE motifs in 20V plants, but that enrichment was not found in non-vernalized plants (Fig. 37A and B). This result indicates that RVE8 binds to the *VIN3* promoter and that this binding is regulated by the presence of cold temperatures.

A transient expression assay was conducted to further identify whether RVEs function as transcriptional activators at the *VIN3* promoter. Because *RVE8* was reported to localize in the cytosol under normal conditions (Kidokoro et al., 2021), *RVE8* was fused to NLS-GFP and expressed with the *pVIN3::LUC* reporter in protoplast cells from 5-week-old *Arabidopsis* plants. The fusion protein increases reporter activity compared with NLS-GFP, suggesting that RVE8 directly binds to the EE on the *VIN3* promoter and acts as a transcriptional activator of *VIN3* (Fig. 38).

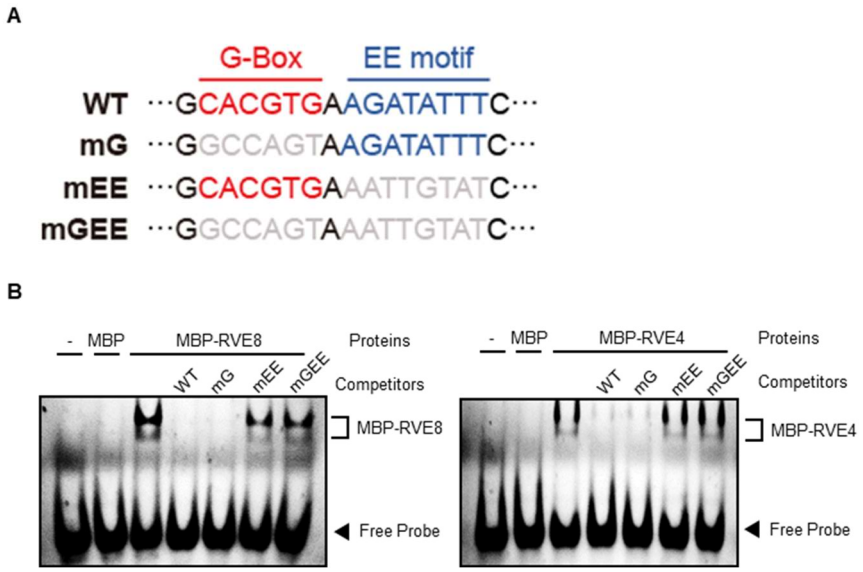

Figure 37. *In vitro* binding of the recombinant RVE8 and RVE4 to *VIN3* promoter sequence.

(A) Description of probe or competitor sequences for EMSA. WT, wild-type sequence; mG, mEE, mGEE represent mutations in G-box, EE, and both G-box and EE, respectively. Gray indicates replaced sequence for mutations.

(B) EMSA assay using recombinant RVE4 or RVE8. Purified recombinant MBP-RVE8, MBP-RVE4 or MBP was incubated with Cy5-labeled 30 bp sequences including EE and G-box as WT probes. Unlabeled competitor DNA (100x molar excess) was added to each reaction, as indicated.

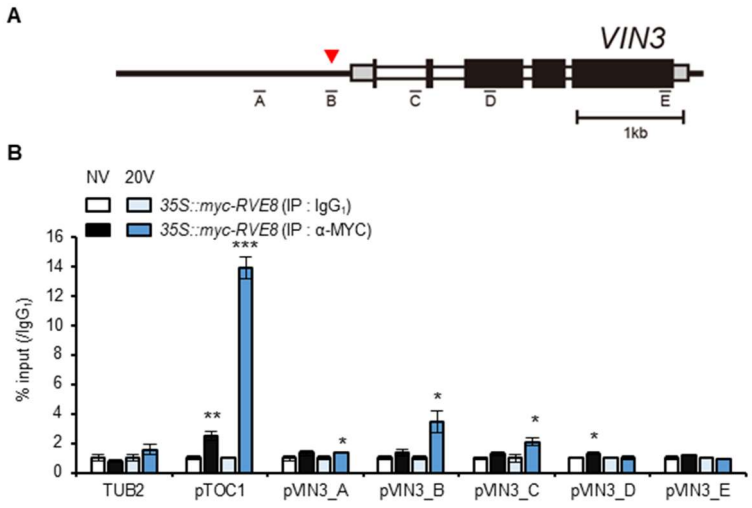

Figure 38. *In vivo* binding of the RVE8 to *VIN3* promoter.

(A) Schematic diagram of *VIN3* with PCR amplicons indicated as letters A-E used for ChIP-qPCR. Red arrowhead marks the position of the EE.

(B) ChIP experiments showing RVE8 occupancy across *VIN3*. The *35S::myc-RVE8* plants without (NV) or with 20 days of cold (20V) were collected at ZT4 for ChIP analysis. Enrichment shown as percentage of input DNA, versus IgG control antibodies. *TUB2* promoter was used as negative control, and *TOC1* promoter was used as positive control. Data are shown as means ± SEM for three replicates. Asterisks indicate a significant difference (*P<0.05, **P<0.01, ***P<0.001; Student's t test).

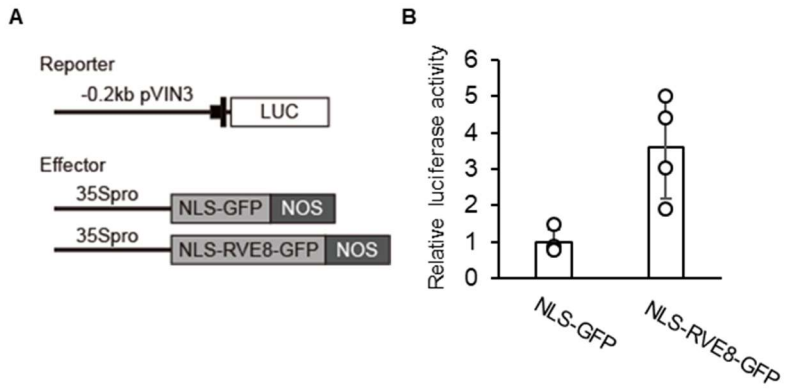

Figure 39. RVE8 acts as a transcriptional activator of *VIN3*.

(A) A schematic diagram showing the vector constructs used for the luciferase assay. The reporter harbors -0.2kb promoter, 5'-UTR, and the 1st exon of *VIN3*. LUC, 35Spro, NLS, and NOS indicate luciferase gene, the 35S promoter, nuclear localization sequence, and NOS terminator, respectively. RVE8-coding sequence were amplified and fused in-frame to control vector containing NLS-GFP.

(B) Luciferase assay showing that *RVE8* activates *VIN3* promoter. Reporter construct and each effector construct were co-transfected into *Arabidopsis* mesophyll protoplasts. Relative luciferase activity was normalized to that of the NLS-GFP control. Data are shown as means ± SD for four replicates. Dots represent each data-point.

IV. Discussion

In this study, I found that cytosolic chaperonin complex functions in the signal transduction process under a specific abiotic stress condition, long-term cold exposure. Chaperonin was required during the cold period to sustain the circadian rhythm controlled by several clock genes (Fig. 27). Among the clock genes, *RVE* family genes were shown to lose rhythm in *cct8* (Fig. 28). I showed that one of those genes, *RVE8,* binds to the *VIN3* promoter and directly regulates *VIN3* expression*,* which plays an important role in vernalization (Fig. 35-37). Indeed, *VIN3* showed a diurnal expression pattern under long-term cold, and this pattern was mainly regulated by *RVEs* (Fig. 25, 30, 31). Both the *cct8* and *rve34568* mutants showed a delayed flowering time after vernalization treatment, suggesting that chaperonin-mediated RVE regulation is responsible for proper vernalization responses (Fig. 19, 34). Collectively, my findings demonstrate that chaperonin affects the circadian rhythm of *RVEs*, and direct regulation of *VIN3* by *RVE* produces *VIN3* rhythms for proper vernalization during long-term cold exposure (Fig. 39).

Previously, *Arabidopsis* chaperonin was reported to have functions in cell-to-cell trafficking for stem cell regulation, tubulin regulation, and phosphatase regulation through protein folding mechanism, which are warm-condition functions (Ahn et al., 2019; Xu et al., 2011). In my study, I found that the chaperonin complex has a novel temperature-dependent regulatory function. Moreover, the *cct8* mutant showed temperature-dependent pleiotropy, such as retarded growth and pigment accumulation when exposed to long-term cold (Fig. 12). These findings suggest the possibility that chaperonin may be involved in

various processes required for adaptation to chronic environmental changes, such as long-term cold.

For a long time, RVE genes have been suggested to serve as circadian clock regulators. However, the upstream regulators of these genes have not yet been intensively studied. Whether the substrate specificity of CCT8 or the folding activity of chaperonin affects the regulation of *RVE* expression remains unclear. Nevertheless, I identified CCT8 as one of the upstream regulators of *RVEs*. Considering that the general function of chaperonin is protein folding, unknown protein X, a regulator of the expression of RVEs, is likely to be folded in a chaperonin-assisted manner. There are several stress-related transcription factors that regulate the activity of core clock components under cold stress conditions. One such potential candidate transcription factor is HsfB2b. HsfB2b regulates the circadian clock by regulating the expression of the clock gene *PRR7*, and its protein structure is predicted to contain disordered domains at the N-terminal and C-terminal ends, which are commonly considered to be domains that are stabilized by chaperones. Further studies are needed to elucidate the possible involvement of HsfB2b in the chaperonin-mediated regulation of *VIN3* expression.

Circadian clock genes have been shown to regulate the cold response through many clock components, including *CCA1, LHY, PRR5, PRR7, PRR9, TOC1*, and the evening complex (Dong et al., 2011; Keily et al., 2013; Liu et al., 2013; Nagel et al., 2015). *CCA1* and *LHY* were long considered regulators of the cold response, including regulation of *VIN3* (Hepworth et al., 2018; Kyung et al., 2022). Because *VIN3* expression showed a

diurnal rhythm and *VIN3* has an EE on its promoter, *CCA1* and *LHY* were indicated as upstream regulators of *VIN3.* While *RVE* genes are also capable of binding to EEs, they were not previously considered *VIN3* regulators. In this study, I analyzed the *VIN3* expression pattern using *cca1 lhy* and *rve34568* mutants, which were reported to have mutation in cycling repressor or activator of circadian clocks, respectively (Shalit-Kaneh et al., 2018b). Among Col-0, *cca1 lhy*, and *rve34568,* only *rve34568* showed an impaired *VIN3* rhythm under long-term cold, whereas the others showed rhythmic expression of *VIN3* (Fig. 31). In addition, transcript levels and rhythmic expression levels of *RVE8* in *cca1 lhy* were not changed from those in the wild-type after 20 days of cold exposure (Fig. 31). Overall, my findings suggest that *RVE8* expression is slightly affected by *CCA1* or *LHY* under long-term cold exposure and that circadian clock-mediated regulation of *VIN3* expression mainly occurs via *RVEs*. The reduction of the *VIN3* levels observed in *cca1 lhy* seems to be a consequence of complex feedback loops of the molecular clock. Considering that RVE4 and RVE8 are involved in cold acclimation by activating the transcription of *CBF3*, it is also possible that RVEs regulate other cold responses in addition to vernalization via EE-containing genes depending on the environmental context.

Previous research has reported found that mutations of EE or G-box result in the partial expression of *VIN3* after vernalization treatment (Kyung et al., 2022), indicating that both EE-binding and G-Box-binding transcription factors are required for the proper activation of *VIN3*. In the present study, although the rhythmic expression of *VIN3* was disrupted in *cct8* mutants after under vernalization (Fig. 27), the *VIN3* levels during night time were

similar in both the wild-type and *cct8*, but were elevated compared to those observed under non-vernalized conditions (Fig. 27). This suggests that the basal expression level of *VIN3* is elevated by the increase in the duration of the cold period and that RVE-mediated transcriptional activation is responsible for the rhythmic expression of *VIN3* but not for the basal *VIN3* expression level (Fig. 40). It was found that due to mutations of both EE and G-box, the *VIN3* promoter almost completely lost its activity under long-term cold exposure (Kyung et al., 2022). Thus, G-Box is likely to be responsible for the elevation of the basal expression level of *VIN3*. On the other hand, considering that *Arabidopsis* could be vernalized even in the dark, during which the rhythmic expression of the circadian clock is abolished (Chandler and Dean, 1994; Dalchau et al., 2011), EE-mediated regulation is likely to serve as a mechanism that contributes to rhythmic *VIN3* expression by rendering environmental signals, which are incorporated into circadian oscillators, for optimal developmental transition (Fig. 40).

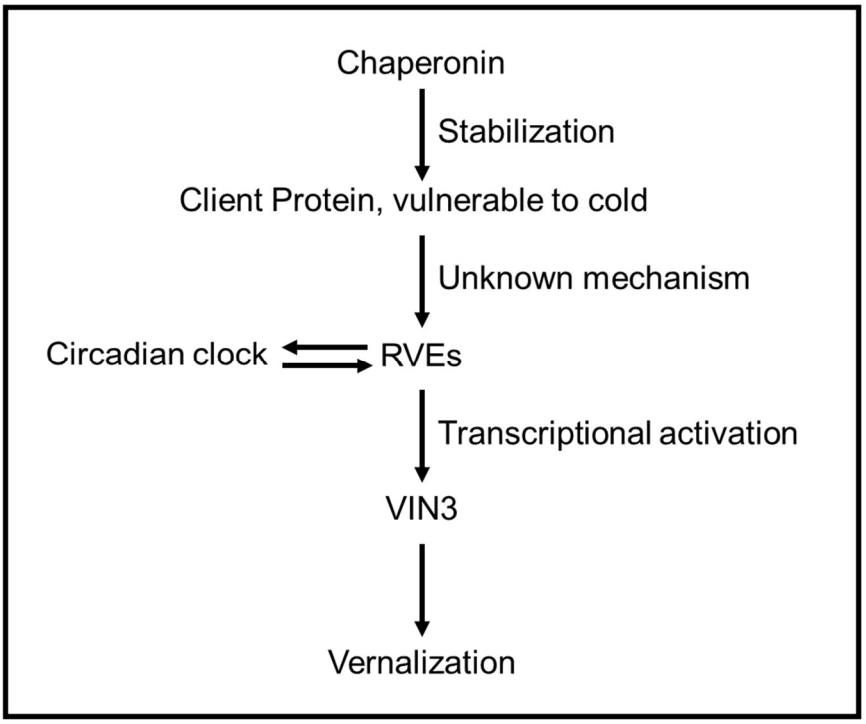

Figure 40. Brief mechanism of chaperonin mediated *VIN3* regulation via circadian clock.

In prolonged cold conditions, chaperonin-mediated mechanism stabilizes unknown protein vulnerable to cold. Unknown protein directly or indirectly regulates RVEs, a transcriptional activator involved in circadian clock regulation. RVE adjusts diurnal rhythm regulated by clock genes, and activates transcription of *VIN3*, a gene required for vernalization response.

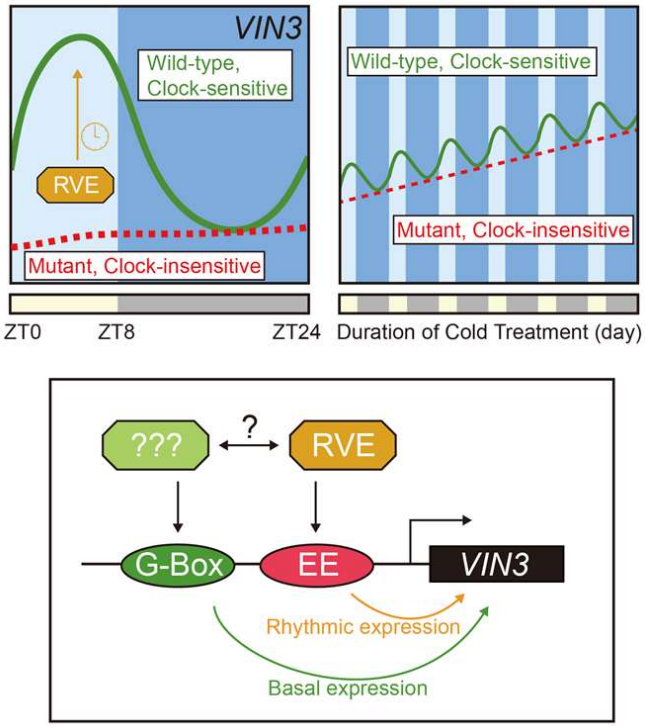

Figure 41. EE is required for overlaying clock oscillation to *VIN3* expression.

On daily scale, expression level of *VIN3* is elevated by RVE-mediated transcriptional activation during daytime. During nighttime, when RVE is not exist, expression level of *VIN3* is showed as basal expression level. However, the basal expression level is elevated by the duration of the cold period. EE-mediated regulation is likely to serve as a mechanism that contributes to rhythmic *VIN3* expression by rendering environmental signals, which are incorporated into circadian oscillators, for optimal developmental transition.

Reference

Ahn, H.-K., J.-T. Yoon, I. Choi, S. Kim, H.-S. Lee, and H.-S. Pai. 2019. Functional characterization of chaperonin containing T-complex polypeptide-1 and its conserved and novel substrates in Arabidopsis. *Journal of Experimental Botany*. 70:2741-2757.

Alabadí, D., T. Oyama, M.J. Yanovsky, F.G. Harmon, P. Más, and S.A. Kay. 2001. Reciprocal regulation between TOC1 and LHY/CCA1 within the Arabidopsis circadian clock. *Science*. 293:880-883.

Amin, J., J. Ananthan, and R. Voellmy. 1988. Key features of heat shock regulatory elements. *Mol Cell Biol*. 8:3761-3769.

Anderson, J.T., C.-R. Lee, and T. Mitchell-Olds. 2011. Life-history QTLS and natural selection on flowering time in Boechera stricta, a perennial relative of Arabidopsis. *Evolution*. 65:771-787.

Andrási, N., A. Pettkó-Szandtner, and L. Szabados. 2021. Diversity of plant heat shock factors: regulation, interactions, and functions. *Journal of Experimental Botany*. 72:1558-1575.

Antoniou-Kourounioti, R.L., J. Hepworth, A. Heckmann, S. Duncan, J. Qüesta, S. Rosa, T. Säll, S. Holm, C. Dean, and M. Howard. 2018. Temperature Sensing Is Distributed throughout the Regulatory Network that Controls FLC Epigenetic Silencing in Vernalization. *Cell Systems*. 7:643-655.e649.

Banti, V., F. Mafessoni, E. Loreti, A. Alpi, and P. Perata. 2010. The heat-inducible transcription factor HsfA2 enhances anoxia tolerance in Arabidopsis. *Plant physiology*. 152:1471-1483.

Bechtold, U., W.S. Albihlal, T. Lawson, M.J. Fryer, P.A. Sparrow, F. Richard, R. Persad, L. Bowden, R. Hickman, C. Martin, J.L. Beynon, V. Buchanan-Wollaston, N.R. Baker, J.I. Morison, F. Schöffl, S. Ott, and P.M. Mullineaux. 2013. Arabidopsis HEAT SHOCK TRANSCRIPTION FACTORA1b overexpression enhances water productivity, resistance to drought, and infection. *J Exp Bot*. 64:3467-3481.

Bond, D.M., E.S. Dennis, B.J. Pogson, and E.J. Finnegan. 2009a. Histone acetylation, VERNALIZATION INSENSITIVE 3, FLOWERING LOCUS C, and the vernalization response. *Mol Plant*. 2:724-737.

Bond, D.M., I.W. Wilson, E.S. Dennis, B.J. Pogson, and E. Jean Finnegan. 2009b. VERNALIZATION INSENSITIVE 3 (VIN3) is required for the response of Arabidopsis thaliana seedlings exposed to low oxygen conditions. 59:576-587.

Bond, D.M., I.W. Wilson, E.S. Dennis, B.J. Pogson, and E. Jean Finnegan. 2009c. VERNALIZATION INSENSITIVE 3 (VIN3) is required for the response of Arabidopsis thaliana seedlings exposed to low oxygen conditions. *The Plant Journal*. 59:576-587.

Busch, W., M. Wunderlich, and F. Schöffl. 2005. Identification of novel heat shock factor-dependent genes and biochemical pathways in Arabidopsis thaliana. *The Plant Journal*. 41:1-14.

Catalá, R., J. Medina, and J. Salinas. 2011. Integration of low temperature and light signaling during cold acclimation response in Arabidopsis. *Proceedings of the National Academy of Sciences*. 108:16475-16480.

Chandler, J., and C. Dean. 1994. Factors influencing the vernalization response and flowering time of late flowering mutants of Arabidopsis thaliana (L.) Heynh. *Journal of Experimental Botany*. 45:1279-1288.

Chouard, P. 1960. Vernalization and its Relations to Dormancy. *Annual Review of Plant Physiology*. 11:191-238.

Clough, S.J., and A.F. Bent. 1998. Floral dip: a simplified method for Agrobacterium-mediated transformation of Arabidopsis thaliana. *Plant J*. 16:735-743.

Dalchau, N., J. Baek Seong, M. Briggs Helen, C. Robertson Fiona, N. Dodd Antony, J. Gardner Michael, A. Stancombe Matthew, J. Haydon Michael, G.-B. Stan, M. Gonçalves Jorge, and A.R. Webb Alex. 2011. The circadian oscillator gene GIGANTEA mediates a long-term response of the Arabidopsis thaliana circadian clock to sucrose. *Proceedings of the National Academy of Sciences*. 108:5104-5109.

De Lucia, F., P. Crevillen, A.M.E. Jones, T. Greb, and C. Dean. 2008. A PHD-Polycomb Repressive Complex 2 triggers the epigenetic silencing of FLC during vernalization. *Proceedings of the National Academy of Sciences*. 105:16831.

Dong, M.A., E.M. Farré, and M.F. Thomashow. 2011. Circadian clock-associated 1 and late elongated hypocotyl regulate expression of the C-repeat binding factor (CBF) pathway in Arabidopsis. *Proc Natl Acad Sci U S A*. 108:7241-7246.

Enoki, Y., and H. Sakurai. 2011. Diversity in DNA recognition by heat shock transcription factors (HSFs) from model organisms. *FEBS Letters*. 585:1293-1298.

Evrard, A., M. Kumar, D. Lecourieux, J. Lucks, P. von Koskull-Döring, and H. Hirt. 2013. Regulation of the heat stress response in Arabidopsis by MPK6-targeted phosphorylation of the heat stress factor HsfA2. *PeerJ*. 1:e59.

Feder, M.E., and G.E. Hofmann. 1999. HEAT-SHOCK PROTEINS, MOLECULAR CHAPERONES, AND THE STRESS RESPONSE: Evolutionary and Ecological Physiology. *Annual Review of Physiology*. 61:243-282.

Fogelmark, K., and C. Troein. 2014. Rethinking Transcriptional Activation in the Arabidopsis Circadian Clock. *PLOS Computational Biology*. 10:e1003705.

Gendron, J.M., J.L. Pruneda-Paz, C.J. Doherty, A.M. Gross, S.E. Kang, and S.A. Kay. 2012. Arabidopsis circadian clock protein, TOC1, is a DNA-binding transcription factor. *Proc Natl Acad Sci U S A*. 109:3167-3172.

Gray, J.A., A. Shalit-Kaneh, D.N. Chu, P.Y. Hsu, and S.L. Harmer. 2017. The REVEILLE Clock Genes Inhibit Growth of Juvenile and Adult Plants by Control of Cell Size. *Plant physiology*. 173:2308-2322.

Guo, Y.-L., M. Todesco, J. Hagmann, S. Das, and D. Weigel. 2012. Independent FLC Mutations as Causes of Flowering-Time Variation in Arabidopsis thaliana and Capsella rubella. *Genetics*. 192:729-739.

Harmer, S.L., J.B. Hogenesch, M. Straume, H.-S. Chang, B. Han, T. Zhu, X. Wang, J.A. Kreps, and S.A. Kay. 2000. Orchestrated Transcription of Key Pathways in Arabidopsis by the Circadian Clock. *Science*. 290:2110.

Heino, P., G. Sandman, V. Lång, K. Nordin, and E.T. Palva. 1990. Abscisic acid deficiency

prevents development of freezing tolerance in Arabidopsis thaliana (L.) Heynh. *Theoretical and Applied Genetics*. 79:801-806.

Heo, J.B., and S. Sung. 2011. Vernalization-mediated epigenetic silencing by a long intronic noncoding RNA. *Science*. 331:76-79.

Hepworth, J., R.L. Antoniou-Kourounioti, R.H. Bloomer, C. Selga, K. Berggren, D. Cox, B.R. Collier Harris, J.A. Irwin, S. Holm, T. Säll, M. Howard, and C. Dean. 2018. Absence of warmth permits epigenetic memory of winter in Arabidopsis. *Nature Communications*. 9:639.

Horwich, A.L., W.A. Fenton, E. Chapman, and G.W. Farr. 2007. Two Families of Chaperonin: Physiology and Mechanism. *Annual Review of Cell and Developmental Biology*. 23:115-145.

Hou, X., L. Li, Z. Peng, B. Wei, S. Tang, M. Ding, J. Liu, F. Zhang, Y. Zhao, H. Gu, and L.J. Qu. 2010. A platform of high-density INDEL/CAPS markers for map-based cloning in Arabidopsis. *Plant J*. 63:880-888.

Hsu, P.Y., U.K. Devisetty, and S.L. Harmer. 2013. Accurate timekeeping is controlled by a cycling activator in Arabidopsis. *eLife*. 2:e00473.

Ikeda, M., N. Mitsuda, and M. Ohme-Takagi. 2011. Arabidopsis HsfB1 and HsfB2b Act as Repressors of the Expression of Heat-Inducible Hsfs But Positively Regulate the Acquired Thermotolerance. *Plant physiology*. 157:1243-1254.

Ikeda, M., and M. Ohme-Takagi. 2009. A novel group of transcriptional repressors in Arabidopsis. *Plant Cell Physiol*. 50:970-975.

Keily, J., D. Macgregor, R. Smith, A. Millar, K. Halliday, and S. Penfield. 2013. Model selection reveals control of cold signalling by evening-phased components of the plant circadian clock. *The Plant journal : for cell and molecular biology*. 76.

Kidokoro, S., K. Hayashi, H. Haraguchi, T. Ishikawa, F. Soma, I. Konoura, S. Toda, J. Mizoi, T. Suzuki, K. Shinozaki, and K. Yamaguchi-Shinozaki. 2021. Posttranslational regulation of multiple clock-related transcription factors triggers cold-inducible gene expression in Arabidopsis</em&gt. *Proceedings of the National Academy of Sciences*. 118:e2021048118.

Kim, D.-H. 2020. Current understanding of flowering pathways in plants: focusing on the vernalization pathway in Arabidopsis and several vegetable crop plants. *Horticulture, Environment, and Biotechnology*. 61:209-227.

Kim, D.-H., and S. Sung. 2013. Coordination of the Vernalization Response through a VIN3 and FLC Gene Family Regulatory Network in Arabidopsis</em&gt. *The Plant Cell*. 25:454.

Kim, D.-H., and S. Sung. 2017a. The Binding Specificity of the PHD-Finger Domain of VIN3 Moderates Vernalization Response. *Plant Physiology*. 173:1258-1268.

Kim, D.H., and S. Sung. 2017b. Vernalization-Triggered Intragenic Chromatin Loop Formation by Long Noncoding RNAs. *Dev Cell*. 40:302-312.e304.

Kim, D.H., Y. Xi, and S. Sung. 2017. Modular function of long noncoding RNA, COLDAIR, in the vernalization response. *PLoS Genet*. 13:e1006939.

Kim, Y., K.S. Schumaker, and J.K. Zhu. 2006. EMS mutagenesis of Arabidopsis. *Methods Mol Biol*. 323:101-103.

Kolmos, E., B.Y. Chow, J.L. Pruneda-Paz, and S.A. Kay. 2014. HsfB2b-mediated repression of PRR7 directs abiotic stress responses of the circadian clock. *Proceedings of the National Academy of Sciences*. 111:16172.

Kuittinen, H., A. Niittyvuopio, P. Rinne, and O. Savolainen. 2008. Natural Variation in Arabidopsis lyrata Vernalization Requirement Conferred by a FRIGIDA Indel Polymorphism. *Molecular Biology and Evolution*. 25:319-329.

Kumar, M., W. Busch, H. Birke, B. Kemmerling, T. Nürnberger, and F. Schöffl. 2009. Heat Shock Factors HsfB1 and HsfB2b Are Involved in the Regulation of Pdf1.2 Expression and Pathogen Resistance in Arabidopsis. *Molecular Plant*. 2:152-165.

Kyung, J., M. Jeon, G. Jeong, Y. Shin, E. Seo, J. Yu, H. Kim, C.-M. Park, D. Hwang, and I. Lee. 2021. The two clock proteins CCA1 and LHY activate VIN3 transcription during vernalization through the vernalization-responsive cis-element. *The Plant Cell*:koab304.

Kyung, J., M. Jeon, G. Jeong, Y. Shin, E. Seo, J. Yu, H. Kim, C.-M. Park, D. Hwang, and

I. Lee. 2022. The two clock proteins CCA1 and LHY activate VIN3 transcription during vernalization through the vernalization-responsive cis-element. *The Plant Cell*. 34:1020-1037.

Lång, V., P. Heino, and E.T. Palva. 1989. Low temperature acclimation and treatment with exogenous abscisic acid induce common polypeptides in Arabidopsis thaliana (L.) Heynh. *Theoretical and Applied Genetics*. 77:729-734.

Lee, I., S.D. Michaels, A.S. Masshardt, and R.M. Amasino. 1994. The late-flowering phenotype of FRIGIDA and mutations in LUMINIDEPENDENS is suppressed in the Landsberg erecta strain of Arabidopsis. *The Plant Journal*. 6:903-909.

Lee, J., J.-Y. Yun, W. Zhao, W.-H. Shen, and R. Amasino. 2015. A methyltransferase required for proper timing of the vernalization response in Arabidopsis. *Proceedings of the National Academy of Sciences of the United States of America*. 112.

Liu, T., J. Carlsson, T. Takeuchi, L. Newton, and E.M. Farré. 2013. Direct regulation of abiotic responses by the Arabidopsis circadian clock component PRR7. *The Plant Journal*. 76:101-114.

Llorca, O., J. Martín-Benito, M. Ritco-Vonsovici, J. Grantham, G.M. Hynes, K.R. Willison, J.L. Carrascosa, and J.M. Valpuesta. 2000. Eukaryotic chaperonin CCT stabilizes actin and tubulin folding intermediates in open quasi-native conformations. *Embo j*. 19:5971-5979.

Lukowitz, W., C.S. Gillmor, and W.-R. Scheible. 2000a. Positional Cloning in Arabidopsis. Why It Feels Good to Have a Genome Initiative Working for You. *Plant Physiology*. 123:795.

Lukowitz, W., C.S. Gillmor, and W.-R.d. Scheible. 2000b. Positional Cloning in Arabidopsis. Why It Feels Good to Have a Genome Initiative Working for You1. *Plant Physiology*. 123:795-806.

Marquardt, S., O. Raitskin, Z. Wu, F. Liu, Q. Sun, and C. Dean. 2014. Functional consequences of splicing of the antisense transcript COOLAIR on FLC transcription. *Mol Cell*. 54:156-165.

Michaels, S.D., and R.M. Amasino. 1999. FLOWERING LOCUS C Encodes a Novel MADS Domain Protein That Acts as a Repressor of Flowering. *The Plant Cell*. 11:949-956.

Michaels, S.D., and R.M. Amasino. 2000. Memories of winter: vernalization and the competence to flower. *Plant, Cell & Environment*. 23:1145-1153.

Minkoff, B.B., K.E. Stecker, and M.R. Sussman. 2015. Rapid Phosphoproteomic Effects of Abscisic Acid (ABA) on Wild-Type and ABA Receptor-Deficient A. thaliana Mutants. *Mol Cell Proteomics*. 14:1169-1182.

Muñoz, I.G., H. Yébenes, M. Zhou, P. Mesa, M. Serna, A.Y. Park, E. Bragado-Nilsson, A. Beloso, G. de Cárcer, M. Malumbres, C.V. Robinson, J.M. Valpuesta, and G. Montoya. 2011. Crystal structure of the open conformation of the mammalian chaperonin CCT in complex with tubulin. *Nat Struct Mol Biol*. 18:14-19.

Nagel Dawn, H., J. Doherty Colleen, L. Pruneda-Paz Jose, J. Schmitz Robert, R. Ecker Joseph, and A. Kay Steve. 2015. Genome-wide identification of CCA1 targets uncovers an expanded clock network in Arabidopsis. *Proceedings of the National Academy of Sciences*. 112:E4802-E4810.

Nagel, D.H., C.J. Doherty, J.L. Pruneda-Paz, R.J. Schmitz, J.R. Ecker, and S.A. Kay. 2015. Genome-wide identification of CCA1 targets uncovers an expanded clock network in <em>Arabidopsis</em&gt. *Proceedings of the National Academy of Sciences*. 112:E4802.

Nishizawa, A., Y. Yabuta, E. Yoshida, T. Maruta, K. Yoshimura, and S. Shigeoka. 2006. Arabidopsis heat shock transcription factor A2 as a key regulator in response to several types of environmental stress. *The Plant Journal*. 48:535-547.

Nover, L., K. Bharti, P. Döring, S.K. Mishra, A. Ganguli, and K.D. Scharf. 2001. Arabidopsis and the heat stress transcription factor world: how many heat stress transcription factors do we need? *Cell Stress Chaperones*. 6:177-189.

Nover, L., K.D. Scharf, D. Gagliardi, P. Vergne, E. Czarnecka-Verner, and W.B. Gurley. 1996. The Hsf world: classification and properties of plant heat stress transcription factors. *Cell Stress Chaperones*. 1:215-223.

O'Malley, R.C., S.C. Huang, L. Song, M.G. Lewsey, A. Bartlett, J.R. Nery, M. Galli, A. Gallavotti, and J.R. Ecker. 2016. Cistrome and Epicistrome Features Shape the Regulatory DNA Landscape. *Cell*. 165:1280-1292.

Ogawa, D., K. Yamaguchi, and T. Nishiuchi. 2007. High-level overexpression of the Arabidopsis HsfA2 gene confers not only increased themotolerance but also salt/osmotic stress tolerance and enhanced callus growth. *Journal of Experimental Botany*. 58:3373-3383.

Park, M.-J., Y.-J. Kwon, K.-E. Gil, and C.-M. Park. 2016. LATE ELONGATED HYPOCOTYL regulates photoperiodic flowering via the circadian clock in Arabidopsis. *BMC Plant Biology*. 16:114.

Poethig, R.S. 1990. Phase change and the regulation of shoot morphogenesis in plants. *Science*. 250:923-930.

Qüesta Julia, I., J. Song, N. Geraldo, H. An, and C. Dean. 2016. Arabidopsis transcriptional repressor VAL1 triggers Polycomb silencing at FLC during vernalization. *Science*. 353:485-488.

Rawat, R., N. Takahashi, P.Y. Hsu, M.A. Jones, J. Schwartz, M.R. Salemi, B.S. Phinney, and S.L. Harmer. 2011. REVEILLE8 and PSEUDO-REPONSE REGULATOR5 Form a Negative Feedback Loop within the Arabidopsis Circadian Clock. *PLOS Genetics*. 7:e1001350.

Richter, K., M. Haslbeck, and J. Buchner. 2010. The heat shock response: life on the verge of death. *Mol Cell*. 40:253-266.

Sabehat, A., S. Lurie, and D. Weiss. 1998. Expression of small heat-shock proteins at low temperatures. A possible role in protecting against chilling injuries. *Plant Physiol*. 117:651-658.

Shalit-Kaneh, A., W. Kumimoto Roderick, V. Filkov, and L. Harmer Stacey. 2018a. Multiple feedback loops of the Arabidopsis circadian clock provide rhythmic robustness across environmental conditions. *Proceedings of the National Academy of Sciences*. 115:7147-7152.

Shalit-Kaneh, A., R.W. Kumimoto, V. Filkov, and S.L. Harmer. 2018b. Multiple feedback

loops of the Arabidopsis circadian clock provide rhythmic robustness across environmental conditions. *Proceedings of the National Academy of Sciences*. 115:7147.

Sheldon, C.C., J.E. Burn, P.P. Perez, J. Metzger, J.A. Edwards, W.J. Peacock, and E.S. Dennis. 1999. The FLF MADS Box Gene: A Repressor of Flowering in Arabidopsis Regulated by Vernalization and Methylation. *The Plant Cell*. 11:445-458.

Shin, J., G. Jeong, J.-Y. Park, H. Kim, and I. Lee. 2018. MUN (MERISTEM UNSTRUCTURED), encoding a SPC24 homolog of NDC80 kinetochore complex, affects development through cell division in Arabidopsis thaliana. *The Plant Journal*. 93:977-991.

Simpson, G., and C. Dean. 2002. Arabidopsis, the Rosetta Stone of Flowering Time? *Science (New York, N.Y.)*. 296:285-289.

Skjærven, L., J. Cuellar, A. Martinez, and J.M. Valpuesta. 2015. Dynamics, flexibility, and allostery in molecular chaperonins. *FEBS Letters*. 589:2522-2532.

Spiess, C., A.S. Meyer, S. Reissmann, and J. Frydman. 2004. Mechanism of the eukaryotic chaperonin: protein folding in the chamber of secrets. *Trends Cell Biol*. 14:598-604.

Sung, S., and R.M. Amasino. 2004. Vernalization in Arabidopsis thaliana is mediated by the PHD finger protein VIN3. *Nature*. 427:159-164.

Sung, S., Y. He, T.W. Eshoo, Y. Tamada, L. Johnson, K. Nakahigashi, K. Goto, S.E. Jacobsen, and R.M. Amasino. 2006. Epigenetic maintenance of the vernalized state in Arabidopsis thaliana requires LIKE HETEROCHROMATIN PROTEIN 1. *Nat Genet*. 38:706-710.

Swindell, W.R., M. Huebner, and A.P. Weber. 2007. Transcriptional profiling of Arabidopsis heat shock proteins and transcription factors reveals extensive overlap between heat and non-heat stress response pathways. *BMC Genomics*. 8:125-125.

Ul Haq, S., A. Khan, M. Ali, A.M. Khattak, W.X. Gai, H.X. Zhang, A.M. Wei, and Z.H. Gong. 2019. Heat Shock Proteins: Dynamic Biomolecules to Counter Plant Biotic

and Abiotic Stresses. *Int J Mol Sci*. 20.

von Koskull-Döring, P., K.-D. Scharf, and L. Nover. 2007. The diversity of plant heat stress transcription factors. *Trends in Plant Science*. 12:452-457.

Wood, C.C., M. Robertson, G. Tanner, W.J. Peacock, E.S. Dennis, and C.A. Helliwell. 2006. The Arabidopsis thaliana vernalization response requires a polycomb-like protein complex that also includes VERNALIZATION INSENSITIVE 3. *Proceedings of the National Academy of Sciences*. 103:14631-14636.

Wu, C. 1995. Heat shock transcription factors: structure and regulation. *Annu Rev Cell Dev Biol*. 11:441-469.

Xu, X.M., J. Wang, Z. Xuan, A. Goldshmidt, P.G.M. Borrill, N. Hariharan, J.Y. Kim, and D. Jackson. 2011. Chaperonins Facilitate KNOTTED1 Cell-to-Cell Trafficking and Stem Cell Function. *Science*. 333:1141.

Xu, Z., K. Mahmood, and S. Rothstein. 2017. ROS Induces Anthocyanin Production Via Late Biosynthetic Genes and Anthocyanin Deficiency Confers the Hypersensitivity to ROS-Generating Stresses in Arabidopsis. *Plant & cell physiology*. 58.

Yang, H., S. Berry, T.S.G. Olsson, M. Hartley, M. Howard, and C. Dean. 2017. Distinct phases of Polycomb silencing to hold epigenetic memory of cold in Arabidopsis. *Science*. 357:1142-1145.

Yoo, S.-D., Y.-H. Cho, and J. Sheen. 2007. Arabidopsis mesophyll protoplasts: a versatile cell system for transient gene expression analysis. *Nature Protocols*. 2:1565-1572.

Yoshida, T., N. Ohama, J. Nakajima, S. Kidokoro, J. Mizoi, K. Nakashima, K. Maruyama, J.M. Kim, M. Seki, D. Todaka, Y. Osakabe, Y. Sakuma, F. Schöffl, K. Shinozaki, and K. Yamaguchi-Shinozaki. 2011. Arabidopsis HsfA1 transcription factors function as the main positive regulators in heat shock-responsive gene expression. *Mol Genet Genomics*. 286:321-332.

Yuan, W., X. Luo, Z. Li, W. Yang, Y. Wang, R. Liu, J. Du, and Y. He. 2016. A cis cold memory element and a trans epigenome reader mediate Polycomb silencing of FLC by vernalization in Arabidopsis. *Nat Genet*. 48:1527-1534.

Zhang, Y., S. Zheng, Z. Liu, L. Wang, and Y. Bi. 2011. Both HY5 and HYH are necessary regulators for low temperature-induced anthocyanin accumulation in Arabidopsis seedlings. *J Plant Physiol*. 168:367-374.

Zhao, Y., R.L. Antoniou-Kourounioti, G. Calder, C. Dean, and M. Howard. 2020. Temperature-dependent growth contributes to long-term cold sensing. *Nature*. 583:825-829.

Abstract in Korean

국문 초록

춘화처리는 겨울과 같은 장기 저온현상 이후의 개화 촉진현상을 지칭하는 것으로, 특히 겨울종 식물의 개화시기 조절 메커니즘에서 주요하게 다루어졌다. 모델 식물인 애기장대에서는 PHD finger domain 을 가지는 단백질인 VERNALIZATION INSENSITVE 3 (VIN3) 가 Polycome Repressive Complex 2 를 강력한 개화 억제자인 *FLC* 에 가져와 후성유전학적 방법을 통해 억제하는 현상이 춘화처리에 있어 필수적이다. *VIN3* 의 발현양은 수 주 단위의 저온에 걸쳐 서서히 증가한다. 그러나, 식물에서 일어나는 저온환경에 따른 *VIN3* 의 정교한 발현조절은 현재까지 완벽하게 밝혀지지 않았다. 본 연구에서는 *VIN3* 의 프로모터에 GUS reporter 를 결합한 형질전환 식물을 이용하였으며, 이 식물체를 사용해 EMS mutagenesis 를 수행, *hov1* 과 *P161* 이라는 두 돌연변이체를 동정하였다.

1장에서는, heat shock transcription factor 를 통한 *VIN3* 의 미세 조절 기작에 대해 다룬다. *VIN3* 의 발현을 GUS reporter gene 으로 파악할 수 있는 형질전환 식물을 이용한 EMS mutagensis 를 통해, *VIN3* 발현이 증가해 있는 돌연변이체, *hov1* 을 동정하였다. Positional cloning 과 whole-genome

resequencing 을 통해, *hov1* 이 전사 억제 기능을 가지고 있는 heat shock transcription factor 인 HsfB2b 가 조기에 종결되도록 하는 돌연변이를 가지고 있다는 것을 알아냈다. HsfB2b 는 *VIN3* 의 프로모터에 직접 결합해 전사를 억제하는 것으로 확인되었으며, HsfB2b 의 과발현이 춘화처리 이후의 개화촉진을 저해하는 것도 확인하였다. 이러한 발견들을 통해 *VIN3* 를 통한 춘화처리 반응의 미세 조절 기작을 규명하였다.

2장에서는, 진핵생물의 샤페로닌에 의해 매개되는 *VIN3* 조절의 분자 기작에 대해 논의한다. 돌연변이 스크리닝 과정에서, 춘화처리 과정 중 *VIN3* 의 발현이 감소해 있는 돌연변이체, *P161* 을 동정하였다. Positional cloning 과 whole-genome resequencing 을 통해, *P161* 이 샤페로닌 소단위체 중 하나인 CCT8 의 아미노산 잔기 하나를 치환하는 점 돌연변이를 가지고 있음이 확인되었다. 이 돌연변이가 생체시계를 구성하는 유전자 중 하나인 *RVE8* 의 일주기 발현 패턴을 저해하는 것이 확인되었으며, *VIN3* 의 일주기 발현패턴 또한 저해되는 것이 확인되었다. RVE8 은 *VIN3* 프로모터에 직접 결합해 일주기 리듬패턴을 만드는 것이 확인되었다. 종합적으로, 이러한 발견들을 통해 *VIN3* 를 조절해 춘화처리를 조절하는 새로운 기작을 규명하였다.

주요어: 개화 조절, 춘화처리, VIN3, CCT8, RVE8, 애기장대

학번: 2013-20317